40356

National Library of Canada | Bibliothèque nationale du Canada

CANADIAN THESES ON MICROFICHE | THÈSES CANADIENNES SUR MICROFICHE

NAME OF AUTHOR/*NOM DE L'AUTEUR* PETER RICHARD WRENSHALL

TITLE OF THESIS/*TITRE DE LA THÈSE* EVALUATION OF HAILFALL FROM RADAR AND HAILPAD DATA

UNIVERSITY/*UNIVERSITÉ* UNIVERSITY OF ALBERTA

DEGREE FOR WHICH THESIS WAS PRESENTED/*GRADE POUR LEQUEL CETTE THÈSE FUT PRÉSENTÉE* MASTER OF SCIENCE

YEAR THIS DEGREE CONFERRED/*ANNÉE D'OBTENTION DE CE GRADE* 1978

NAME OF SUPERVISOR/*NOM DU DIRECTEUR DE THÈSE* DR. ROBERT CHARLTON

Permission is hereby granted to the NATIONAL LIBRARY OF CANADA to microfilm this thesis and to lend or sell copies of the film.

The author reserves other publication rights, and neither the thesis nor extensive extracts from it may be printed or otherwise reproduced without the author's written permission.

L'autorisation est, par la présente, accordée à la BIBLIOTHÈQUE NATIONALE DU CANADA de microfilmer cette thèse et de prêter ou de vendre des exemplaires du film.

L'auteur se réserve les autres droits de publication; ni la thèse ni de longs extraits de celle-ci ne doivent être imprimés ou autrement reproduits sans l'autorisation écrite de l'auteur.

DATED/*DATÉ* JULY 24 1978 SIGNED/*SIGNÉ* P.R. Wrenshall

PERMANENT ADDRESS/*RÉSIDENCE FIXÉ* 220 NORMANDY AVENUE
PINCOURT, QUEBEC J7V 3V7

NL-91 (3-74)

NOTICE

The quality of this microfiche is heavily dependent upon the quality of the original thesis submitted for microfilming. Every effort has been made to ensure the highest quality of reproduction possible.

If pages are missing, contact the university which granted the degree.

Some pages may have indistinct print especially if the original pages were typed with a poor typewriter ribbon or if the university sent us a poor photocopy.

Previously copyrighted materials (journal articles, published tests, etc.) are not filmed.

Reproduction in full or in part of this film is governed by the Canadian Copyright Act, R.S.C. 1970, c. C-30. Please read the authorization forms which accompany this thesis.

THIS DISSERTATION
HAS BEEN MICROFILMED
EXACTLY AS RECEIVED

AVIS

La qualité de cette microfiche dépend grandement de la qualité de la thèse soumise au microfilmage. Nous avons tout fait pour assurer une qualité supérieure de reproduction.

S'il manque des pages, veuillez communiquer avec l'université qui a conféré le grade.

La qualité d'impression de certaines pages peut laisser à désirer, surtout si les pages originales ont été dactylographiées à l'aide d'un ruban usé ou si l'université nous a fait parvenir une photocopie de mauvaise qualité.

Les documents qui font déjà l'objet d'un droit d'auteur (articles de revue, examens publiés, etc.) ne sont pas microfilmés.

La reproduction, même partielle, de ce microfilm est soumise à la Loi canadienne sur le droit d'auteur, SRC 1970, c. C-30. Veuillez prendre connaissance des formules d'autorisation qui accompagnent cette thèse.

LA THÈSE A ÉTÉ
MICROFILMÉE TELLE QUE
NOUS L'AVONS REÇUE

THE UNIVERSITY OF ALBERTA

EVALUATION OF HAILFALL FROM RADAR AND HAILPAD DATA

by

© PETER WRENSHALL

A THESIS

SUBMITTED TO THE FACULTY OF GRADUATE STUDIES AND RESEARCH

IN PARTIAL FULFILMENT OF THE REQUIREMENTS FOR THE DEGREE OF

MASTER OF SCIENCE

in

METEOROLOGY

DEPARTMENT OF GEOGRAPHY

EDMONTON, ALBERTA

FALL 1978

THE UNIVERSITY OF ALBERTA

FACULTY OF GRADUATE STUDIES AND RESEARCH

The undersigned certify that they have read, and recommend to the Faculty of Graduate Studies and Research, for acceptance, a thesis entitled "Evaluation of Hailfall from Radar and Hailpad Data", submitted by Peter Wrenshall in partial fulfilment of the requirements for the degree of Master of Science in Meteorology.

Robert R. Gilbert
Supervisor

Henry G. Hogan

D. A. McLeish

Date June 30/1978.

DEDICATION:

To F.B.

ABSTRACT

Weather radar data is used to extrapolate hailfall energy to locations where the energy was not measured by hailpads. A formula to convert radar echo intensities to energy fluxes of hail was developed. These fluxes were summed over the duration of the storm at a given location to obtain a raw estimate of energy density of hailfall at the ground in Jm^{-2}. This areal energy density was then adjusted by the hailpad network using a linear regression of the energy densities known from hailpad analyses against the raw radar estimates from the same locations.

Radar data from August 7 and 18, 1974, produced by the Alberta Hail Project C-band system, was used in this study. This data is logged on magnetic tape, and was extracted by computer programs developed during the study. Hailpad data from August 7 and 18 was used with the radar data. Supplementary hailpad information from July 30 and August 15, 1974 was also used.

The radar-hailpad method of estimating hail energy density had a spatial resolution equal to that of the radar itself, which was about 1 kilometer. The density of information that can be obtained by this method is much higher

than that of the existing hailpad network. The error in the radar-hailpad method was found by statistical analysis to be substantially less than the error in methods based on hailpad information alone. Farmers' reports of hailfall were also used in the analysis.

The storms on the two days studied were different enough to produce changes in the parameters used in adjusting radar estimates with hailpad data. This implies that radar estimates of hailfall should be adjusted on a day-to-day basis using ground-based measurements.

A continuous grid of estimates of hailfall energy density was calculated by the radar-hailpad method for a 109 square mile ($282 km^2$) area hit by the storm of August 18, 1974. The details of the resulting pattern agreed strongly with the known properties of the distribution of hailfall on that scale. The estimated energy densities also agreed with the observations of hailfall by farmers in the area.

ACKNOWLEDGEMENTS

I would like to acknowledge my sincere gratitude to Dr. Robert Charlton in helping to guide this project to completion, in spite of the setbacks encountered over the last three years.

I would also like to express thanks to Dr. Brian Barge and Dr. Robert Humphries for clearing up problems I had in the theory of weather radar, and to the other members of the Alberta Hail Project research staff for their many useful suggestions. Dr. Carlton Ulbrich of Clemson University in South Carolina sent some interesting correspondence on the results of his work, which was closely related to this project.

Thanks also go to Dr. Guy Goyer and Dr. D. L. MacLeish for serving on my examining committee.

I would also like to express my appreciation to Lynne Rowen, who typed the final draft of this thesis.

This study was amply funded by a grant from the Interim Weather Modification Board under the Alberta Ministry of Agriculture.

TABLE OF CONTENTS

Table of Contents, Continued

LIST OF TABLES

LIST OF FIGURES

List of Figures, Continued

CHAPTER 1

INTRODUCTION

1.1 THE PROBLEM

The Alberta Hail Project is involved in cloud seeding to reduce crop damage by hail over a 20,000 km^2 area of central Alberta. The spatial pattern of hailfall is very intricate and the Alberta Hail Project would like to detect hail damage reductions in the order of ten percent. Therefore, it is desirable to document the fine-scale features of hailfall for individual storms to the greatest extent possible using all available information.

The damage to grain crops which is caused by a hail storm has been shown to be closely related to the kinetic energy per unit area of the hailstones which fell during the storm. For instance, 100 joules per square meter means slight crop damage and 1000 joules per square meter usually means 100 percent crop damage. Although some of a falling stone's kinetic energy is tied up in its horizontal travel with horizontal winds, most of its energy is usually incorporated in its vertical fall speed. In this study, the sum of the vertical kinetic energies of

the hailstones which fell on a unit area during a storm will be called the "kinetic energy density" although it is really a kinetic energy per unit area.

This study investigates the use of weather radar to estimate hailfall from individual storms between points where hailfall information is already available. Since the resolution of the radar is about one kilometer it is theoretically possible to estimate the hailfall from a storm over every square kilometer of land.

The Alberta Hail Project relies on several sources to obtain data on hail activity: hailpads, radar, ground surveys by mail or telephone, field trips in specially-instrumented trucks, and crop insurance statistics.

Telephone and mail surveys, called farmers' reports, cover a wide area and can yield a high areal density of hail information. This information is rather imprecise, since observing conditions during a hailstorm are hardly ideal for the amateur observer who is expected to produce quantitative information. Field trips by professional observers are expensive and time-consuming. In the history of a typical hailstorm, all the field trips undertaken will cover only about twenty locations. While crop insurance statistics reveal a great deal about total storm damage and seasonal losses, they have insufficient resolution to delineate the fine-scale storm effects. They can, however, be used in conjunction with high-

density, area-averaged information for general assessments of storm damage.

Until 1974, the Alberta Hail Project has used its radar facilities mainly for hailstorm research. In July 1974 a PDP-11 computer was added to the radar system. The computer makes a digital record on magnetic tape of all radar echoes on hailstorm days as well as providing instantaneous storm-tracking information.

A hailpad is a piece of Styrofoam about 30 centimeters square and 3 centimeters thick. In the field, it is mounted on a firm, level surface. Each hailstone impacting the Styrofoam will dent it, providing a record of the storm's passage over the pad. The principles of hailpad analysis are described in Chapters 2 and 3. In the 1974 operations seasons, about 600 hailpad stations were maintained in the "Project" area. The regular network consisted of 491 hailpads. The hailpad spacing varied from three per township (36 square miles or 93.2 square kilometers) near the central region, to about one per township on the fringes. Farmers who maintained hailpad stations also kept raingauges and collected hail samples. For finer-scale studies the Project also maintained a dense network of about 100 hailpads over ten townships between the towns of Rimbey and Eckville.

In 1973 Strong (1975) studied the use of hailpads in providing quantitative information. He found that this information would be useful in studying

entire storms only if the density of the hailpad network was made much higher than it has been to date. His conclusions are based on the use of hailpads as the only source of information on spatial distribution of hailfall energy. The suggested number of hailpads required to successfully capture these variations over the entire Project area was clearly impracticable. A good alternative is to supplement the data from the existing hailpad network with radar information. The use of radar and hailpads instead of hailpads alone has two major advantages. First, the radar can cover the entire area under observation. The second advantage is its comparatively low cost. The required information can be abstracted from data collected during regular radar operation which involves detection of storms and the guidance of seeding aircraft.

1.2 HISTORICAL BACKGROUND OF THE STUDY

Since weather radars were used to study rainfall rate before they were used to study hailfall, it is best to review the historical developments in that order.

Early in the history of radar meteorology, it was realized that the intensity of radar echoes from rain could be correlated with the rainfall rate. An empirical relationship between the radar reflectivity Z, and the rate of rainfall R, was suggested by Marshall, Langille and Palmer as early as 1947. This and similar formulae

have since been referred to as Z-R relationships. Using observations of raindrop-size distributions, Marshall and Palmer (1948) developed the following theoretical Z-R relationship:

$$Z = 220R^{1.6} \qquad 1.1$$

with Z in mm^6m^{-3} and R in $mm\ hr^{-1}$.

In the 1960's Soviet scientists used raingauges to verify Z-R relationships. Some of these studies were reported by Dimaksian, Zotimov and Zykov (Dimaksian *et al.*, 1965).

From 1963 onward, studies of the Z-R relationship proliferated rapidly. Wilson (1966) showed that storm-to-storm variability exists in the relationship. Stout and Mueller (1968) discovered significant regional as well as storm-to-storm variation. It became clear that a ground network of precipitation gauges was needed to calibrate the radar for each storm if it was to successfully estimate rainfall rate over the area of radar coverage. There is an implication here that hailfall-radar studies may also need ground-based gauges.

Raingauges were actively used in calibrating or adjusting radar estimates of rainfall in a major study in Illinois in 1964 and 1965. Estimates of the total volume of fallen rain from the existing "climatological" raingauge network were compared with estimates from radar data cali-

brated by the raingauges. The known statistical properties of the raingauge network were used to judge the relative accuracy of the two methods. The study showed that the radar, calibrated by raingauges, was equivalent in accuracy to a raingauge-only network of 150mi^2/gauge. The climatological raingauge network had an actual density of 225mi^2/gauge (Huff, 1966).

Newer techniques of integrating raingauge and radar data improved the accuracy of areal rainfall estimates in the Florida Area Cumulus Experiment (Woodley *et al.*, 1974). Other studies have consistently demonstrated the value of combined radar-ground gauge methods (Changnon, 1967; Wilson, 1970; Brandes, 1974, 1975).

The possibility that hailfall could be analysed in a similar way to rainfall depended on the development of a simple and reliable instrument for measuring the important parameters associated with hail at the ground. These parameters are mass, kinetic energy or momentum per unit area. The hailpad has become the favorite instrument for this purpose. It was first used by Schleusener and Jennings (1960). They used the 30-centimeter size, covered with aluminum foil, which was in common use until 1975. Hailpad usage was first described by Decker and Calvin (1961). The Alberta Hail Project used this type of hailpad in 1974, but it abandoned the use of aluminum foil in the following year. Quantitative methods of analysing foil-covered and "styrofoam only" hailpads were

developed in Alberta (Strong, 1974; Strong and Lozowski, 1977).

The theory of the radar detection and evaluation of hailfall has been studied by many researchers. Practical applications were recognized as early as 1960 (Douglas). A comprehensive review can be found in "Radar Meteorology" (Battan, 1973). It has been shown that the intensity of hailfall can be related to the strength and other characteristics of the radar echoes in much the same way as rainfall (Barge, 1977). It is possible, therefore, that hailpads and radar can be used to delineate the pattern of hailfall in an analogous way to the use of raingauges and radar for rainfall. The problem is somewhat more difficult than rainfall evaluation because of the generally smaller dimensions of hailshafts and because echoes from hail are generally masked to some extent by those from rain.

1.3 DESCRIPTION AND OBJECTIVES

The main objective of the study was to develop a method of estimating the kinetic energy density of hailfall at locations where only radar data was available. The digitized output of meteorological radar and hailpad information were used. Such an analysis of hailfall could probably be related to statistics of crop damage by hail, and it could, therefore, aid in the assessment of the ef-

fectiveness of cloud seeding.

This study uses radar and hailpad information from two hail-days in central Alberta in 1974. August 7 and August 18, 1974 yielded a large number of useful hailpads, while the quality of the radar data was better than any available on other hail-days during the season. Supplementary hailpad information from July 30 and August 15 was also used. The radar was the Alberta Hail Project C-band, operating at a wavelength of 5.5 centimeters. The S-band, 10-centimeter unit, which would normally be used, was under repair throughout the summer of 1974.

When the data for this study was being collected, the method of digitizing the radar output was new, and defects in the data extraction were still in the process of being removed. As a result, there are weaknesses and interruptions in the radar data even under the best conditions, and the overall quality is poor in comparison to the data from later years. This dissertation describes the analysis of this data and the development of a method of radar-hailpad interpolation. The results of this method are shown in Chapter 4. Their accuracy, in comparison to methods using hailpads alone, is determined by elementary statistical tests. The radar and hailpad data from 1975 and 1976 are expected to provide a more thorough test of the method described here.

CHAPTER 2

SOURCES AND PREPARATION OF DATA

2.1 THEORY OF THE HAILPAD

This section summarizes how a hailpad measures the energy density of hailfall.

Strong and Lozowski (1977) have shown that a simple relationship exists between the size of the dent on a hailpad and the size of the hailstone which produced it. By assuming values for parameters such as the density, shape and drag coefficient of the hailstone and the air density, one gets the following equation for the terminal velocity V_+.

$$V_+ = kD^{\frac{1}{2}} \qquad 2.1$$

D is the diameter of the spherical hailstone and k is the constant of proportionality which depends on the factors mentioned above. The momentum and kinetic energy of the hailstone can be inferred from this equation. A count of the dents in particular size categories will, by application of the proper formulae, yield the kinetic energy per

unit area of the hail that fell on the pad.

The hailpads used by the Alberta Hail Project are made of a brand of Styrofoam (Type *FR) manufactured by the Dow Chemical Company. In 1974 they were covered with heavy (.001 inch) aluminum foil. A key assumption made by Strong and Lozowski is that the hailpad exerts a constant pressure against the surface of a solid, homogeneous sphere as it undergoes collision. Most of the kinetic energy of the hailstone is assumed to be used in creating the dent in the styrofoam. The center of the stone does not penetrate below the undisturbed surface of the hailpad, and the sphere does not penetrate so deeply that the support underneath the pad affects the dynamics of the collision. Fracturing of the Styrofoam and the effect of deforming the aluminum foil cover are assumed to be unimportant. Using these assumptions, the authors derived an equation

$$R = \left[\frac{4}{9}\,\frac{\rho_i^{\,2}}{\rho_a}\,\frac{g}{C_D p}\right]^{\frac{1}{4}} r^{\frac{5}{4}} \qquad 2.2$$

where R is the hailstone radius, r is the radius of the dent it produces, p is the pressure the Styrofoam exerts against the hailstone, g the gravitational acceleration, C_D the drag coefficient, and ρ_i and ρ_a are the densities of ice and air, respectively.

Based on laboratory experiments the authors developed a polynomial to express the hailstone-dent rela-

"tion:

$$D = 0.15 + 1.11d - 0.09d^2 \qquad 2.3$$

with D being the hailstone diameter and d the dent diameter, both in centimeters. The vertical kinetic energy of a hailstone of diameter D falling at terminal velocity is:

$$E_D = \left(\frac{\pi}{9} \frac{\rho i^2}{\rho_a} \frac{g}{C_D}\right) D^4 \qquad 2.4$$

Summing the kinetic energy given by Equations 2.3 and 2.4 from all dents on the hailpad and dividing by the area of the pad gives the energy per unit area, or energy density, of the hail that fell at the hailpad site. To get the hailstone's kinetic energy in units of joules the coefficient of D^4 in Equation 2.4 is typically 0.042 if D is in centimeters. The methods actually used to calculate energy density are described in the following section.

2.2 ANALYSIS OF THE HAILPADS

The original analysis of the hailpads from the 1974 Hail Project operations was performed by part-time helpers and the author of this study throughout 1975 and 1976, using a method developed by Wojtiw (1975).

Each analyst was supplied with sheets of clear

acetate plastic to cover the exposed faces of the hailpads to be analysed, and a transparent template marked with circles of various diameters ranging from 0.1 inches to 2.25 inches. The borders of the dents on the hailpads are traced on the acetate sheets. This prevents damage to the hailpads and provides a convenient means to mark off dents as the analysis proceeds.

Using the template, a count is made of the number of dents in diameter classes at intervals of 0.05 inches. Diameter classes not represented on the template are counted by the dents whose diameters lie between the two nearest available circle sizes. Large, irregular dents are counted by using the circles of approximately the same area. The counts of the dent sizes are entered in the left-hand blank column of the analysis sheet, an example of which is shown in Figure 2.1. The kinetic energy per dent in each diameter class is listed beside the blank center column. The counts of the dents are multiplied by the corresponding kinetic energies per dent and the resulting figures, in joules, are entered in the center column. This column is totalled to give the kinetic energy density in joules per square foot, then multiplied by 10.76 to give the result in joules per square meter.

Subsequent publication of the results of hailpad calibration by Lozowski and Strong (1977) led to the discovery of a discrepancy between their calibration formulae (Equations 2.3 and 2.4) and the ones implicit in

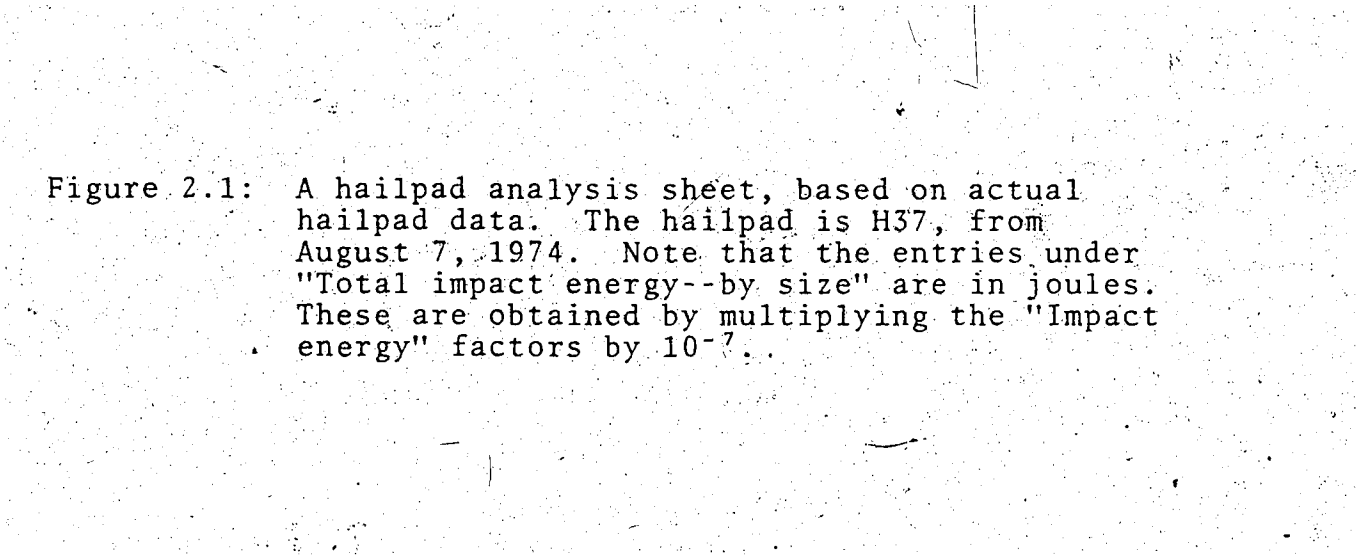

Figure 2.1: A hailpad analysis sheet, based on actual hailpad data. The hailpad is H37, from August 7, 1974. Note that the entries under "Total impact energy--by size" are in joules. These are obtained by multiplying the "Impact energy" factors by 10^{-7}.

HAILPAD ANALYSIS SHEET

22 Oct./73

HAILPAD NO.: N219 STORM DATE/ TIME: 7/8, 16:50 ANALYSIST'S INITIALS: _____

STATION NO.: H37 LAND LOCATION: NE20,41,26,4 DATE OF ANALYSIS: _____

OPERATOR: _____ CHECK BOX(ES) IF AND WHEN ANALYSIS REPEATED ☐☐

	dent diameter (inches)	no. dents: by size	no. dents: size ranges	impact energy (ergs)	total impact energy (joules - ergs x 10^{-7}): by size	total impact energy (joules - ergs x 10^{-7}): size ranges	equivalent hailstone size: diam. (in.)	equivalent hailstone size: X-sctn. area(in^2)	total areas dented on hailpad(in^2)
shot	< .05		shot	2.59×10^6		shot	<.20	.0020	
pea	.10	34	no. pea size	6.99×10^6	0.238	pea size E_1	.25	.0079	
	.15	27		1.35×10^7	0.919		.31	.0177	
	.20	35		3.01×10^7	1.054		.36	.0314	
	.25	8		5.31×10^7	0.425		.42	.0491	
	.30	3		8.74×10^7	0.252		.47	.0707	
grape	.35	1	no. grape size	1.36×10^8	0.136	grape size E_1	.53	.096	
	.40			2.03×10^8			.58	.126	
	.45			2.91×10^8			.64	.159	
	.50			4.06×10^8			.69	.196	
	.55			5.52×10^8			.75	.237	
	.60			7.33×10^8			.80	.283	
walnut	.65		no. walnut size	9.57×10^8		walnut size E_1	.86	.332	
	.70			1.23×10^9			.91	.385	
	.75			1.49×10^9			.96	.436	
	.80			1.76×10^9			1.00	.502	
	.85			2.07×10^9			1.04	.567	
	.90			2.42×10^9			1.08	.636	
	.95			2.81×10^9			1.12	.708	
	1.00			3.24×10^9			1.16	.785	
	1.05			3.73×10^9			1.20	.865	
	1.10			4.26×10^9			1.24	.950	
golfball	other sizes up to 2.00		no. golfball size			golfball size E_1			
greater golfball	others > 2.00		golfball			>golfball E_1			
	total no. hailstones			total E_1 ($j\text{-}ft^{-2}$)	2.524		total dented area (in^2)		
	total no. excluding "shot" size			$E_1 \times 10.76 = j\text{-}m^{-2}$	27.158		$\div 1.44$ = % of hailpad		

Summary of hailpad/hailcard:

		from hailpad	operator's hailcard
1.	Apparent wind direction (16 pts.) as indicated by pad (check if not apparent)		☒
2.	Total no. hailstones (excluding "shot" size)		☒
3.	Size (range) of largest hail		
4.	Size (range) of most common hail/% of total no. hailstones		
5.	Approximate spacing of most common hail (inches) = $24/\sqrt{(N+1-2/N)}$		
6.	Estimated damage (%) at operator's location (farm)/crop type	☒	
7.	Impact energy/unit area (joules-meter^{-2})		☒
8.	Size (range) of greatest contributor to impact energy		☒
9.	% contribution to total impact energy		☒
10.	Percent area of pad dented by hail (all sizes)		☒

the calculations of energy done in the original analyses. There is no difference in the basic method of hailpad analysis. However, calculation of the hail energy density from the dent counts by Equations 2.3 and 2.4 led to a value smaller than the value from the original analysis by approximately a factor of 3. This new calibration, as described by Strong and Lozowski (1977), was judged to be more reliable because of the care and thoroughness with which Strong and Lozowski established their calibration formulae. The significance of this finding will be discussed in Chapter 4.

The error from the theoretical uncertainties in the procedure is about 10 percent. The variations in the kinetic energy density for the same hailpad obtained by different analysts indicate that an additional error of up to 15 percent can sometimes be produced by the analysis method (Strong, 1974). The energy density of hailfall determined by a hailpad analysis will, however, be accepted as the "true" value. Hailpads have an operational range of 0 to about $2{,}000 jm^{-2}$. Some damage to grain crops is usually detected at energy densities of $50 jm^{-2}$ or more. Crops are often totally lost at $400 jm^{-2}$ or greater. Above $2{,}000 jm^{-2}$, the hailpad is usually destroyed (Strong, 1974). Storms of this magnitude cause massive damage, not only to crops, but to cars and buildings as well.

Thirty-one hailpads from July 30, 1974; 49 from August 7; 7 from August 15; and 44 from August 18 were analysed. Not all hailpads within the areas of these storms were avail-

able. Many pads were missing or had faulty or inadequate documentation, so that the mean effective spacing was just over one per standard township (93km^2). The pertinent information on all the hailpads used in this study, including the results of both the original and later calibrations, is given in Appendix A. Dent size distributions for all these hailpads were compiled, but they are not tabulated here. The hailpad locations are recorded as the quarter-section of land on which the hailpad was set up. This is a 0.25mi^2 area (about 0.65km^2).

2.3 RADAR

The C-band radar data has undergone considerable processing to reduce it to the form used here. The first stage was an analog-to-digital conversion which transformed the standard PPI (plan-position indicator) display into an array of "bins". Each bin occupied 1.05 kilometers of range and 0.545 degrees of azimuth. The bins covered a range of from 3 to 147 kilometers. The returned power of the radar in each bin was converted into a numerical value as the radar beam scanned elevations from 0° to 21.0° at 1.5° intervals.

The second stage was the recording of the bin values on magnetic tape. Computer programs handled such aspects as placing the bin values on tape and labelling them for azimuth, range and time, indicating changes in antenna elevation and the beginning and end of scan cycles. Other programs handled the calibration of the radar after

analog-to-digital conversion of the received power.

The magnetic tapes containing the radar data were copied and run on the University of Alberta computer, using programs designed especially for this study by Fred McDougall and Michel Delorme. The first program, called PLOT, was activated by a series of land locations which were selected by the operator. The land location description used was the standard code of quarter-section, section, township, range and meridian placement (see Appendix F). PLOT accepted any land location within range of the radar, whether or not it contained a hailpad. The operator also supplied the slope and intercept of the calibration curve and the radar calibration constant for the desired date. The radar calibration constant was the difference, in dB, between the transmitted power and the radar constant, both in dBm. The calibration curve determined the relation between the returned power of the radar echo and the digital value stored on tape. The radar constant corrects for the range of the target.

The program PLOT selected the nearest bin, at all elevations, to each land location. It then surveyed the entire history of the radar echoes represented by the bin set over a time span selected by the operator, after converting the raw bin values to equivalent radar reflectivity in decibels (dBZ). These data were recorded on a

second tape. The program also calculated a general hourly summary of the echo history over each selected land location. An example of the output from PLOT appears in Figure 2.2.

The second program, PLOTPAD, used the tape generated by PLOT to produce a graphic time-height summary of the echoes over land locations selected by the operator. The correct file created by PLOT had to be specified in order to use the desired land locations, and only those locations used in PLOT could be run, since a single run of PLOT opened and closed a single file on the output tape. The result was effectively a radar history of the storm as it passed over the land location in question. Indeed, most of these time-height summaries resembled the thunderstorm cross-sections that appear in meteorology textbooks. Figure 2.3 shows an example of the output from PLOTPAD.

Complete texts of PLOT and PLOTPAD are given in Appendix C. The output of these programs had direct applications in establishing the timing and local severity of the storms. PLOTPAD, in particular, was able to show subtle changes in the structure and development of the storms when continuous grids of land locations were surveyed. The tape output from PLOT was applied to direct calculations of radar-based estimates of hail energy density.

Good radar data was available throughout the afternoon and evening of August 7, 1974 so that all hail-

Figure 2.2: A portion of the output from the program PLOT. The input data described on page 17 appear at the head of the listing. The list of times immediately following the tape-mount lines are the times when the antenna returns to the 0-degree elevation, 0-degree azimuth position. They provide a check on the continuity of the data. Limitations of space prevented showing the complete data summary, which would include hailpad G39. In the complete output listing, sets of 0-degree time markers and data summaries would be printed at hourly intervals through the time period specified by the operator.

```
 INPUT BEGINNING TIME AND ENDING TIME OF SURVEY

16:00:00 18:00:00


INPUT SLOPE,INTERCEPT,AND RADAR CONSTANT

?0.473 -89.95 73.2


INPUT QUARTER,SECTION,TOWNSHIP,RANGE,
MERIDIAN, AND IDENTIFICATION FOR EACH LOCATION.
ne20,41,26,4,h37
sw19,32,25,4,q18
se28,42,25,4,g39

PAD IDENT AZM D RNGE KM      3
Q18          153.     53
H37           14.     42
G39           23.     56
 ENTER TAPE MOUNT#

?4
#003261 9TP *T* SIZE=6144

#*T*: MOUNTED ON T3C2
 PLS ENTER NAME OF FILE TO BE CREATED ON TAPE

?sample1
#$MOUNT 003470 9TP *TAPE* RING=IN POSN=*EOT* VOL=OUTPUT FMT=FB LRECL=212 SIZE=21200
#003470 9TP *TAPE* RING=IN POSN=*EOT* VOL=OUTPUT FMT=FB LRECL=212 SIZE=21200 DSN=sample

#*TAPE*: MOUNTED ON T780
 16:01:28
 16:04:33
 16:08:05
 16:11:37
 16:15:09
 16:18:41
 16:22:12
 16:25:44
 16:29:15
 16:32:47
 16:36:07
 16:39:39
 16:43:11
 16:46:42
 16:50:14
 16:53:46
 16:57:18



SUMARY OF DATA FOR THE LAST PERIOD
NUMBER OF TIMES RADAR REFLECTIVITY WAS IN RANGE OF
PAD IDENT  0-9 10-19 20-29 30-39 40-49 50-59 60-69 70-79 80-89 90-99 DBZ
Q18        209    13    24     9     0     0     0     0     0     0
H37        205     8    15    20     7     0     0     0     0     0
```

Figure 2.3: The output from PLOTPAD for hailpad H37, using the original radar data. The radar record of a single, complete storm is shown. The antenna elevation is listed in degrees at the extreme left, and the corresponding height in kilometers at the extreme right. The bottom line in each frame is the time, in minutes, from the first non-zero echo appearing on the current data tape. Several data tapes may be used to produce a PLOTPAD summary.

h37

TIME-HEIGHT-REFLECTIVITY FOR PAD H37
START TIME=16:29:15 DISTANCE= 42 KM. AZIMUTH= 14. DEG

DEG																				KM.
21.0?	0	0	0	0	0	0	0	0	0	0	0	0	0	0	0	0	0	0	0	0?15.4
19.5?	0	0	0	0	0	0	0	0	0	0	0	0	0	0	0	0	0	0	0	0?14.3
18.0?	0	0	0	0	0	0	0	0	0	0	0	0	0	0	0	0	0	0	0	0?13.2
16.5?	0	0	0	0	0	0	0	0	0	0	0	0	0	0	0	0	0	0	0	0?12.1
15.0?	0	0	0	0	0	0	0	0	0	0	0	0	0	0	0	0	0	0	0	0?11.0
13.5?	0	0	0	0	0	0	0	0	0	0	0	0	0	0	0	0	0	0	0	0? 9.9
12.0?	0	0	0	0	0	0	0	0	0	0	0	0	0	0	0	0	0	0	0	0? 8.8
10.5?	13	0	0	0	24	19	0	17	14	0	0	0	0	0	0	0	0	0	0	0? 7.7
9.0?	12	0	0	0	31	27	23	25	24	29	0	0	0	0	0	0	0	0	0	0? 6.6
7.5?	14	0	0	12	37	31	32	30	0	37	14	11	13	0	0	0	0	0	0	0? 5.5
6.0?	11	22	0	0	32	30	32	36	35	40	14	20	13	11	0	0	12	11	14	14? 4.4
4.5?	16	14	16	0	27	35	32	37	32	35	31	21	13	12	13	12	12	13	14	12? 3.3
3.0?	0	15	23	14	18	33	22	32	23	40	39	20	14	12	13	0	0	0	0	0? 2.2
1.5?	0	0	27	0	15	28	26	35	38	35	44	12	0	0	0	0	0	0	0	0? 1.1
0.0?	0	0	0	0	0	28	25	23	29	31	30	13	0	0	0	0	0	0	0	0? 0.0
TIME	0	3	6	10	13	17	20	24	28	31	34	38	41	45	49	52	56	59	63	66 MIN

TIME-HEIGHT-REFLECTIVITY FOR PAD H37
START TIME=16:29:15 DISTANCE= 42 KM. AZIMUTH= 14. DEG

DEG																				KM.
21.0?	0	0	0	0	0	0	0	0	0	0	0	0	0	0	0	0	0	0	0	0?15.4
19.5?	0	0	0	0	0	0	0	0	0	0	0	0	0	0	0	0	0	0	0	0?14.3
18.0?	0	0	0	0	0	0	0	0	0	0	0	0	0	0	0	0	0	0	0	0?13.2
16.5?	0	0	0	0	0	0	0	0	0	0	0	0	0	0	0	0	0	0	0	0?12.1
15.0?	0	0	0	0	0	0	0	0	0	0	0	0	0	0	0	0	0	0	0	0?11.0
13.5?	0	0	0	0	0	0	0	0	0	0	0	0	0	0	0	0	0	0	0	0? 9.9
12.0?	0	0	0	0	0	0	0	0	0	0	0	0	0	0	0	0	0	0	0	0? 8.8
10.5?	0	0	0	0	0	0	0	0	0	0	0	0	0	0	0	0	0	0	0	0? 7.7
9.0?	0	0	0	0	0	0	0	0	0	0	0	0	0	0	0	0	0	0	0	0? 6.6
7.5?	0	0	0	0	0	0	0	0	0	0	0	0	0	0	0	0	0	0	0	0? 5.5
6.0?	12	12	0	0	0	0	0	0	0	0	0	0	0	0	0	0	0	0	0	0? 4.4
4.5?	12	12	0	0	0	0	0	0	0	0	0	0	0	0	0	0	0	0	0	0? 3.3
3.0?	0	0	0	0	0	0	0	0	0	0	0	0	0	0	0	0	0	0	0	0? 2.2
1.5?	0	0	0	0	0	0	0	0	0	0	0	0	0	0	0	0	0	0	0	0? 1.1
0.0?	0	0	0	0	0	0	0	0	0	0	0	0	0	0	0	0	0	0	0	0? 0.0
TIME	70	73	77	80	84	87	91	95	98	0	0	0	0	0	0	0	0	0	0	0 MIN

INPUT DESIRED PAD IDENTIFICATION OR "STOP"

pads collected from that day had complete radar histories. The radar data from August 18, 1974 was good until 1832 (6:32 p.m.), after which numerous tape and software breakdowns rendered the radar output unusable. Thus, complete radar histories were available for only the eighteen hailpads dented by the storm had finished by 1832 on August 18. Neither July 30 nor August 15 had good radar data, but were selected mainly for their good hailpad data.

The radar data initially was extracted by PLOT using a radar calibration constant of 68.4dB. More recently Humphries (1978) pointed out that this figure did not take into account line losses in the waveguide and a discrepancy between the way a radar system with a linear response to returned power and one with a logarithmic response (the C-band) processes reflectivity data. The combination of these effects adds 4.8dB to the radar calibration constant. Thus all the original radar data was re-analysed using a radar calibration constant of 73.2dB. The significance of this, along with the modifications introduced to the hailpad data, will be examined in the fourth chapter. Figure 2.4 illustrates the output from PLOTPAD over the same hailpad as Figure 2.3, except using the improved radar data.

h37

```
        TIME-HEIGHT-REFLECTIVITY FOR PAD H37
      START TIME=16:29:15  DISTANCE= 42 KM.  AZIMUTH= 14. DEG
DEG                                                                  KM.
21.0?  0  0  0  0  0  0  0  0  0  0  0  0  0  0  0  0  0  0  0  0  0?15.4
19.5?  0  0  0  0  0  0  0  0  0  0  0  0  0  0  0  0  0  0  0  0  0?14.3
18.0?  0  0  0  0  0  0  0  0  0  0  0  0  0  0  0  0  0  0  0  0  0?13.2
16.5?  0  0  0  0  0  0  0  0  0  0  0  0  0  0  0  0  0  0  0  0  0?12.1
15.0?  0  0  0  0  0  0  0  0  0  0  0  0  0  0  0  0  0  0  0  0  0?11.0
13.5?  0  0  0  0  0  0  0  0  0  0  0  0  0  0  0  0  0  0  0  0  0? 9.9
12.0?  0  0  0  0  0  0  0  0  0  0  0  0  0  0  0  0  0  0  0  0  0? 8.8
10.5? 17  0  0  0 29 24  0 22 18  0  0  0  0  0  0  0  0  0  0  0  0? 7.7
 9.0? 16  0  0  0 35 32 27 30 29 34  0  0  0  0  0  0  0  0  0  0  0? 6.6
 7.5? 18  0  0 16 42 36 36 34  0 42 19 16 17  0  0  0  0  0  0  0  0? 5.5
 6.0? 16 26  0  0 37 34 37 41 40 44 18 25 18 16  0  0 16 16 19 18 18? 4.4
 4.5? 21 19 21  0 32 40 37 42 37 40 35 26 18 17 17 16 16 17 18 16? 3.3
 3.0?  0 20 28 18 23 38 26 37 28 45 43 25 18 17 17  0  0  0  0  0  0? 2.2
 1.5?  0  0 32  0 20 33 31 40 43 40 49 17  0  0  0  0  0  0  0  0  0? 1.1
 0.0?  0  0  0  0  0 33 30 28 34 36 34 17  0  0  0  0  0  0  0  0  0? 0.0
      ..... ..................................................................
 TIME  0  3  6 10 13 17 20 24 28 31 34 38 41 45 49 52 56 59 63 66 MIN


        TIME-HEIGHT-REFLECTIVITY FOR PAD H37
      START TIME=16:29:15  DISTANCE= 42 KM.  AZIMUTH= 14. DEG
DEG                                                                  KM.
21.0?  0  0  0  0  0  0  0  0  0  0  0  0  0  0  0  0  0  0  0  0  0?15.4
19.5?  0  0  0  0  0  0  0  0  0  0  0  0  0  0  0  0  0  0  0  0  0?14.3
18.0?  0  0  0  0  0  0  0  0  0  0  0  0  0  0  0  0  0  0  0  0  0?13.2
16.5?  0  0  0  0  0  0  0  0  0  0  0  0  0  0  0  0  0  0  0  0  0?12.1
15.0?  0  0  0  0  0  0  0  0  0  0  0  0  0  0  0  0  0  0  0  0  0?11.0
13.5?  0  0  0  0  0  0  0  0  0  0  0  0  0  0  0  0  0  0  0  0  0? 9.9
12.0?  0  0  0  0  0  0  0  0  0  0  0  0  0  0  0  0  0  0  0  0  0? 8.8
10.5?  0  0  0  0  0  0  0  0  0  0  0  0  0  0  0  0  0  0  0  0  0? 7.7
 9.0?  0  0  0  0  0  0  0  0  0  0  0  0  0  0  0  0  0  0  0  0  0? 6.6
 7.5?  0  0  0  0  0  0  0  0  0  0  0  0  0  0  0  0  0  0  0  0  0? 5.5
 6.0? 16 17  0  0  0  0  0  0  0  0  0  0  0  0  0  0  0  0  0  0  0? 4.4
 4.5? 17 16  0  0  0  0  0  0  0  0  0  0  0  0  0  0  0  0  0  0  0? 3.3
 3.0?  0  0  0  0  0  0  0  0  0  0  0  0  0  0  0  0  0  0  0  0  0? 2.2
 1.5?  0  0  0  0  0  0  0  0  0  0  0  0  0  0  0  0  0  0  0  0  0? 1.1
 0.0?  0  0  0  0  0  0  0  0  0  0  0  0  0  0  0  0  0  0  0  0  0? 0.0
      ..................................................................
 TIME 70 73 77 80 84 87  0  0  0  0  0  0  0  0  0  0  0  0  0  0  0 MIN


INPUT DESIRED PAD IDENTIFICATION OR 'STOP'
```

Figure 2.4: Same as figure 2.3, except using the revised radar data. Note that the echoes are about 5dB higher than in the original radar data.

CHAPTER 3

THEORETICAL BACKGROUND

3.1 THE RADAR REFLECTIVITY-ENERGY DENSITY RELATIONSHIP

In this section a relationship between the radar echo and the downward flux of hailfall kinetic energy is developed. The time-integrated flux of kinetic energy determines the total hailstone energy intercepted by a hailpad during a hailstorm. The influence of hailstone melting between the echo level and the ground is taken into account. Following evaluation in Chapters 4 and 5 problems associated with this method are discussed in Chapter 6.

By using some simplifying assumptions, a formula can be developed that converts the reflectivity factor of a radar echo (in dBZ) to a quantity expressing the downward energy flux density of hail (in joules per square meter per second) illuminated by the radar beam. A derivation of this formula based on studies by Barge (1977), Smith *et al.* (1975), and Ulbrich (1977), follows.

The kinetic energy flux (E) of spherical hailstones passing through a unit horizontal area can be expressed as

$$E = \sum_{\text{volume}} \tfrac{1}{2}mv^2 \cdot v \qquad 3.1$$

The form of Equation 3.1 is based on the kinetic energy formula for each particle having mass m and fall velocity v. "Volume" refers to the unit volume occupied by the hailstones. The kinetic energy flux $\dot{E}$ is therefore equal to the product of the kinetic energy per hailstone and its fall velocity, summed over all hailstones in the unit volume.

Assuming that there are no updrafts or downdrafts hailstones will fall at their terminal velocity inside a storm. Numerous studies have shown that the terminal velocity, v, of a hailstone of diameter D is

$$v = kD^{\frac{1}{2}} \qquad 3.2$$

where k is a parameter that is discussed shortly. The mass, m, per stone is given by

$$m = \tfrac{\pi}{6}\rho_i D^3 \qquad 3.3$$

where ρ_i is the approximate density of ice, $920 kgm^{-3}$. Equation 3.1 becomes

$$\dot{E} = \tfrac{\pi}{12}\rho_i k^3 \sum_{\text{volume}} D^{4.5} \qquad 3.4$$

by substituting Equations 3.2 and 3.3 for m and v. In

practice, Equation 3.4 can be replaced by an integration:

$$\dot{E} = \tfrac{1}{12}\rho_i \pi k^3 \int_{D=0}^{D=D_{MAX}} n(D) D^{4.5} dD \qquad 3.5$$

where $n(D)dD$ is the number of hailstones per unit volume in a diameter interval $(D, D+dD)$. D_{MAX} is the maximum hailstone diameter in the unit volume.

Justification for approximating $n(D)$ in the form of a Marshall-Palmer exponential is given in a study by Smith *et al.* (1975), in which case:

$$n(D) = N_0 \exp(-\Lambda D) \qquad 3.6$$

N_0 and Λ are distribution parameters. N_0 is assumed to be constant for all hailfalls and Λ is assumed to depend on hailfall rate in equivalent depth of liquid water per unit time. In earlier studies by Douglas (1963, 1964), a similar exponential distribution was postulated, except that Λ was held fixed and N_0 left to vary.

Using a Marshall-Palmer distribution allows the assumption that D_{MAX} is very large, so that Equation 3.5 takes the form

$$\dot{E} = \tfrac{1}{12}\rho_i \pi k^3 N_0 \int_{D=0}^{\infty} \exp(-\Lambda D) D^{4.5} dD \qquad 3.7$$

The integral is easily evaluated:

$$\dot{E} = \tfrac{1}{12}\rho_i \pi k^3 N_0 \Gamma(5.5)\Lambda^{-5.5} \qquad 3.8$$

where $\Gamma(x)$ is the complete gamma function. For instance, $\Gamma(5.5)$ has a value of 52.3.

A relationship between Λ, N_0 and Z_e is now required. Z_e, the effective or equivalent reflectivity factor, is the reflectivity factor of an ensemble of Rayleigh-scattering particles that would give the same returned radar beam power as the precipitation particles under observation. The Rayleigh reflectivity factor is given by

$$Z = \int_{D=0}^{\infty} n(D) D^6 dD$$

Hence, for a Marshall-Palmer distribution of particles,

$$Z = \int_0^{\infty} N_0 \exp(-\Lambda D) D^6 dD$$

Integrating this expression yields

$$Z = 720 N_0 \Lambda^{-7} \qquad 3.9$$

If $N_0 = 3\times10^{-4}$ cm^{-4} (Smith *et al.*, 1975), Λ has units of cm^{-1} and Z is in cm^3. The question of converting N_0 into SI units and Z into standard units of mm^{6}m^{-3} will be dealt with shortly.

Smith *et al.* (1975) adjust the right-hand side of Equation 3.9 by a power of 0.95 to obtain the effective reflectivity factor, Z_e, at a 10.6cm radar wavelength.

A calculation, similar to that of Smith *et al.* (1975), showed that at the 5.5cm wavelength, the corresponding power ranged from 0.97 to 0.93 for all hailstone diameters less than 3cm. Thus, the relationship of Smith *et al.* (1975),

$$Z_e = (720 N_0 \Lambda^{-7})^{0.95} \qquad 3.9a$$

was sufficiently accurate for the purpose of this study.

Equation 3.8 for energy flux can now be written in terms of Z_e by using Equation 3.9a to eliminate Λ, the hailfall rate parameter:

$$\dot{E} = \frac{\pi}{12} \rho_i k^3 \Gamma(5.5) N_0 \cdot \frac{1}{(720 N_0)^{\frac{5}{7}}} \cdot Z_e^{0.83} \qquad 3.10$$

To evaluate k (in Equation 3.2) one assumes that the hailstone is falling at terminal velocity, so that its weight equals its drag. Therefore,

$$V_t = \left(\frac{4}{3} \frac{\rho_i}{\rho_a} \frac{g}{C_D} \right)^{\frac{1}{2}} D^{\frac{1}{2}} \qquad 3.11$$

$$= k D^{\frac{1}{2}} \qquad 3.11a$$

where ρ_a is the ambient air density, g is the acceleration due to gravity, and C_D is the drag coefficient. The value of C_D for a smooth sphere with a diameter less than 11cm

is approximately 0.45. For hailstones of average roughness a more realistic value of 0.5 is used. The freezing level in most Alberta hailstorms is near 750mb, corresponding to an air density of $0.95\times10^{-3}kgm^{-3}$. Using these values and the density of ice as previously given, k is found to be $159m^{\frac{1}{2}}sec^{-1}$. The freezing level is a good typical level for radar observations used in this study. In Alberta a typical ground level k based on a pressure of 900mb and a temperature of 20°C would be $133m^{\frac{1}{2}}sec^{-1}$. This was confirmed by photographic studies by Beattie (1975).

When N_0 is expressed as $3\times10^{4}m^{-4}$, the constants and parameters in Equation 3.10 can be evaluated, so that

$$\dot{E} = 2.625\times10^{9}Z_e^{\,0.83} \qquad 3.12$$

where $\dot{E}$ is in units of $Jm^{-2}sec^{-1}$. As Equation 3.12 is written, Z_e has units of m^3, or m^6m^{-3}. To adjust Equation 3.12 so that Z_e has the usual units of mm^6m^{-3}, the numerical coefficient is multiplied by a factor of 1.30×10^{-15}, leaving

$$\dot{E} = 3.40\times10^{-6}Z_e^{\,0.83} \qquad 3.13$$

or

$$\dot{E} = 3.40\times10^{-6}\times10^{\frac{Z_e}{12.1}} \qquad 3.14$$

where the observed effective reflectivity factor, Z_e, is

in dBZ (Z_e[dBZ] = 10 logZ_e[mm^{6}m^{-3}]). Z_e will be given in units of dBZ from here onwards, unless specified otherwise. Equation 3.14 is valid in a hail cloud but it must be adjusted for melting and air density changes if $\dot{E}$ is to be integrated as ground energy flux, while Z_e is observed near the freezing level.

3.2 THE EFFECT OF MELTING ON KINETIC ENERGY FLUX

Equation 3.14 assumes that no melting occurs in the hail's descent from the freezing level to the ground. However, the diameters of hailstones, and consequently the kinetic energy flux, can change appreciably from melting. To determine the effect, a simplified model of hail melting was developed.

Mason (1971), based on studies by Ludlam (1958) and Macklin (1963), gives the relationships between the radius of a hailstone at the freezing level and its radius upon reaching the ground after melting as

$$R_0^{\frac{7}{4}} - R_g^{\frac{7}{4}} = 2.23\times10^{-3} b \int_0^{Z_0} Pr^{\frac{1}{3}} K \Delta T \rho_a^{\frac{3}{4}} \mu^{-\frac{1}{2}} dz \qquad 3.15$$

where R_0 and R_g are the radii, in centimeters, of a hailstone at the freezing level and at the ground, respectively. b is a shape factor, which for spheres is 0.658 (Macklin, 1963). Z_0 is the height above ground of the freezing level in kilometers. P_r is the Prandtl number,

which has a value of 0.71 for air. K is the thermal conductivity of air, in $Jm^{-1}sec^{-1}°K^{-1}$. In the range of temperatures considered here, K is approximately 2.4×10^{-2}. ΔT is the air temperature in °C (a function of Z_c ρ_a is the ambient air density in g m^{-3}, and μ is the dynamic viscosity of air, which is approximately 1.75×10^{-4} g $cm^{-1}sec^{-1}$ for the range of temperatures assumed in this model. To a good approximation, the right-hand side of Equation 3.15 is proportional to the surface temperature, in °C, and the square of the depth of the melting layer. Conditions typical of Alberta hailstorms were taken to be ρ_a = 1.0kg m^{-3}, ΔT = 18°C at the surface with a constant lapse rate from the surface to the freezing level, and z_0 = 3km. Using these values, Equation 3.15 becomes

$$R_0^{\frac{7}{4}} - R_G^{\frac{7}{4}} = 0.242 \qquad 3.16$$

In terms of the initial and final diameters, D_0 and D_G, in centimeters, Equation 3.16 becomes

$$D_0^{\frac{7}{4}} - D_G^{\frac{7}{4}} = 0.814 \qquad 3.16a$$

Equation 3.16a assumes that the hail is a sphere falling in still, clear air. The actual melting may be different from what Equation 3.16a implies, when the falling stone is caught in an updraft or downdraft, but this effect is difficult to assess.

Re-writing Equation 3.16a gives

$$D_G = (D_0^{\frac{7}{4}} - 0.814)^{\frac{4}{7}} \qquad 3.17$$

The kinetic energy of a hailstone of diameter D is:

$$E = \frac{\pi}{12}\rho_i k^2 D^4 \qquad 3.18$$

If k (the air density dependent terminal velocity coefficient), ρ_i and D are in cgs units, substituting Equation 3.17 into Equation 3.18 yields

$$E = \frac{\pi}{12}\rho_i k^2_G (D_0^{\frac{7}{4}} - 0.814)^{\frac{16}{7}} \qquad 3.19$$

which is the ground level kinetic energy in ergs, of the hailstone in terms of its freezing level diameter, D_0. k takes on its ground level value, k_G, in Equation 3.19. The problem of the change in k from the freezing level to the ground as it influences radar and hailpad estimates of $\dot{E}$ will be treated in Chapter 4. The velocity of the melted hailstone at the ground, using Equation 3.2 and 3.17 is

$$v = k_G(D_0^{\frac{7}{4}} - 0.814)^{\frac{2}{7}} \qquad \text{--c.g.s. units--} \qquad 3.20$$

The kinetic energy of the hailstone at cloud level is given by Equation 3.18 when $D = D_0$. An ensemble of hailstones is assumed to have a Marshall-Palmer size distribution,

$N_0 \exp(-\Lambda D_0)$, before melting. N_0 here has units of cm^{-4}. The kinetic energy flux of the ensemble at the ground is the product of:

a. the number of unmelted hailstones per unit volume as a function of diameter (the Marshall-Palmer formula);

b. the initial kinetic energy per stone,

$$\frac{\pi}{12}\rho_i k_0^2 D_0^4;$$

c. the factor by which the energy per stone changes due to melting (the ratio of Equation 3.19 to Equation 3.18 in terms of D_0),

$$\frac{k_G^2}{K_0^2} \cdot \frac{(D_0^{\frac{7}{4}} - .814)^{\frac{16}{7}}}{D_0^4}; \text{ and}$$

d. the velocity at the ground per stone,

$$k_G(D_0^{\frac{7}{4}} - 0.814)^{\frac{2}{7}},$$

integrated over all diameters of hailstones that reach the ground. Thus,

$$\dot{E}_{ground} = \int_{D_{0MIN}}^{D_{0MAX}} N_0 \exp(-\Lambda D_0) \cdot \frac{\pi}{12}\rho_i k_0^2 D_0^4 \frac{k_G^2}{k_0^2} \frac{(D_0^{\frac{7}{4}} - 0.814)^{\frac{16}{7}}}{D_0^4} \cdot$$

$$k_G(D_0^{\frac{7}{4}} - 0.814)^{\frac{2}{7}} dD_0,$$

$$\dot{E}_{ground} = \frac{\pi}{12}\rho_i k_G^3 N_0 \int_{D_{0MIN}}^{D_{0MAX}} \exp(-\Lambda D_0)(D_0^{\frac{7}{4}} - 0.814)^{\frac{18}{7}} dD_0 \qquad 3.21$$

$\dot{E}_{ground}$ is in ergs $cm^{-2}sec^{-1}$, and $D_{0\,MIN}$ is the diameter of the smallest hailstone which just reaches the ground after melting. The energy flux of the hail before melting is

$$\dot{E}_{cloud} = \frac{\pi}{12}\rho_i k_0^3 N_0 \int_0^{D_{0MAX}} \exp(-\Lambda D_0) D_0^{4.5} dD_0 \qquad 3.22$$

The ratio of Equation 3.21 to 3.22 will therefore give the ground energy flux as a fraction of the cloud energy flux (at the freezing level). D_{0MAX} is set at 11cm to avoid problems with supercritical fall regimes. Fortunately for this model, hailstones with diameters greater than 11cm are extremely rare. From Equation 3.17, D_{0MIN} is found to be 0.90cm. Equations 3.21 and 3.22 were evaluated by Simpson's Rule to obtain the ratio of the ground energy to the cloud energy for values of Λ from 7.5 to $4.0cm^{-1}$. The reasonableness of this range of Λ was checked by the formula

$$W_i = \frac{\pi N_0 \rho_i}{\Lambda^4} \qquad 3.23$$

which relates W_i, the water mass concentration of hail in the cloud, to Λ when a Marshall-Palmer hail size distribution is assumed. Here W_i and ρ_i are in the same units, gm^{-3}, and $N_0 = 3\times10^4 m^{-4}$. When $\Lambda = 4.0cm^{-1}$, W_i is $3.31gm^{-3}$, which is close to the highest water mass concentration of

hail believed to exist in hail-producing clouds (Charlton, 1978). At a Λ of 7.5cm^{-1}, W_i = 0.40gm^{-3}. The ratio of Equations 3.21 and 3.22 is plotted, ignoring variations in k, as a dotted line in Figure 3.1. The correct form of Equation 2.14 would include this ratio as a coefficient.

A true verification of this melting model would require direct measurements of the vertical hail energy flux at the freezing level, and comparing them to the energy flux recorded by hailpads on the ground immediately below. This procedure was impractical.

A partial check with hailpads on the validity of the model was done by translating the hailstone diameters at the ground into the corresponding diameters at the freezing level by Equation 3.16a, calculating the kinetic energy at each diameter by Equation 3.18, and summing over the size spectrum observed from the hailpad, making sure that the resulting quantity was in the appropriate units (SI). The hailstone diameters at the ground were determined by the calibration formulae, Equations 2.3 and 2.4, of Strong and Lozowski (1977). The contribution to the total kinetic energy flux at the freezing level by the hailstones that melted completely before reaching the ground was

$$\frac{\pi}{12}\rho_i k^3 N_0 \int_0^{0.90} \exp(-\Lambda D_0) D_0^{4.5}\, dD_0$$

This quantity was found by rough calculation to be negligible for all hailpads used in this procedure. The kinetic

energy flux was obtained by dividing the total kinetic energy calculated above by the duration of the hailfall, in seconds, reported by the farmer operating the hailpad. A total of 53 hailpads from August 7 and 18 carried hailfall duration data and had a flux at the ground high enough to be usefully plotted. Such estimates of hail energy flux are very crude because the hailfall durations are given roughly to the nearest minute. The ratios of these estimates of ground flux to freezing-level flux are plotted as points in Figure 3.1. An estimated best fit to these points is indicated by the dashed line. Figure 3.1 shows that the melting model correctly predicts the trend (with increasing kinetic energy flux) and order of magnitude of the ratio of the flux at the ground to the flux at the freezing level, assuming that the calculated fluxes at the freezing level are close to the real fluxes. However, Figure 3.1 indicates that the model may overestimate the effect of melting on hail kinetic energy flux. Both the model and the estimates show that the fraction of the kinetic energy flux retained by the hail has increased with increasing energy flux at the ground.

A comparison of hailpad kinetic energy densities with the corresponding estimated kinetic energy densities at the freezing level was done by following the procedure used for the kinetic energy fluxes, except without dividing through by the hailfall durations. This method was applied to all the hailpads from August 7 and 18 that recorded

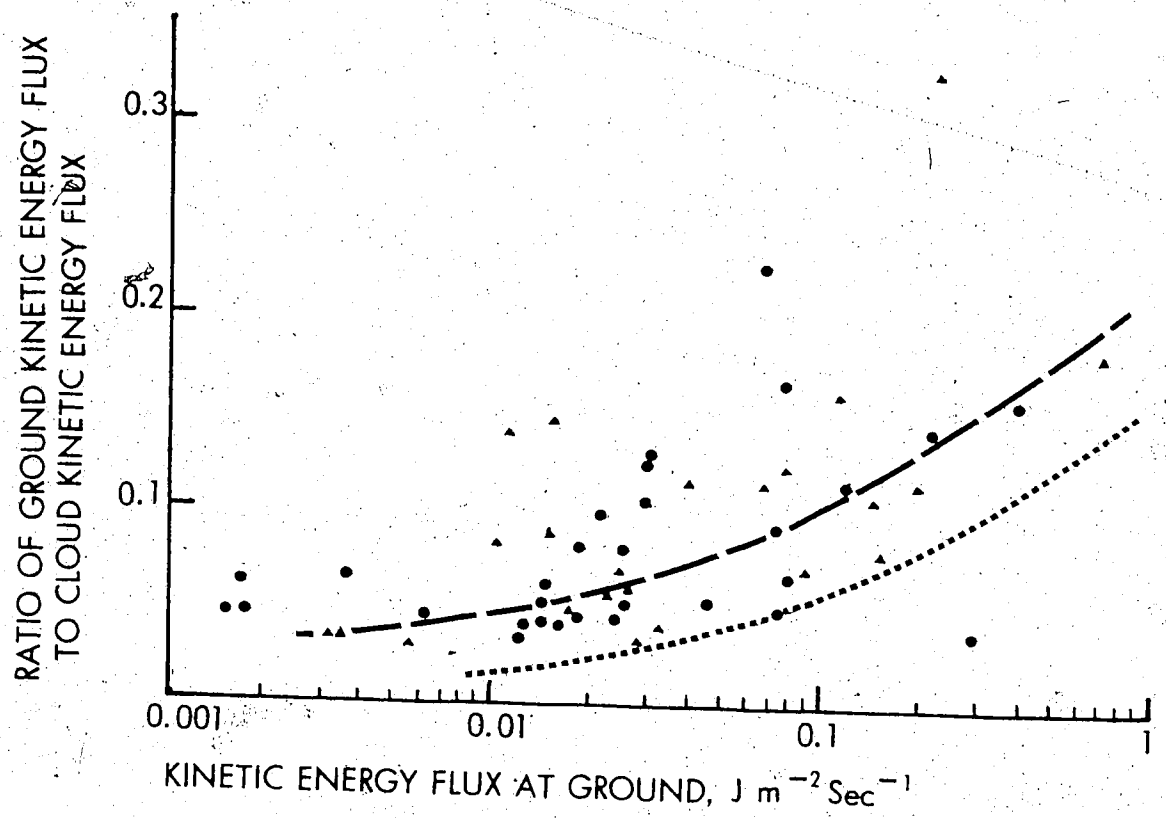

Figure 3.1: The ratio of the ground-level kinetic energy flux of hail to cloud (freezing level) kinetic energy flux for 53 hailpads from August 7 (circles) and August 18, 1974 (triangles). This ratio is plotted on the vertical scale against ground-level kinetic energy flux in $Jm^{-2}sec^{-1}$. Upper curve is the best fit, drawn by eye, to the hailpads. Lower curve gives the theoretical ratio for the given ground-level energy flux.

measurable hailfalls. These pads are plotted in Figure 3.2, except for those with energy densities too low to appear on the graph. Again, a trend toward higher retention of kinetic energy at high overall energy densitites is evident in Figure 3.2. An estimated best-fit line to the plotted points is drawn in. The ratio of ground to freezing level energy density reached 0.2 at a ground-level energy density of about $80 Jm^{-2}$. The value of 0.2 was chosen as the melting coefficient to be added to Equation 3.14. It should again be emphasized that the effect of the slowing-down of the hailstones in the denser air near the surface was not taken into account (i.e., "k" variations) in producing Figure 3.2.

The choice of 0.2 as the melting factor was somewhat arbitrary since the effect is markedly non-linear and depends strongly on the freezing-level (or ground-level) kinetic energy flux of hail. The value was chosen because it is reasonably accurate at high ground-level energy densities, which is the main situation of interest in this study. Thus, Equation 3.14 becomes

$$\dot{E} = 0.20 \times 3.40 \times 10^{-6} \times 10^{\frac{Z_e}{12.1}} \qquad 3.24$$

or

$$\dot{E} = 6.80 \times 10^{-7} \times 10^{\frac{Z_e}{12.1}} \qquad 3.25$$

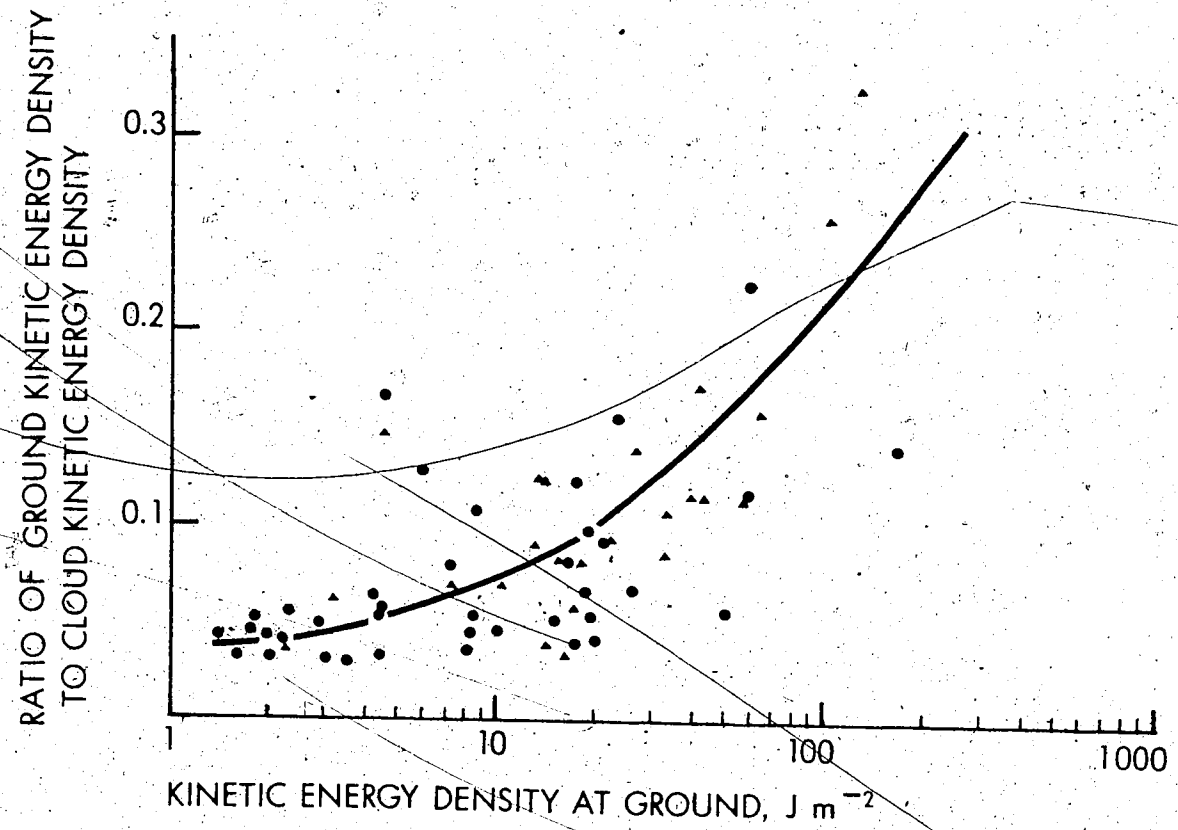

Figure 3.2: The ratio of the ground-level kinetic energy density of hail to cloud (freezing level) kinetic energy density for 62 hailpads from August 7 (circles) and August 18, 1974 (triangles). The ratio is plotted on the vertical scale against the ground-level kinetic energy density in Jm^{-2}. The curve is the estimated best fit to the hailpad points.

with $\dot{E}$ in $Jm^{-2}sec^{-1}$ and Z_e in dBZ. It will be shown in Chapter 4 that the adjustment for the change in air density from the freezing level to the ground is a simple multiplicative constant.

CHAPTER 4

METHOD OF RADAR-HAILPAD INTERPOLATION AND PRELIMINARY RESULTS

4.1 DEVELOPMENT OF OPERATIONAL FORMULA

Equation 3.25 will be used to develop an operational procedure that interpolates the energy density of hail at points without hailpads when radar and hailpads are available. The procedure is based on a time integration of Equation 3.25, but three important considerations entered in the choice of integration method.

The first is that not all altitudes in the storm cloud will provide radar information that correlates equally well with the hailfall at the ground. At very high altitudes, the hail is in the process of formation, giving it a size spectrum that may be different from the one it will have by the time it reaches the ground. The hailstone's surface will furthermore be dry and cold, rather than wet and melting. Also, because hail is carried horizontally to some extent by wind, hail at high altitudes is less likely to fall on the land location intended as the correction area. For these reasons, it will have different

radar reflectivity properties from those it should have at lower levels. On the other hand, radar information from very close to the ground will be affected by phenomena such as ground clutter. Time integration of Equation 3.25 was therefore carried out only for echoes at heights between 1.5 and 4 kilometers.

The radar executes a complete scan cycle every 211 seconds, making a complete revolution approximately every 14 seconds. The elevation starts at 0 degrees and increases 1.5 degrees with every revolution up to 21 degrees, and returning to 0 degrees to begin the next scan cycle. From one to five echoes per scan cycle are available at altitudes between 1.5 and 4 kilometers, depending on the range of the land location. The hail corresponding to these echoes was assumed to be representative of the hail that fell during the entire $3\frac{1}{2}$ minute scan cycle. All echoes within the interval were weighted equally, in the absence of any other information on their representativeness of hailfall at the ground (see below for details).

The second consideration is that it is desirable to eliminate the contribution of rain to the echoes. Rain contributes most of the returned power in echoes of less than about 35 dBZ (Marge, 1972, 1977). For this reason a threshold equivalent reflectivity was assumed such that echoes less than the threshold did not enter the calculation of the hail energy density. Thresholds of 30, 35, 40 and 45 dBZ were tested as a crude method of eliminating the

rain contribution.

Finally, falling hailstones will lose kinetic energy as a result of being slowed down by the increasing air density. Recalling Equation 3.18, the kinetic energy of a hailstone of a given diameter is proportional to k^2. Thus we have, for any hailstone,

$$\frac{E_{ground}}{E_{cloud}} \alpha \frac{k_G^2}{k_0^2} \qquad 4.1$$

E_R, which is the total kinetic energy density of the hail at the freezing level, estimated by radar, is given by

$$E_R = \sum_{i=1}^{N} \dot{E}_i \Delta t \qquad 4.2$$

when N observations are taken, Δt is the mean time interval between in-cloud radar observations and $\dot{E}_i$ is the energy flux of the hail. Since the kinetic energy density of all hailstones is altered by the factor (k_G^2/k_0^2), the total energy density at the ground, estimated by radar is

$$E_R = \frac{k_G^2}{k_0^2} \sum_{i=1}^{N} \dot{E}_i \Delta t \qquad 4.3$$

apart from any melting effect. It should be noted that energy flux density varies as k^3 between cloud and ground (Equations 3.2 and 3.22) but energy density varies as k^2 because the time of hailfall is different between cloud

and ground. Since k near the freezing level is $159 m^{\frac{1}{2}} sec^{-1}$, and at the ground is about $133 m^{\frac{1}{2}} sec^{-1}$, the formula becomes

$$E_R = \frac{133^2}{159^2} \sum_{i=1}^{N} \dot{E}_i \Delta t \qquad 4.4$$

or

$$E_R = 0.70 \sum_{i=1}^{N} \dot{E}_i \Delta t \qquad 4.5$$

The complete formula, based on Equation 3.25 and including the melting effect, now becomes

$$E_R = 0.70 \times 6.80 \times 10^{-7} \frac{T_s}{N_{SCAN}} \sum_{t=0}^{t=t_e} 10^{\frac{Z_e}{12.1}}$$

or

$$E_R = 4.76 \times 10^{-7} \frac{T_s}{N_{SCAN}} \sum_{t=0}^{t=t_e} 10^{\frac{Z_e}{12.1}} \qquad 4.6$$

where $[0, t_e]$ is the time interval in the radar record during which echoes above the threshold value occurred. N_{SCAN} is the number of scans appearing between 1.5 and 4.0 kilometers. T_s is the time, in seconds, it takes the radar to undergo a complete scan cycle, which in the case of the Alberta Hail Project C-band is 211 seconds. Z_e is the strength of any echo, in dBZ, within the height interval and equal to or greater than the threshold value. E_R has units of joule m^{-2}. The quantity E_R will from now onward

be referred to as the "raw radar estimate" of hailfall kinetic energy.

A first attempt at using Equation 4.6 was made with the original radar data (with calibration constant 68.4dB), and comparing the results with the hailpads using the older calibration scheme. The use of Equation 4.6 is illustrated in Figure 4.1(a). This is the sample of PLOTPAD made with the original data, representing the echo history over hailpad H37 of August 7, 1974. Here, there are 2 scans between 1.5 and 4 kilometers; hence $N_{SCAN} = 2$. A program called PADEN, similar to PLOTPAD, was used to calculate E_R. Using thresholds of various values, E_R worked out to the following:

Threshold (dBZ)	E_R (J m^{-2})
45	0.0
40	0.099
35	0.321
30	0.437

The following sample calculation shows how the values listed above were derived:

In Figure 4.1(a) at the 35dBZ threshold, the following echoes were found to be within the required height interval:

35, 37, 35, 40, 39 dBZ (indicated by boxes)

$N_{SCAN} = 2$; $T_s = 211$ sec.

$$E_R = 4.76 \times 10^{-7} \times \frac{211}{2}\left[10^{\frac{35}{12.1}} + 10^{\frac{37}{12.1}} + 10^{\frac{35}{12.1}} + 10^{\frac{40}{12.1}} + 10^{\frac{39}{12.1}}\right] =$$

Figure 4.1a,b: This is the same PLOTPAD output shown in Figures 2.3 and 2.4 for (a) the original radar data and (b) the revised radar data, except showing the echoes which contribute to the calculation of equation 4.6. In both (a) and (b), the echoes are outlined by boxes. The vertical interval in which echoes can contribute to Equation 4.6 is shown by the bracket at the extreme right of each frame. In these examples, two scans fall between heights of 1.5 and 4.0 kilometers, so that N_{SCAN} equals 2. The threshold reflectivity is 35dBZ.

h37

TIME-HEIGHT-REFLECTIVITY FOR PAD H37
START TIME=16:29:15 DISTANCE= 42 KM. AZIMUTH= 14. DEG

DEG																				KM.
21.0?	0	0	0	0	0	0	0	0	0	0	0	0	0	0	0	0	0	0	0	0?15.4
19.5?	0	0	0	0	0	0	0	0	0	0	0	0	0	0	0	0	0	0	0	0?14.3
18.0?	0	0	0	0	0	0	0	0	0	0	0	0	0	0	0	0	0	0	0	0?13.2
16.5?	0	0	0	0	0	0	0	0	0	0	0	0	0	0	0	0	0	0	0	0?12.1
15.0?	0	0	0	0	0	0	0	0	0	0	0	0	0	0	0	0	0	0	0	0?11.0
13.5?	0	0	0	0	0	0	0	0	0	0	0	0	0	0	0	0	0	0	0	0? 9.9
12.0?	0	0	0	0	0	0	0	0	0	0	0	0	0	0	0	0	0	0	0	0? 8.8
10.5?	13	0	0	0	24	19	0	17	14	0	0	0	0	0	0	0	0	0	0	0? 7.7
9.0?	12	0	0	0	31	27	23	25	24	29	0	0	0	0	0	0	0	0	0	0? 6.6
7.5?	14	0	0	12	37	31	32	30	0	37	14	11	13	0	0	0	0	0	0	0? 5.5
6.0?	11	22	0	0	32	30	32	36	35	40	14	20	13	11	0	0	12	11	14	14? 4.4
4.5?	16	14	16	0	27	35	32	37	32	35	31	21	13	12	13	12	12	13	14	12? 3.3
3.0?	0	15	23	14	18	33	22	32	23	40	39	20	14	12	13	0	0	0	0	0? 2.2
1.5?	0	0	27	0	15	28	26	35	38	35	44	12	0	0	0	0	0	0	0	0? 1.1
0.0?	0	0	0	0	0	28	25	23	29	31	30	13	0	0	0	0	0	0	0	0? 0.0
TIME	0	3	6	10	13	17	20	24	28	31	34	38	41	45	49	52	56	59	63	66 MIN

TIME-HEIGHT-REFLECTIVITY FOR PAD H37
START TIME=16:29:15 DISTANCE= 42 KM. AZIMUTH= 14. DEG

DEG																				KM.
21.0?	0	0	0	0	0	0	0	0	0	0	0	0	0	0	0	0	0	0	0	0?15.4
19.5?	0	0	0	0	0	0	0	0	0	0	0	0	0	0	0	0	0	0	0	0?14.3
18.0?	0	0	0	0	0	0	0	0	0	0	0	0	0	0	0	0	0	0	0	0?13.2
16.5?	0	0	0	0	0	0	0	0	0	0	0	0	0	0	0	0	0	0	0	0?12.1
15.0?	0	0	0	0	0	0	0	0	0	0	0	0	0	0	0	0	0	0	0	0?11.0
13.5?	0	0	0	0	0	0	0	0	0	0	0	0	0	0	0	0	0	0	0	0? 9.9
12.0?	0	0	0	0	0	0	0	0	0	0	0	0	0	0	0	0	0	0	0	0? 8.8
10.5?	0	0	0	0	0	0	0	0	0	0	0	0	0	0	0	0	0	0	0	0? 7.7
9.0?	0	0	0	0	0	0	0	0	0	0	0	0	0	0	0	0	0	0	0	0? 6.6
7.5?	0	0	0	0	0	0	0	0	0	0	0	0	0	0	0	0	0	0	0	0? 5.5
6.0?	12	12	0	0	0	0	0	0	0	0	0	0	0	0	0	0	0	0	0	0? 4.4
4.5?	12	12	0	0	0	0	0	0	0	0	0	0	0	0	0	0	0	0	0	0? 3.3
3.0?	0	0	0	0	0	0	0	0	0	0	0	0	0	0	0	0	0	0	0	0? 2.2
1.5?	0	0	0	0	0	0	0	0	0	0	0	0	0	0	0	0	0	0	0	0? 1.1
0.0?	0	0	0	0	0	0	0	0	0	0	0	0	0	0	0	0	0	0	0	0? 0.0
TIME	70	73	77	80	84	87	91	95	98	0	0	0	0	0	0	0	0	0	0	0 MIN

INPUT DESIRED PAD IDENTIFICATION OR "STOP"

Figure 4.1a

h37

TIME-HEIGHT-REFLECTIVITY FOR PAD H37
START TIME=16:29:15 DISTANCE= 42 KM. AZIMUTH= 14. DEG

DEG																				KM.
21.0?	0	0	0	0	0	0	0	0	0	0	0	0	0	0	0	0	0	0	0	0?15.4
19.5?	0	0	0	0	0	0	0	0	0	0	0	0	0	0	0	0	0	0	0	0?14.3
18.0?	0	0	0	0	0	0	0	0	0	0	0	0	0	0	0	0	0	0	0	0?13.2
16.5?	0	0	0	0	0	0	0	0	0	0	0	0	0	0	0	0	0	0	0	0?12.1
15.0?	0	0	0	0	0	0	0	0	0	0	0	0	0	0	0	0	0	0	0	0?11.0
13.5?	0	0	0	0	0	0	0	0	0	0	0	0	0	0	0	0	0	0	0	0? 9.9
12.0?	0	0	0	0	0	0	0	0	0	0	0	0	0	0	0	0	0	0	0	0? 8.8
10.5?	17	0	0	0	29	24	0	22	18	0	0	0	0	0	0	0	0	0	0	0? 7.7
9.0?	16	0	0	0	35	32	27	30	29	34	0	0	0	0	0	0	0	0	0	0? 6.6
7.5?	18	0	0	16	42	36	36	34	0	42	19	16	17	0	0	0	0	0	0	0? 5.5
6.0?	16	26	0	0	37	34	37	41	40	44	18	25	18	16	0	0	16	16	19	18? 4.4
4.5?	21	19	21	0	32	40	37	42	37	40	35	26	18	17	17	16	16	17	18	16? 3.3
3.0?	0	20	28	18	23	38	26	37	28	45	43	25	18	17	17	0	0	0	0	0? 2.2
1.5?	0	0	32	0	20	33	31	40	43	40	49	17	0	0	0	0	0	0	0	0? 1.1
0.0?	0	0	0	0	0	33	30	28	34	36	34	17	0	0	0	0	0	0	0	0? 0.0
TIME	0	3	6	10	13	17	20	24	28	31	34	38	41	45	49	52	56	59	63	66 MIN

TIME-HEIGHT-REFLECTIVITY FOR PAD H37
START TIME=16:29:15 DISTANCE= 42 KM. AZIMUTH= 14. DEG

DEG																				KM.
21.0?	0	0	0	0	0	0	0	0	0	0	0	0	0	0	0	0	0	0	0	0?15.4
19.5?	0	0	0	0	0	0	0	0	0	0	0	0	0	0	0	0	0	0	0	0?14.3
18.0?	0	0	0	0	0	0	0	0	0	0	0	0	0	0	0	0	0	0	0	0?13.2
16.5?	0	0	0	0	0	0	0	0	0	0	0	0	0	0	0	0	0	0	0	0?12.1
15.0?	0	0	0	0	0	0	0	0	0	0	0	0	0	0	0	0	0	0	0	0?11.0
13.5?	0	0	0	0	0	0	0	0	0	0	0	0	0	0	0	0	0	0	0	0? 9.9
12.0?	0	0	0	0	0	0	0	0	0	0	0	0	0	0	0	0	0	0	0	0? 8.8
10.5?	0	0	0	0	0	0	0	0	0	0	0	0	0	0	0	0	0	0	0	0? 7.7
9.0?	0	0	0	0	0	0	0	0	0	0	0	0	0	0	0	0	0	0	0	0? 6.6
7.5?	0	0	0	0	0	0	0	0	0	0	0	0	0	0	0	0	0	0	0	0? 5.5
6.0?	16	17	0	0	0	0	0	0	0	0	0	0	0	0	0	0	0	0	0	0? 4.4
4.5?	17	16	0	0	0	0	0	0	0	0	0	0	0	0	0	0	0	0	0	0? 3.3
3.0?	0	0	0	0	0	0	0	0	0	0	0	0	0	0	0	0	0	0	0	0? 2.2
1.5?	0	0	0	0	0	0	0	0	0	0	0	0	0	0	0	0	0	0	0	0? 1.1
0.0?	0	0	0	0	0	0	0	0	0	0	0	0	0	0	0	0	0	0	0	0? 0.0
TIME	70	73	77	80	84	87	0	0	0	0	0	0	0	0	0	0	0	0	0	0 MIN

INPUT DESIRED PAD IDENTIFICATION OR "STOP"

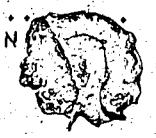

Figure 4.1b

$$5.00 \times 10^{-5}[781 + 1142 + 781 + 2022 + 1671]$$

$$= 0.321 \text{ J m}^{-2}.$$

The hailpad value of energy density, according to the original analysis, was 27.3 Jm^{-2}. The raw radar estimate by the above calculation is about 85 times smaller than the hailpad value. A discrepancy of this size occurred systematically throughout the radar and hailpad data. This prompted a re-evaluation of all the data and led to the revisions described in Chapter 2.

Figure 4.1(b) illustrates the PLOTPAD output based on the revised radar data (calibration constant 73.2dB) for hailpad H37. Repeating the calculation, E_R is now found to be the following:

Threshold (dBZ)	$E_R(Jm^{-2})$
45	0.281
40	0.847
35	1.143
30	1.166

The sample calculation is again illustrated for the 35 dBZ threshold:

Echoes at or above 35dBZ (see Figure 4.1b)

38, 40, 37, 37, 42, 37, 45, 40, 43, 35 dBZ

N_{SCAN} = 2; T_s = .211 sec

$$E_R = 5.00 \times 10^{-5}\left[10^{\frac{38}{12.1}} + 10^{\frac{40}{12.1}} + 10^{\frac{37}{12.1}} + 10^{\frac{37}{12.1}} + 10^{\frac{42}{12.1}} + 10^{\frac{37}{12.1}} + 10^{\frac{45}{12.1}} + 10^{\frac{40}{12.1}} + 10^{\frac{43}{12.1}} + 10^{\frac{35}{12.1}}\right]$$

$$= 1.143 \times \text{Jm}^{-2}$$

$$\simeq 1.1 \text{ Jm}^{-2}$$

The corresponding hailpad energy density, using the revised calibration of Strong and Mozowski (1977), is 8.7 Jm^{-2}. The raw radar estimate is too small by a factor of 8. In general, the radar-based calculation still underestimates the hailpad energy density. Radar beam attenuation would account for this effect, and will be discussed in a later chapter.

The radar estimates, using a 30dBZ threshold, and the corresponding hailpad values of kinetic energy density were plotted for August 7 and 18, using the revised data [Figures 4.2(a) and 4.2(b)]. If the radar estimation method is valid, some sort of linear relationship between the radar estimate and the corresponding hailpad value would be expected. The desired relationship does appear in both Figures 4.2(a) and 4.2(b), although in the case of August 7, the relationship is obscured to some extent by the strong scatter. An important feature of the August 7 data is the large number of zero or very small raw radar estimates associated with appreciable hailfalls. The relationship between the raw radar estimate and the hailpad value of energy density is much clearer in the case of August 18.

Figure 4.2a, b: Raw radar estimates of hail energy density are plotted against the energy densities as determined by the corresponding hailpad analyses for (a) August 7 and (b) August 18, 1974. The raw radar estimate (E_R, in Jm^{-2}) is given along the horizontal scale, while the hailpad value (E_R, in Jm^{-2}) is given along the vertical scale. The least-squares fitting line for E_H and E_R is shown in both cases and the values of "a" and "b" in $E = aE_R + b$, determined by the lines, are also indicated. Note that the horizontal scale has been expanded for greater clarity.

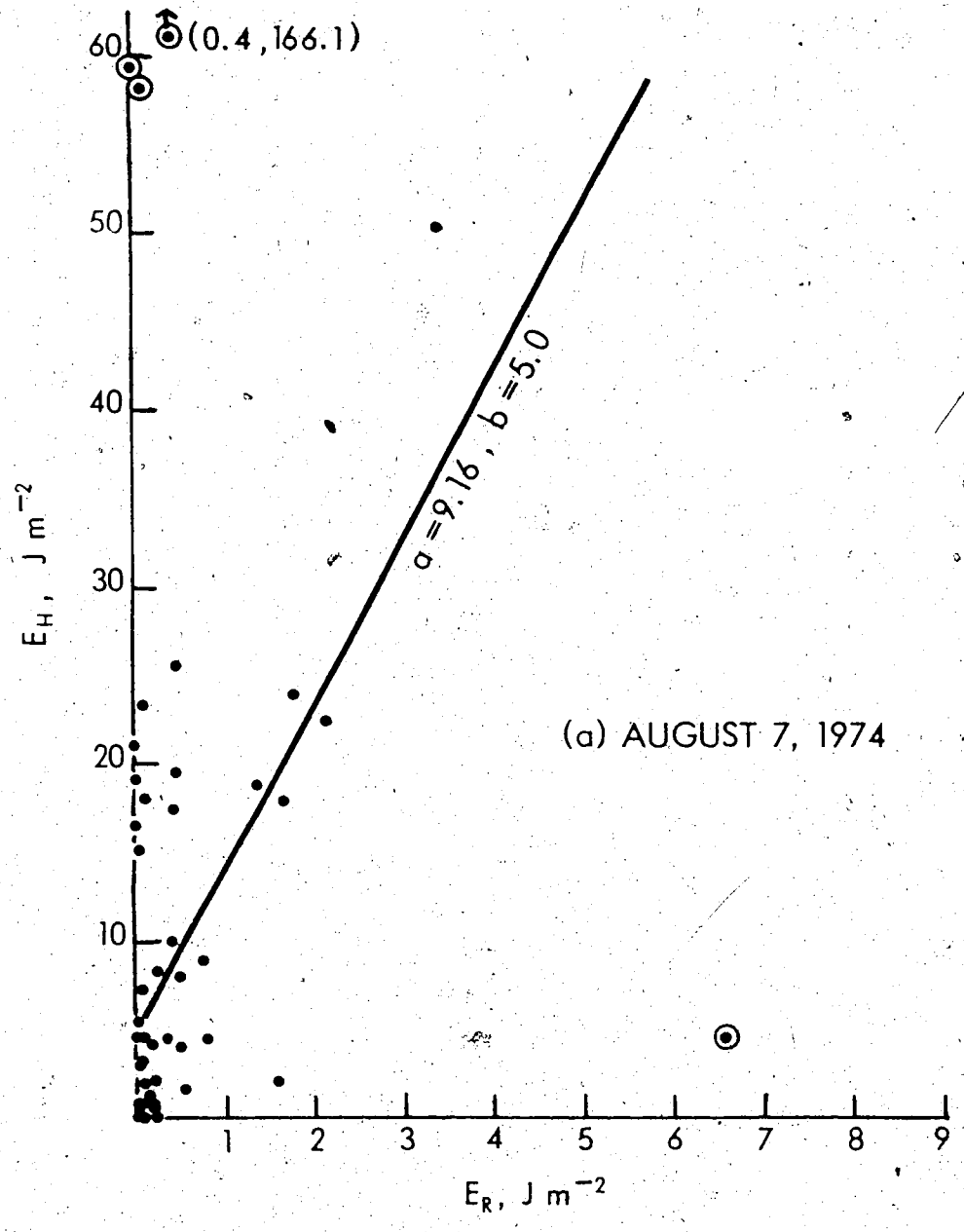
(0.4, 166.1)
60
50
40
30
20
10
E_H, J m^{-2}
a=9.16, b=5.0
(a) AUGUST 7, 1974
1
2
3
4
5
6
7
8
9
E_R, J m^{-2}

Figure 4.2a

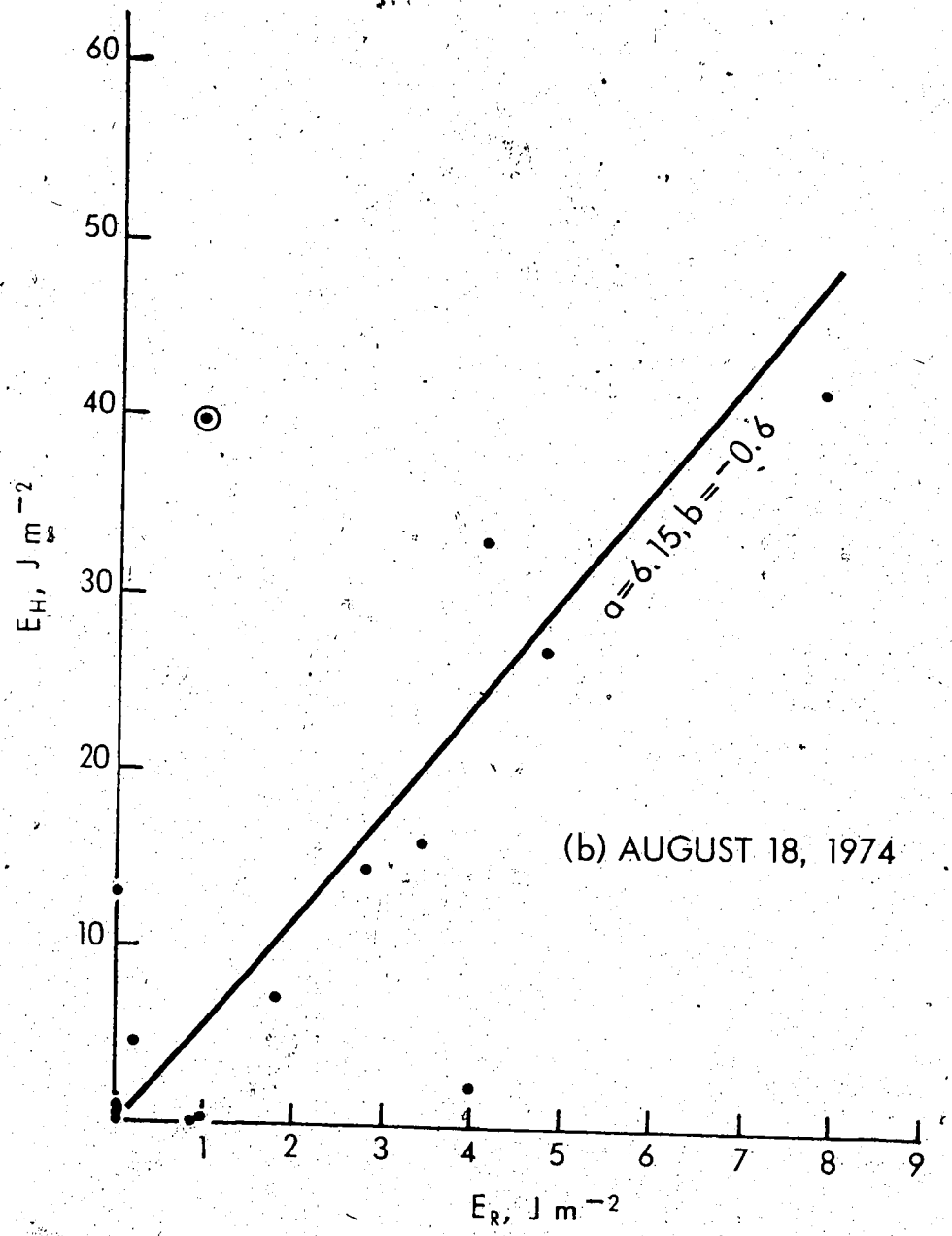
60
50
40
30
20
10
E_H, J m^{-2}
a=6.15, b=−0.6
(b) AUGUST 18, 1974
1
2
3
4
5
6
7
8
9
E_R, J m^{-2}

Figure 4.2b

Occasionally, the raw radar estimates and hailpad values did not conform at all to the overall pattern. For three cases in August 7 and one in August 18, heavy hail fell but the raw radar estimate was very low, a result of anomalously low echo strengths. These points are circled in Figures 4.2(a) and 4.2(b). Unusually severe attenuation of the radar beam is the probable cause, although this is difficult to prove. In one other case, in August 7, the radar estimate was very high relative to the hailpad value. This anomaly is more difficult to explain. This point corresponds to hailpad G27. The output of PLOTPAD from the hailpad site and from the eight surrounding quarter-sections was examined. Echo-trace maps for August 7 were also consulted. These maps are produced by the Hail Project, and are drawn every 15 minutes at the 1.5 degree elevation. General inferences can be made from these maps about the direction of a storm's movement and the stage of its development at a particular time. The PLOTPAD charts and the echo-trace maps indicate that the storm that affected hailpad G27 was undergoing rapid changes at the time it was passing over the hailpad. The storm had a long, narrow configuration and probably consisted of several cells in a line. Two distinct cells show in the PLOTPAD charts. The larger cell, the first one to cross the hailpad, was declining. If it still contained some small ice particles, it would produce a strong radar echo, although it would produce only light hail at the ground. The result would be an

anomalously high raw radar estimate of hail energy density.

The linear correlation coefficient r, between the hailpad values of kinetic energy density and the raw radar estimates, where

$$r = \Sigma \frac{(E_{Ri} - \bar{E}_R)(E_{Hi} - \bar{E}_H)}{s_R s_H} \qquad 4.7$$

was calculated for August 7 and 18 at the 45, 40, 35 and 30 dBZ thresholds. In Equation 4.7, E_{Ri} and E_{Hi} are the raw radar estimates and corresponding hailpad values of kinetic energy density. $\bar{E}_R$ and $\bar{E}_H$ are the mean values of these quantities, and s_R and s_H are the standard deviations. r measures the consistency of the relationship between E_R and E_H. A value of r of ±1 indicates that there is an exact linear relationship, while a value of 0 indicates that there is no relationship between E_R and E_H, i.e., they are uncorrelated. The anomalous hailpads mentioned above were not included in the calculation of the correlation coefficient. The correlation coefficient was calculated and listed in Table 4.1. These results agree with the results of Waldvogel *et al* (1978), who report a correlation of 0.66 between radar and hailpad estimates of energy density for 286 hailpads.

If the threshold echo levels were really useful in improving the accuracy of the raw radar estimate by eliminating rain echoes, the correlation would be noticeably lower at low threshold levels. No appreciable difference was found in the correlation coefficients on a given day in any of the cases, except for the 45 dBZ threshold on August 7, which was somewhat lower than the other correlations

Table 4.1

LINEAR CORRELATION COEFFICIENT, r, OF RADAR ESTIMATE AND HAILPAD VALUE OF ENERGY DENSITY FOR AUGUST 7 AND 18, 1974 AT RADAR CALCULATION THRESHOLDS OF 45, 40, 35 AND 30 dBZ

Threshold (dBZ)	r	
	August 7	August 18
45	0.547	0.891
40	0.630	0.875
35	0.636	0.870
30	0.637	0.873

on that day. It was concluded that the threshold echo levels used here were not effective in improving the accuracy of the radar estimate. However, note that the correlation between the radar estimates and hailpad values is stronger on August 18 than on August 7. Given these qualifications, the correlations between the raw radar estimates and hailpad values were significant at all threshold levels on both days. Echoes below 35 dBZ did not contribute significantly to the total raw radar estimates, due to the exponential increase in the contribution from individual echoes with increasing dBZ.

The final step in obtaining a storm-adjusted estimator for hail energy density is to perfor a linear regression of the raw radar estimates against the hailpad values at the chosen threshold for the storm of interest. The final adjusted estimate, E, is obtained from the least-squares fit of the raw radar estimate against hailpad value for the given storm-day:

$$E = a E_R + b \qquad 4.8$$

where a and b are fitting parameters. Figures 4.2(a) and 4.2(b) show the least-squares fitting lines for August 7 and 18 at the 30dBZ threshold. In deriving Equation 4.8 the four anomalous hailpads from August 7 and the one from August 18 were deleted. E can be calculated for any location by Equation 4.8 provided there is complete radar data

data available to calculate E_R. If at any time Equation 4.8 yields a negative value for E, E can be set to 0.0 Jm^{-2}. In situations where there are not enough hailpads to set up a true least-squares fit, average values of a and b based on many storms may be substituted in Equation 4.8. In general, the more hailpads that are available, the more reliable will be the adjusted hail energy density estimate, E. Chapter 6 will discuss some of the factors which affected the observed relationship between the raw radar estimate and the hailpad value of energy density. The next section will describe the preliminary results of the use of Equations 4.6 and 4.8.

4.2 PRELIMINARY RESULTS: THE EFFECT OF VARYING QUANTITY OF INFORMATION ON THE DELINEATION OF HAIL AREAS

Two attempts were made at delineating hailfall for August 7 and 18 without the use of radar. First, the maps of Figures 4.3(a) and 4.3(b) were produced using the hailpad analyses only. The contours are unrealistically smooth and their placement is extremely imprecise. None of the intricate structure known to exist in most hailswaths shows up in these maps.

Figures 4.4(a) and 4.4(b) are the same as the previous pair of maps, except farmers' maximum hail size reports were also used. About ten farmers' reports per township were usually available from the storm area. The outer edge of the area that received any hail at all (shot-

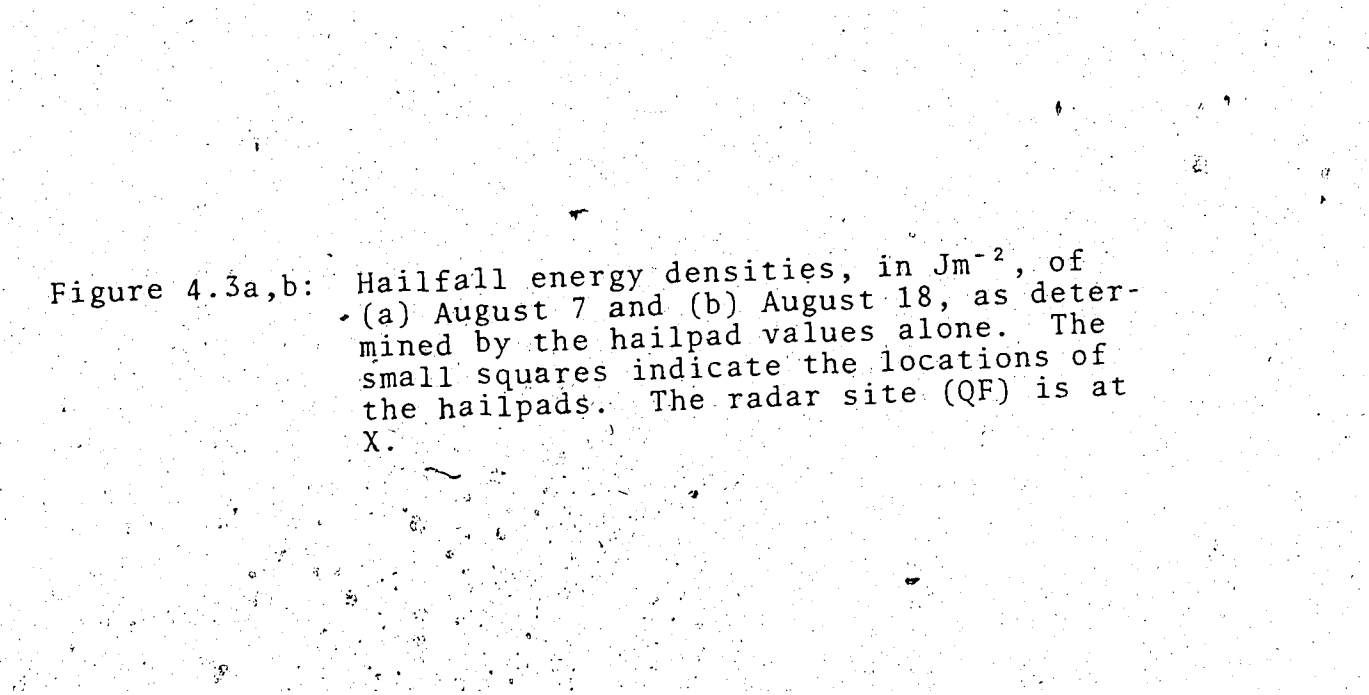

Figure 4.3a,b: Hailfall energy densities, in Jm^{-2}, of (a) August 7 and (b) August 18, as determined by the hailpad values alone. The small squares indicate the locations of the hailpads. The radar site (QF) is at X.

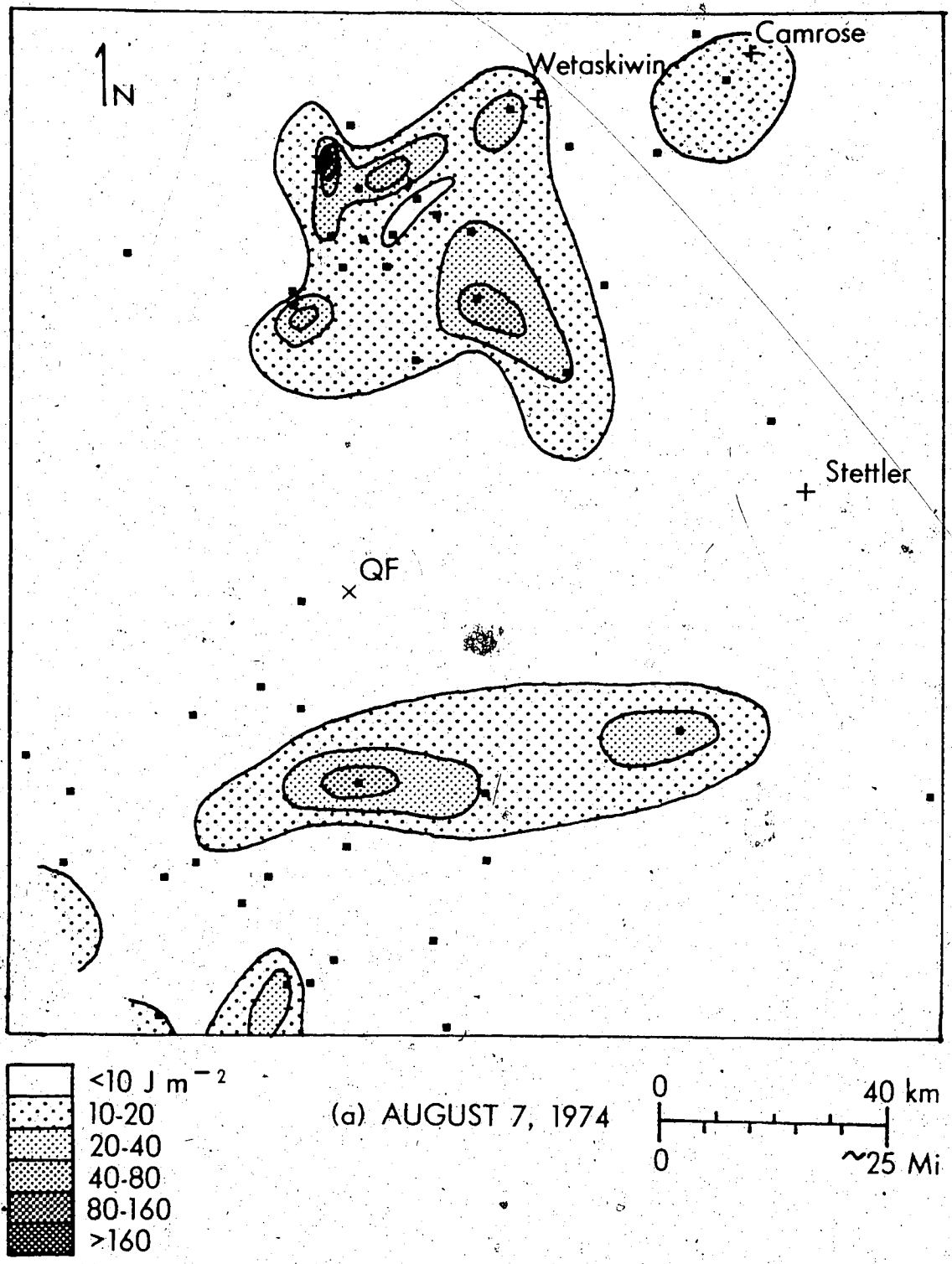
N
Camrose
Wetaskiwin
Stettler
QF
<10 J m⁻²
10-20
20-40
40-80
80-160
>160
(a) AUGUST 7, 1974
0
40 km
0
~25 Mi

Figure 4.3a

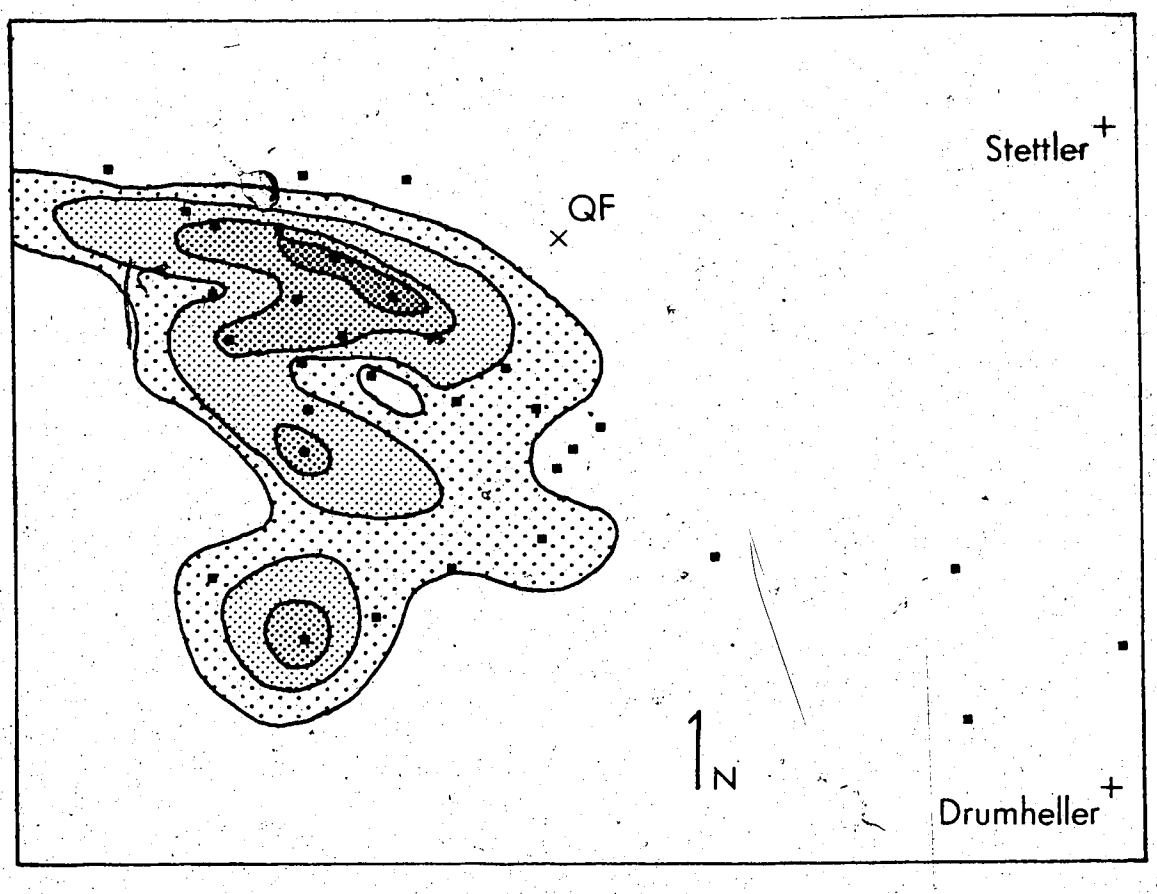

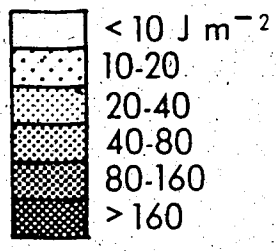

(b) AUGUST 18, 1974

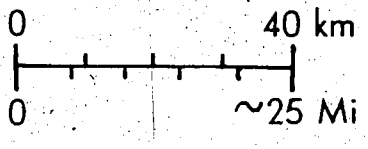

Figure 4.3b

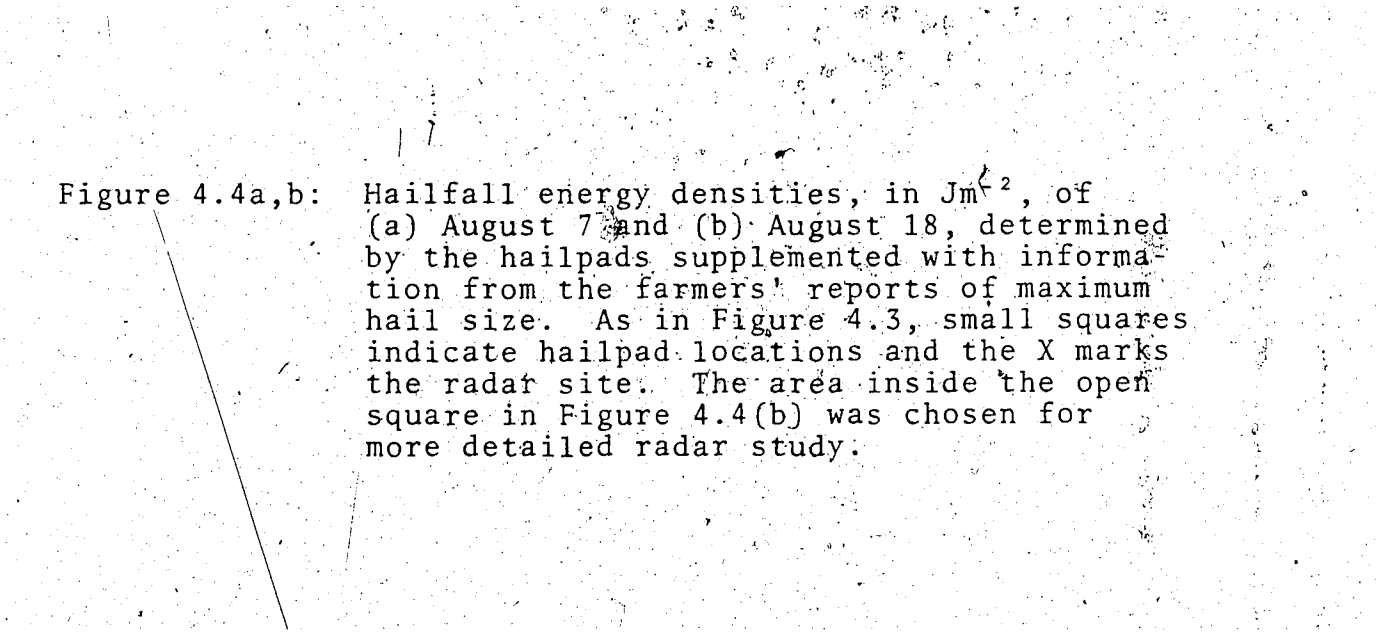

Figure 4.4a,b: Hailfall energy densities, in Jm^{-2}, of (a) August 7 and (b) August 18, determined by the hailpads supplemented with information from the farmers' reports of maximum hail size. As in Figure 4.3, small squares indicate hailpad locations and the X marks the radar site. The area inside the open square in Figure 4.4(b) was chosen for more detailed radar study.

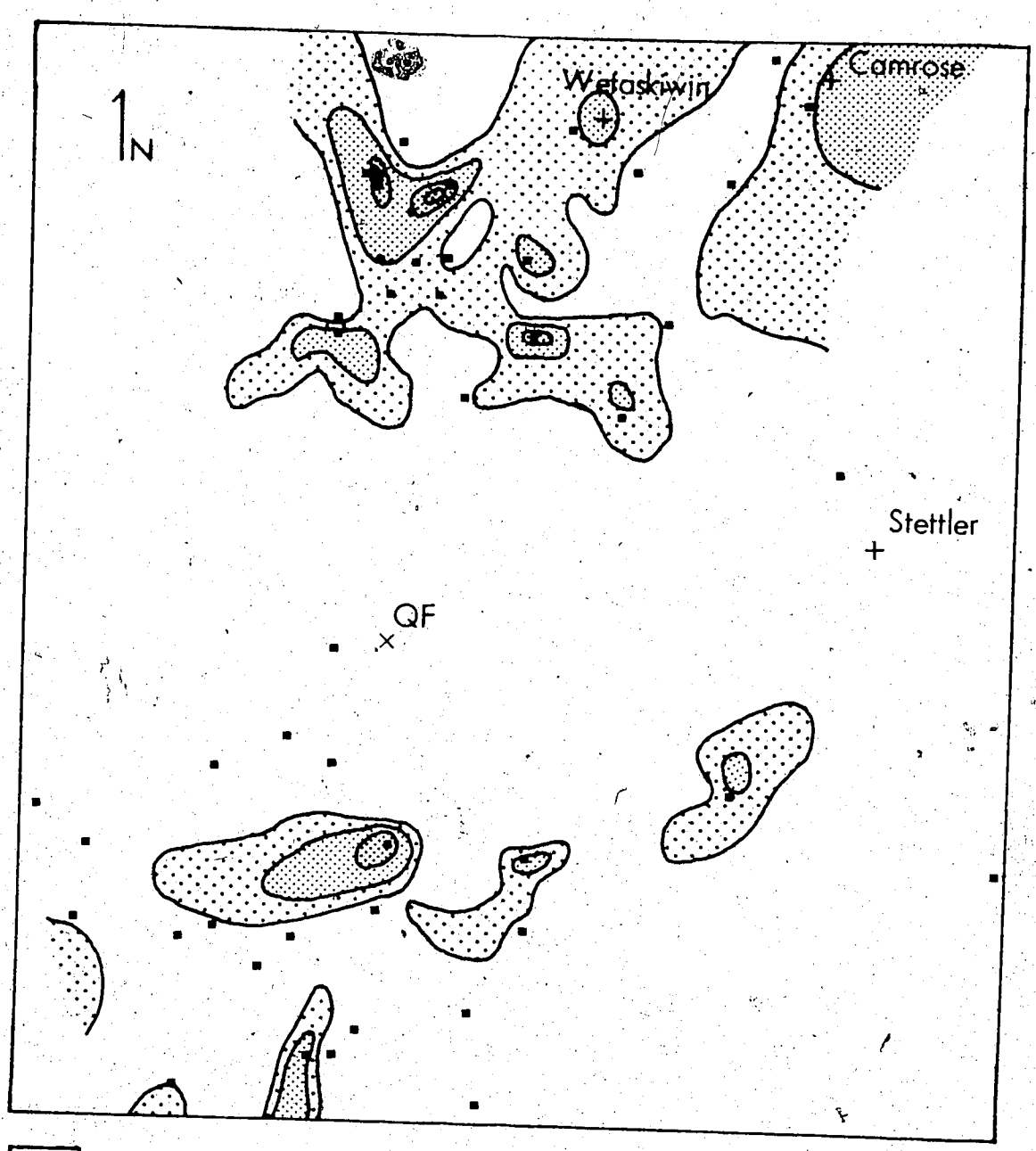
1N
Wetaskiwin
Camrose
Stettler
QF
<10 J m⁻²
10-20
20-40
40-80
80-160
>160
(a) AUGUST 7, 1974
0
40 km
0
~25 Mi

Figure 4.4a

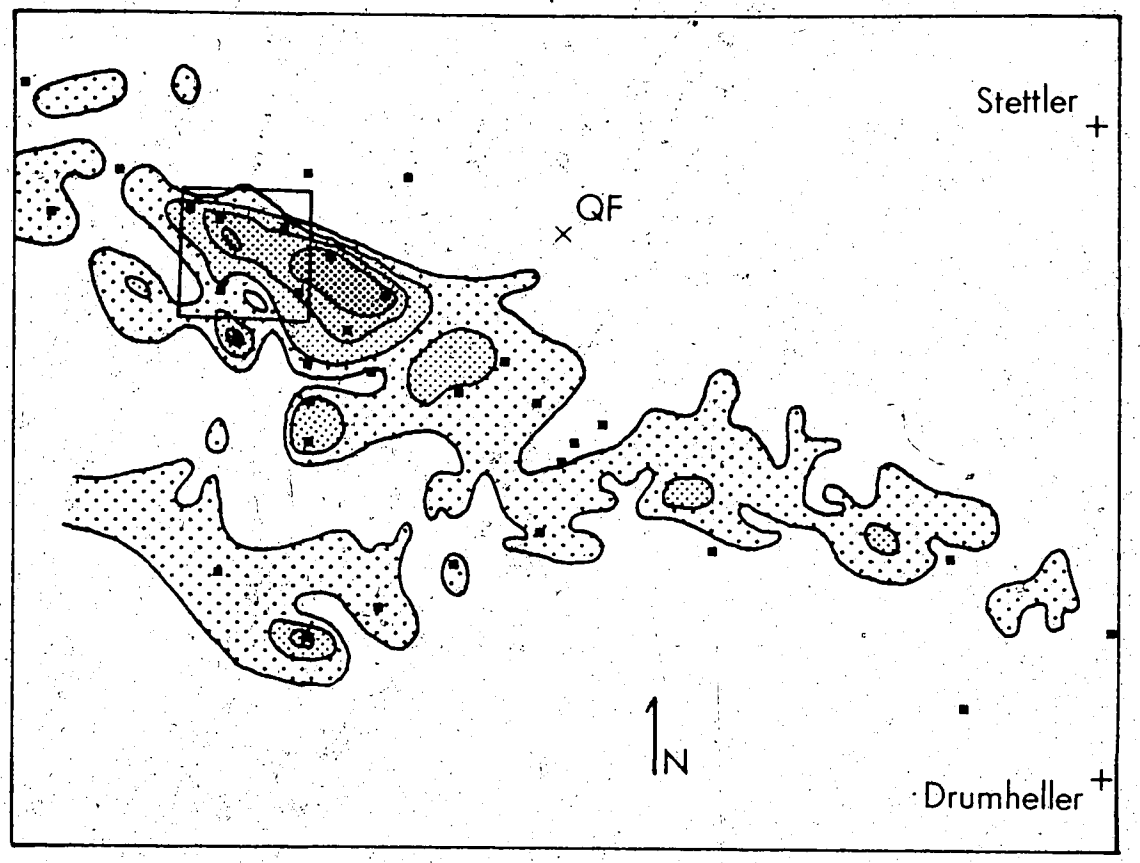

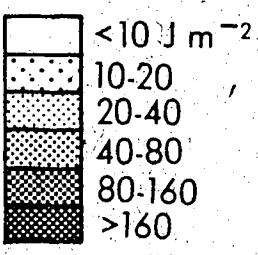

(b) AUGUST 18, 1974

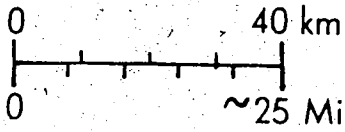

Figure 4.4b

size being the largest reported size) defined the lowest contour value, $10 Jm^{-2}$, of hail energy density. The farmers' reports of maximum hail size were used as a visual aid in drawing successively higher contours of energy density. At hailpad locations, the hailpad value itself determined the contour placement.

This use of finer-scale farmers' report information already showed significant smaller-scale features of the hailswaths. Major changes were made from the hailpad-only maps, especially in the case of August 7, supporting the belief that more detail could be discovered at higher information densities. A portion of the August 18 storm, covering 144 square miles, was then chosen for more intensive radar and hailpad analysis. This area, marked by a square in Figure 4.4(b), is shown at a larger scale in Figure 4.5.

Using the program PADEN and Equation 4.8, where $a = 6.18$ and $b = 0.5\ Jm^{-2}$, radar-based estimates of hail energy density were calculated for all quarter-sections with complete radar data. These estimates were plotted and then contoured to give Figure 4.6. The irregular eastern border of the plotted area marks the limit of complete radar data on August 18.

The most striking feature of the map is the intricate structure and strong variations in the radar-estimated hail energy density field. While the radar-

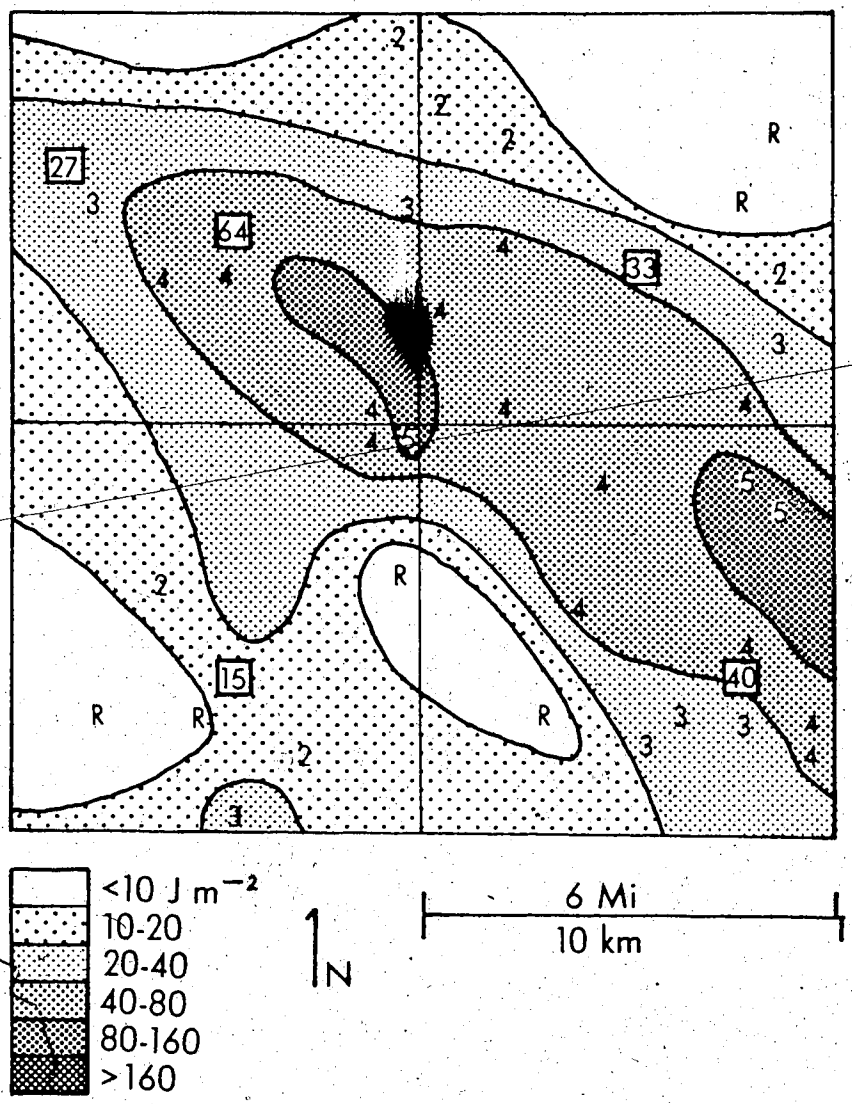

Figure 4.5: Detail of August 18, which was indicated in Figure 4.4b. Numbers inside squares are the kinetic energy densities, in Jm^{-2}, given by the hailpads at those locations. Maximum hail sizes reported by farmers are identified by the following codes: X = no rain or hail, R = rain only, 1 = shot, 2 = pea, 3 = grape, 4 = walnut, 5 = golfball, 6 = larger than golfball, and 0 = maximum size unknown.

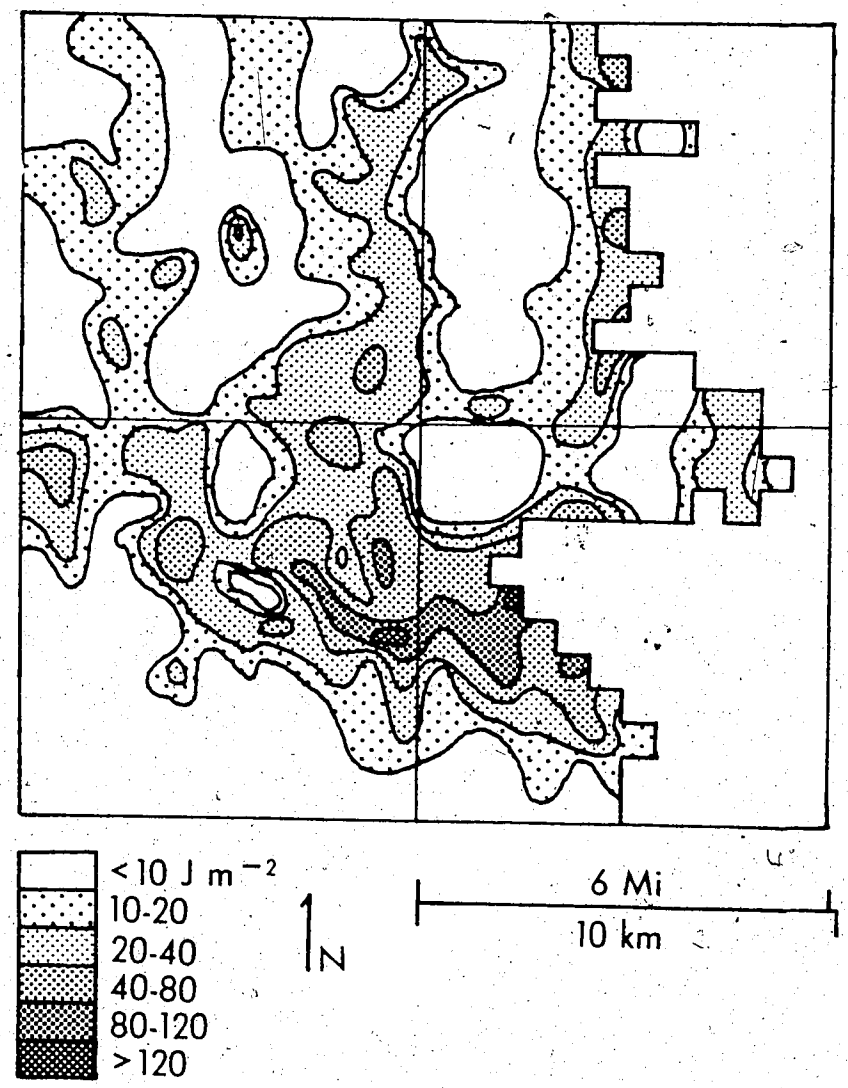

Figure 4.6: Kinetic energy density of hailfall in Jm^{-2}, based on adjusted radar estimates (E in Equation 4.8) in the area covered by Figure 4.5.

based estimates are not direct observations, the structure and scale of the features are generally in agreement with the observations of the spatial distribution of hailfall at the ground by Strong (1974), Changnon (1970) and others. Close examination of Figure 4.6 shows that, apart from local maxima and minima having diameters of 1.5 miles or less, there are some important larger-scale features. Three elongated areas of moderate (10-40Jm^{-2}) activity, oriented north-south, between 2 and 5 kilometers wide and 12-16 kilometers long are visible in the northern half of the map. All these features correspond in size and shape to the hailstreaks described by Changnon (1970).

Examination of echo trace maps of the kind described in the last section shows that two distinct storms crossed the region of the map of Figure 4.6. The first storm was maturing as it crossed the southern half of the region between 1530 and 1630, moving east-southeastward. The second storm, at its peak of development, moved through the area almost due east between 1740 and 1830, sweeping the northern three-quarters of the region.

The later storm contributed most of the hailfall energy in the intermediate areas that experienced both storms. Superimposed hailstreaks from both storms could explain the small areas of estimated energy density exceeding 80 Jm^{-2} which occurred near the southern ends of the north-south oriented streaks. Small cells embedded in the second storm, moving rapidly northward, could explain the

unusual orientation of these streaks. Such cell movement is commonly observed in squall lines.

The average energy density of hailfall over the four townships was 18.2 Jm^{-2} when calculated from the hailpad-adjusted radar estimates. As given by the mean of the five hailpads in the area, the average energy density is 35.8 Jm^{-2}. There is a difference of a factor of 2 in these results.

The sparseness of farmers' reports (about 10 per township) relative to the radar data (up to 144 calculations per township) made the consistency of the two sources of information difficult to ascertain. In most [illegible]s, there was reasonably good agreement between the [illegible]s' reports of maximum hail size and the nearby energy [illegible]sity estimates. A major discrepancy occurred in the south center of the map region where two farmers reported rain only, but the radar indicated hail in excess of 80 Jm^{-2}. Two land locations in that locality yielded radar energy estimates of more than 120 Jm^{-2}. The owner of one of the two apparently hard hit land locations, at NW S18, T36, R4, W5, was interviewed by telephone on April 1, 1977. He recalled receiving very heavy damage to his crops, and seeing hail on the ground on the evening of August 18, more than two hours after the storm had passed over. His comments tend to confirm the radar evidence of heavy hail at that land location. This observation suggests that radar data may be very reliable in the detection of severe hail, although this should be confirmed by more study.

CHAPTER 5

EVALUATION OF THE RADAR-HAILPAD ESTIMATION SCHEME AND ALTERNATIVE METHODS

5.1 TRIPLETS

A quantitative assessment of the radar-hailpad estimation scheme described in the last chapter is needed. That scheme will be compared using two different procedures. Each uses only the information routinely supplied with the hailpads. Some simple statistical tests will be applied to determine whether any of the methods was able to make valid estimates of local energy density.

The hailpads were grouped into series of three, called "triplets". The three pads in each triplet experienced the same storm, and lay within thirty degrees of a straight line. The distance to either end pad from the centerpad did not exceed 24 miles (38 km). The center pad is referred to as H_C, and its measured hail energy density as E_C. The end pads are H_1 and H_2, with energy densities of E_1 and E_2, respectively. Similarly, the distances of H_1 and H_2 to the center pad are d_1 and d_2. Estimates, called E_C', were made of the value of E_C using E_1 and E_2 and various

combinations of radar information. Figure 5.1 illustrates a typical triplet. A complete listing of triplets appears in Appendix C. A description of the estimation methods to be tested follows in the next section.

5.2 DESCRIPTION OF THE ESTIMATION METHODS

Arithmetic mean: this method is based on the assumption that the energy density at the center pad of the triplet lies somewhere between the values at either end pad. No other information is used, and the center-pad estimate is the arithmetic mean of the end-pad values. Thus,

$$E_c' = \tfrac{1}{2}(E_1 + E_2) \qquad 5.1$$

Distance-weighted mean: this method assumes that the energy density of hailfall between two end pads varies linearly. The implicit assumption of this scheme is that the length scale of the most significant features of the hailfall pattern is larger than the average distance between hailpads. The formula for E_c' is

$$E_c' = \frac{d_2 E_1 + d_1 E_2}{d_1 + d_2} \qquad 5.2$$

Radar-hailpad estimate: the formula has already been described in Chapter 4. In this case E_c' is simply

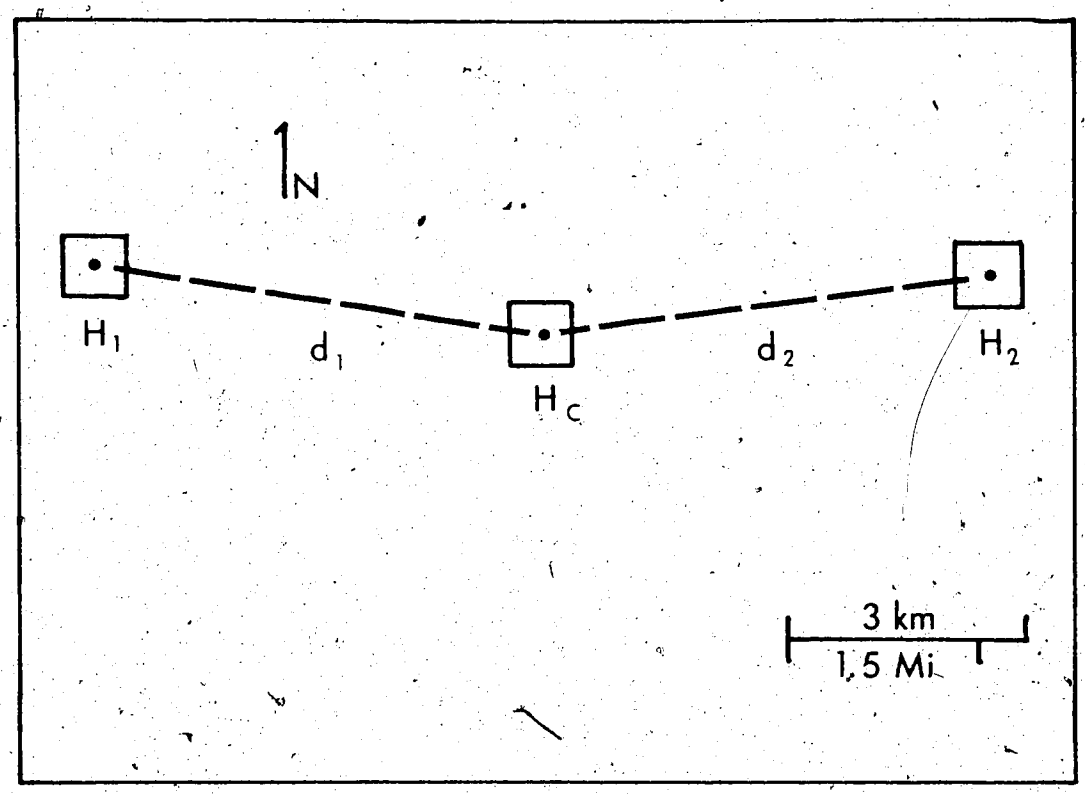

Figure 5.1: An actual hailpad triplet, drawn to scale. The squares represent the quarter-sections containing the hailpads, rather than the hailpads themselves. The triplet shown is No. 719. The data for this triplet appears in Appendix C.

the value of E for that location given by Equations 4.6 and 4.8. Note that this radar estimate is calibrated using hailpad data from the whole storm, not just hailpad data at the ends of the triplet.

Estimation of the center-pad value by the arithmetic and distance-weighted means will serve mainly as controls in the evaluation of the relative accuracy of the radar-hailpad method.

5.3 EVALUATION AND COMPARISON

Estimation by the arithmetic mean, the distance-weighted mean and the radar-hailpad method will be referred to as Method 1, Method 2 and Method 3, respectively. 123 triplets drawn from both the regular and the supplementary (July 30 and August 15) hailpad sample were originally chosen for the analysis, but because of the limited radar data, only 60 were suitable for evaluating all three methods. The test variable chosen was the error,

$$|E_c' - E_c|$$

or the absolute difference between the estimate and actual center-pad energy density. The more common measure of error, the fractional error;

$$\frac{|E_c' - E_c|}{E_c}$$

could not be used because some of the center pads recorded zero hail. Also, in terms of crop damage, the absolute error is more relevant.

The center-pad estimates and errors are listed in Appendix D. The mean error of all triplets was calculated for Methods 1 and 2, and the mean error for 60 triplets for Method 3. The mean over these 60 triplets was also calculated for Methods 1 and 2. The standard deviations were calculated as well. Table 5.1 summarizes these results.

A number of observations emerged from Table 5.1. The first is the high standard deviations of the errors in all three methods. In most cases it is higher than the mean values. The second is that the addition of distance information had no effect on center-pad estimates based only on hailpad information, implying that the assumptions behind Method 2 are false. The size scale of the significant variations in hail activity is much smaller than the average triplet length of about 16 miles, or 27 km (Changnon, 1970). Finally, the mean error of the estimates by Method 3 is substantially less than those of the other methods, indicating that the radar provides real information on local intensity of hailfall. This result requires further testing.

5.4 ANOTHER STATISTICAL TEST

The procedure adopted for this final statistical test was to compare the size of the mean error in each of

Table 5.1

MEANS AND STANDARD DEVIATIONS FOR THE ERRORS LISTED IN APPENDIX D, IN Jm^{-2}

	METHOD 1	METHOD 2	METHOD 3
1. All Available Triplets (N=123)			
Mean	22.5	22.7	
Standard Deviation	23.4	26.9	
2. Triplets Available for Method 3			
a. August 7 (N=43)			
Mean	21.5	23.6	13.7
Standard Deviation	23.0	30.5	21.8
b. August 18 (N=17)			
Mean	16.4	18.6	6.4
Standard Deviation	16.7	19.6	5.3
c. August 7 and August 18 (N=60)			
Mean	20.1	22.2	11.7
Standard Deviation	21.5	27.8	18.7

the methods with that of a similarly calculated "error" from a randomized set of numerical values. If an estimation method has any validity, the mean error associated with it should be significantly smaller than the corresponding error from the randomized data set. A Monte Carlo method was used to test this hypothesis (McLeish, 1978).

The data used in this analysis were the sixty triplets used to calculate the mean error in Method 3. The energy densities observed at the center pads of these triplets were randomized, first by numbering them in the order in which they appeared in Appendix D. These observations were then re-listed in the order in which their numbers appeared in a computer-generated random permutation of the integers from 1 to 60. The estimates of the center-pad energy density by each method, in their original order, were subtracted serially from the randomized observations. The absolute values of the resulting figures will be called the "randomized errors". The mean of the actual errors for each method was compared to the mean of the randomized errors.

The objective of the randomization was to simulate a situation in which there was total ignorance of the true hailfall energy density pattern, except for the overall severity of the storms. It thus served as a control data set, so that the only differences between the randomized and the actual errors were those that resulted from application of the estimation methods.

The procedure described above was repeated 10,000 times using a different permutation of the center-pad values each time. A count was made of the number of times the mean error of each method equalled or exceeded the mean randomized error. This number, as a fraction of the 10,000 trials, is a measure of the level of significance at which the mean actual error is less than the mean randomized error.

The "level of significance" is defined as the probability that a random results will appear to support the hypothesis under test at least as strongly as the observed result. For example, the statement "the observed results are different at the 5 percent level of significance" means that the probability is 0.05, that results arising purely from chance will have a difference at least as large as that between the observed results. It follows that the lower the numerical value of the significance level, the stronger is the probability that the result is physically meaningful. In statistics, a 5 percent significance level is commonly accepted as a criterion for judging a result as having physical meaning, instead of arising from chance.

By implication, the fraction mentioned above is also a measure of the skill of the estimation procedure. The lower the fraction, the more significant is the skill. A computer program, called PERMS, was composed by the author of this study to perform the repeated-trial statistical test. Table 5.2 lists (1) the level of significance described above for the accuracy of each of the center-pad

Table 5.2

RESULTS OF TEST ON SIZE OF MEAN ERROR IN ESTIMATING CENTER-PAD ENERGY, DESCRIBED IN SECTION 5.4

1. Level of significance in reduction of mean error (percentage)
2. Randomized error
3. Observed mean error (from in Table 5.1)
4. Percentage reduction of mean error from randomized error

	METHOD 1	METHOD 2	METHOD 3
1	3.57	5.63	- 0.00
2	23.1	25.0	20.2
3	20.1	22.2	11.7
4	13.1	11.1	42.4

estimation methods; (2) the population mean randomized error. This is the error that can be expected from random guesses of the center-pad value. It can be estimated by taking the mean (over 10,000 trials) of the mean randomized error within each trial. Finally (3) the observed mean error and (4) the percentage difference between the observed mean error and the population mean randomized error are listed.

The results in the table show that only Method 3 achieves a substantial reduction in the mean error from the case of random guesses. Method 1 may show significant skill (based on a maximum 5 percent level of significance), but the reduction in error is not large enough to justify its routine use. The 0.0 percent level of significance recorded under Method 3 indicates that the value is smaller than this statistical test can detect, i.e., the actual level of significance is probably smaller than 0.001 percent. This means that Method 3 showed highly significant skill.

On the basis of the analyses in this section and section 5.3 it was concluded that the combined radar and hailpad method, outlined in Chapter 4, provided a reliable estimate of the energy density of hail at places without hailpads.

CHAPTER 6

FACTORS AFFECTING THE RELATIONSHIP BETWEEN THE HAILPAD ENERGY DENSITY AND THE RAW RADAR ESTIMATE

As noted in Chapter 4, the relationship between E, the actual hail energy density at the ground, and E_R, the radar estimate, is not $E = E_R$, but more like $E = aE_R + b$, where $a \sim 5\text{-}10$ and b is of the order of $\pm 1\text{-}10 Jm^{-2}$, in the case of 5cm radar observations of hail. The relationship is furthermore not perfect, but in practice shows strong scatter. This chapter will describe some of the important factors which influence the relationship between E and E_R. These include attenuation of the radar beam by intervening precipitation (affecting mainly the value of "a" mentioned above), the statistical bias error due to non-uniform beam-filling (probably affecting both "a" and the scatter), inaccurate registration of the receiver, and the presence of spatial scales of hail below the resolution of the radar.

6.1 ATTENUATION

Ordinarily, calculations of the reflectivity of a radar target are made with the assumption that there is

nothing between the target particles and the receiver. In practice, however, a radar beam passes through air, cloud and precipitation. The result is a loss of power in both the incident and reflected beam through absorption and scattering. At the microwave wavelength involved in this study (5.5cm), precipitation is by far the most important attenuating material (Battan, 1973). Estimates of attenuation are usually given by the attenuation coefficient, in units of decibels per kilometer ($dBkm^{-1}$). The magnitude of the attenuation coefficient due to precipitation will depend on the radar wavelength and the type, composition and intensity of the precipitation. The total attenuation is the integral of the local attenuation coefficient, between the transmitter and the target and back.

The value of the one-way attenuation coefficient at a given location can be estimated by

$$k_T = 0.4343 \sum_{volume} Q_+. \qquad 6.1$$

(Battan, 1973), where Q_+ is the attenuation cross-section of each particle in a unit volume and k_T is the attentuation coefficient. As Equation 6.1 is written, Q_+ has units of cm^2, and the volume is $1m^3$. This gives k_T in units of $dBkm^{-1}$. The attenuation cross-section, Q_+, is defined as the area which, when multiplied by the incident beam intensity, gives the total power taken from the beam (Battan, 1973). Equation 6.1 can be written as

$$K_T = 0.4343 \sum_{volume} \sigma_D a_D N_{OD} \qquad 6.2$$

where σ_D is the attenuation cross section at particle diameter D, normalized to unit area (when D is in cm). a_D is the cross-sectional area of the particle in cm , and N_{OD} is the number of particles of diameter D in the unit volume at a given time. This summation is over all diameter classes D in the volume. Equation 6.2 enables the local attenuation coefficient at the freezing level to be calculated from hailpad data. N_{OD} can be expressed in terms of observable hailpad quantities by the following relationship (Barge, 1977):

$$N_{OD} = \frac{N_D}{Av_+t} \qquad 6.3$$

where N_D is the total number of hailstones with diama
D passing through the unit volume in time t. t is t
tion of the hailfall in seconds. N_D is equivalent t
number of hailstones of diameter D intercepted by the
pad. A is the unit area. If A is $1m^2$, N_D must be expr
as the number of hailstones intercepted per square meter,
or 10.76 times the number per square foot. v_+ is the fall velocity of a hailstone as a function of its diameter, in meters per second. At the freezing level, $v_+ = 15.9D^{\frac{1}{2}}$ (see Chapter 4).

Equation 6.3 assumes that the hailfall is steady-state, although for a rough calculation this assumption is

not critical. Substitution of Equation 6.3 into Equation 6.2 yields

$$k_T = 0.4343 \sum_{\text{volume}}^{D} \sigma_D a_D \frac{N_D}{Av_t t} \qquad 6.4$$

or

$$k_T = 0.4343 \sum_{\text{volume}}^{D} \sigma_D \cdot \frac{\pi}{4} D^2 \cdot \frac{N_{Df} \cdot 10.76}{1m^2 \cdot 15.9D^2 t} \qquad 6.4a$$

N_{Df} is the number of hailstones of diameter D per square foot, a value directly obtainable from the hailpad analysis described in Chapter 2. Equation 6.4a simplifies to the following:

$$k_T = \frac{0.2353}{t} \sum_{\text{volume}}^{D} N_{Df} \sigma_D D^{1.5} \qquad 6.5$$

Equation 6.5 gives k_T, the one-way attenuation. Two-way attenuation, or the attenuation in both the incident and returned beam, would be simply twice that value. Each diameter class represented in the hailpad must be converted to the equivalent diameter class at the freezing level, D, by Equation 3.16a. Values of σ_D have been calculated by Battan *et al.* (1971) for diameters from 0.1 to 4 centimeters, at radar wavelengths including 5.5cm, for various proportions of ice and water in the hail. The quantity of water in the hailstone or on its surface was expressed as a water shell of a particular thickness surrounding a core

of solid ice. Since the hailstones were at the freezing level, they would have been wet, so for the purpose of calculation they were assumed to be coated with a film of water 0.05cm thick.

Using Equation 6.5, the attenuation coefficient at the freezing level above some hailpads was calculated and listed in Table 6.1. These values of the attenuation coefficient are probably conservative, because they do not take into account the contribution to the attenuation from heavy rain and from the hailstones which completely melted before reaching the hailpad. Attenuation coefficients in the S-band for the same hailpads were included in Table 6.1 for comparison. Note that attenuation in the S-band is usually an order of magnitude lower than in the C-band.

The values calculated above for typical hail situations under observation by C-band radar show that attenuation was substantial on the storm-days in question. It may be possible in principle to calculate the total attenuation along the radar beam. However, such a calculation would be too complex to be practical and furthermore, future applications of the radar-hailpad method will be made with the 10.6cm S-band system, in which attenuation should not be a major problem. The C-band attenuation coefficients listed in Table 6.1 indicate that a 4 to 8km depth of hail between the hailpads and the radar could easily account for the relative deficiency in echo strength involved in the estimation of energy density by C-band

Table 6.1

TWO-WAY ATTENUATION COEFFICIENTS, IN dB km^{-1},
FOR SOME HAILPADS AT C-BAND AND S-BAND RADAR WAVELENGTHS

Hailpad	Date	k_T, two-way (dB km^{-1})	
		at 5.5cm (C-band)	at 10.0cm (S-band)
E36	August 7	0.28	0.02
D37	August 7	3.12	0.60
D36	August 7	3.30	0.31
L0	August 18	1.64	0.14
L2	August 18	1.66	0.30

radar. This deficiency is about 6-12dB in most cases if the radar estimate is a factor of 5-10 smaller than the hailpad value.

One effect of attenuation that could contribute to the scatter in the E-E_R relation may be the orientation of the storm track relative to the radar. If the storm tracks tangentially relative to the radar site, echoes over some hailpads will be much more strongly affected than others, because some hailpads will always have a large depth of storm between them and the radar. A typical example would be hailpad D37 of August 7. When hail was falling at D37, there was always well over 20km of precipitation between the pad and the radar, according to the echo-trace map. D37 received about 166 Jm^{-2} of hail energy, but yielded a raw radar estimate of less than $0.5Jm^{-2}$. On the other hand, if the storm tracks directly toward or away from the radar, all the hailpads will, on the average, be looked at by the radar through roughly the same depth of storm as it passes over each pad. The echoes over the hailpads will therefore tend to be equally affected by attenuation.

This possibility may have some bearing on the difference in the scatter apparent in Figures 4.2a and 4.2b. On August 7, the storm cells that affected most of the hailpads never approached closer than 40km to the radar, tracking tangentially in an east-northeastward direction. The scatter was very severe in the E-E_R relation. On August 18,

the storms were heading almost directly toward the radar, and the E-E_R relation was relatively coherent.

6.2 NON-UNIFORM BEAM-FILLING

Rogers (1971) showed that in conditions of highly non-uniform filling of the beam by precipitation, radars with a linear or logarithmic response will tend to underestimate the actual mean reflectivity in the target volume. If the precipitation reflectivity varies by 20dB within the resolution volume of the beam (~1km^3 in the case of the Hail Project C-band), the underestimate by a logarithmic receiver can be as high as 3dBZ, and for a 30dB variation, as much as 6dBZ. A pencil-and-paper calculation, using Equation 4.6 and data from Strong's (1974) hailpad network show that such variations are possible in a realistic hailstorm.

Equation 4.6 also shows that a 3dBZ underestimate of reflectivity corresponds to an underestimate of energy density of roughly a factor of 1.8, and an underestimate of 6dBZ to a factor of 3.2 in the energy density. In marginal storms or hailfall areas, the actual average echo strength may already be near the threshold value assumed in the energy density calculation. The statistical bias may be enough in such situations to reduce the observed echo strength below the threshold. This consideration will hold true for any other effect, such as attenuation, which

introduces a downward bias in the observed reflectivity and in turn increases the error in the energy density estimate.

If the statistical bias effect occurred uniformly throughout the storm it may, to some extent, be accounted for automatically by the regression procedure used to form Equation 4.8. However, at hailswath boundaries or during periods of rapid change in the fine-scale structure of a storm, radar returns from some locations may be much more prone to the statistical bias effect than others.

6.3 ERROR IN REGISTRATION OF RADAR

Accuracy of registration, or the accuracy with which the actual position of the echo corresponds to the position given by the radar system output, is a critical limitation on the quality of any information derived from radar echo data. Echoes in convective conditions can vary by 20dB or more over distances on the scale or the radar's spatial resolution of about 1km. If the position given by the radar output is out by this distance, errors of that magnitude in the echo strength may result.

To determine the accuracy of registration of the C-band radar on the storm dates under study, the azimuth and range of every hailpad to within 0.1 degree and 0.1km were recorded from an 8-mile-to-1-inch scale map of the Hail Project area, for August 7 and 18, 1974. The co-

ordinates were measured from the center of the quarter-section containing the hailpad to the radar site. These co-ordinates were then compared to the sets supplied with the PLOTPAD charts, and which also appear in the output of PLOT. In addition, 14 hailpads from August 7, and 14 from August 18 were chosen at random for an independent check. This was done by selecting an echo from a PLOTPAD chart and loating it on a PPI segment generated by computer from the tape data containing the echo. The azimuth and range of the echo are then read off from the PPI segment (see Figures 6.1 and 6.2) and compared to the map co-ordinates as before. The computer-generated PPI was verified by checking the position of Limestone Mountain, a "landmark" echo whose exact position was known. The positions given for this and another "landmark" echo agreed with the true position on both storm dates. The co-ordinates of the hailpads from both the PPI and PLOTPAD were cross-checked, and in all instances except one, the two computer results agreed, within round-off limits.

The results of the preceding tests are tabulated in Appendix E. The total registration error, in kilometers, was the Pythagorean sum of the range and tangential errors. The range error was the difference, in kilometers, between the range of the hailpad calculated by computer and the actual map range. The tangential error is the difference between the computer-calculated azimuth and the map azimuth. It is expressed in kilometers by converting to radians and

AZIMUTH		249.5	250.1	250.7	251.3	251.8	252.4	253.0	253.5
RAY#		1	2	3	4	5	6	7	8
MILES	KM								
18.6	30	18	19	20	22	19	23	24	26
19.3	31	22	25	25	24	23	26	25	27
19.9	32	25	28	25	27	27	29	31	32
20.5	33	29	30	30	30	33	30	33	35
21.1	34	36	37	36	34	34	36	37	39
21.8	35	45	43	40	37	36	40	44	42
22.4	36	51	46	48	51	46	42	38	32
23.0	37	47	50	54	52	49	39	28	27
23.6	38	50	51	45	40	31	23	22	23
24.2	39	20	21	18	16	0	0	0	0

Figure 6.1: A PPI segment generated by the computer program PPI. These data are from August 7, 1974 at 16:24MDT at an elevation of 1.5 degrees. The first two columns on the left give the range, miles and kilometers, of the echoes. The azimuths of the echoes, in degrees, and the "ray numbers" are given along the top. A "ray" is the set of all bins along a given azimuth (see page 16). Echoes are in dBZ.

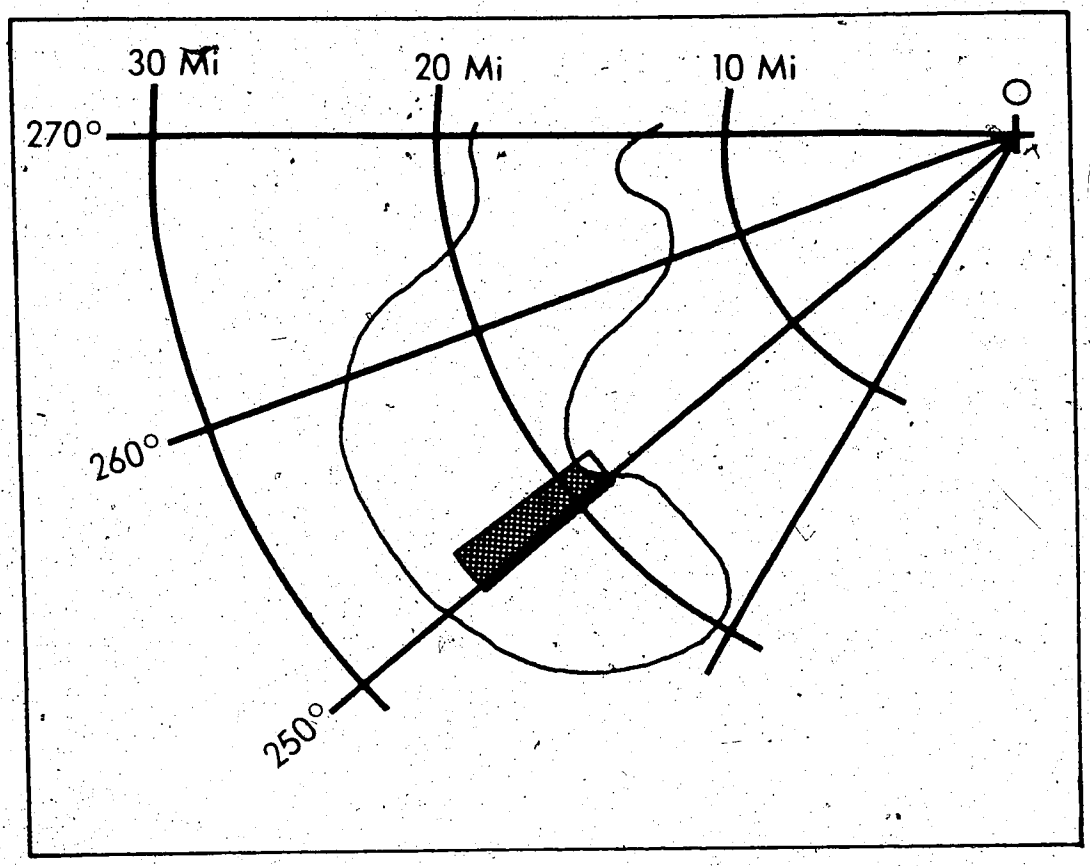

Figure 6.2: The data of Figure 6.1 as they would appear in a true PPI display. The data are outlined by the small shaded sector near 250 degrees. The radar site is at "O". Ranges, in miles, are marked at the top of the diagram while azimuths from true north are marked at the left. The curve indicates the approximate boundary of echoes 10dBZ or higher. The area of strong echoes in the lower left of Figure 6.1 would be in the lower right corner of the sector.

multiplying by the map range. The errors are expressed by the following equations:

$$X_R = |r_{PPI} - r_M| \text{ or } X_R = |r_{OUT} - r_M| \qquad 6.6$$

$$X_T = \frac{r}{57.3} |a_{PPI} - a_M| \text{ or } X_T = \frac{r}{57.3} |a_{OUT} - a_M| \qquad 6.7$$

$$X_{TOTAL} = (X_R^2 + X_T^2)^{\frac{1}{2}} \qquad 6.8$$

X_{TOTAL} is the total registration error, in kilometers. X_R and X_T are the range and tangential errors, respectively. r_M and a_M are the map range of the hailpad in kilometers, and the map azimuth in degrees. r_{PPI} and a_{PPI} are the range in kilometers and the azimuth in degrees given by the computer-generated PPI, while r_{OUT} and a_{OUT} are the range and azimuth given by PLOTPAD. The errors are summarized in Table 6.2.

There is an uncertainty of $\frac{1}{2}$ mile (~ 1km) in a hailpad's position, since its location is given only by the quarter-section on which it is set up. PLOT and PLOTPAD selected the correct radar data within the uncertainty in the hailpad location in a majority of cases. The problems caused by inaccurate registration become significant with appreciably larger errors. Fortunately, none of the hailpads with complete radar data had to be rejected because of excessively poor registration. More sophisticated echo-location routines, such as those used in the handling of

Table 6.2

SUMMARY OF RADAR REGISTRATION ERRORS, X_{TOTAL}

Error Size Class (KM)	Breakdown of Errors by Size Class							
	Number in Size Class				Percentage in Size Class			
	≤1.0	1-2	2-3	>3.0	≤1.0	1-2	2-3	>3.0
August 7								
PLOT-MAP ERRORS ONLY	17	11	2	0	56.7	36.7	6.7	0
DETAILED ANALYSES:								
PLOT-MAP	9	5	0	0	64.3	35.7	0	0
PPI-MAP	9	3	2	0	64.3	21.4	14.3	0
ALL PLOT-MAP ERRORS	26	16	2	0	59.1	36.4	4.5	0
August 18								
PLOT-MAP ERRORS ONLY	18	5	0	2	72.0	20.0	0	18.0
DETAILED ANALYSES:								
PLOT-MAP	9	5	0	0	64.3	35.7	0	0
PPI-MAP	7	5	2	0	50.0	35.7	14.3	0
ALL PLOT-MAP ERRORS	27	10	0	2	69.2	25.6	0	5.2
TOTAL								
PLOT-MAP ERRORS ONLY	35	16	2	2	63.0	29.6	3.7	3.7
DETAILED ANALYSES:								
PLOT-MAP	18	10	0	0	64.3	35.7	0	0
PPI-MAP	16	8	4	0	57.1	28.6	14.3	0
ALL PLOT-MAP ERRORS	53	26	2	2	63.9	31.3	2.4	2.4

the Hail Project S-band data, will help to alleviate the registration problem.

6.4 THE PROBLEM OF RESOLUTION-SCALE MISMATCH

The work of Strong (1974) and Changnon (1970) shows that significant variation in hail activity can exist at scales finer than the size of a quarter-section. This size scale is similar to the resolution of the C-band at a range of 40 to 80 kilometers.

As estimate of the energy density of hail in the beam resolution volume at these ranges is averaged over the volume. The ground hailfall parameter that actually corresponds to the radar estimate would be the energy density averaged over the quarter-section under the beam, rather than the hailpad value. The energy density from a hailpad can deviate markedly from the area average, causing strong scattering in the E-E_R relationship. A rough illustration of the fine-scale variation can be made from the data in the above-mentioned work of Strong. In 1973 he operated a high-density network in Section 6, T42, R2, W5, southwest of Rimbey, Alberta, consisting of a 5 × 5 hailpad array. He produced a hailfall map from this network of a storm which in that area was comparable in intensity to the ones analysed in this study. The map showed maxima of hail activity (about 200Jm^{-2}) in the center of the section and near the southwestern corner. Hail activity varied

widely over the network. In the northwest quarter, the energy density varied from 171Jm^{-2} in the southeast corner to less than 10Jm^{-2} in the northeast corner.

The results indicate that a radar estimate of energy density may be more useful as a mean figure for the hail activity over an extended area, such as a quarter-section. While it will give a good rough estimate of the energy density on a hailpad below the beam, it does not yet show promise of being a highly accurate point estimator.

CHAPTER 7

CONCLUSION

7.1 SUMMARY

A method of estimating kinetic energy density of hailfall at locations without hailpads, using radar data and the existing hailpad network was developed. The method was tested on the hailstorms of August 7 and 18, 1974 in central Alberta.

The radar-hailpad estimation method was compared to methods which use only hailpad information. The hailpads-only methods showed little or no skill at extrapolating energy density, while the radar-hailpad method showed highly significant skill. The average error of estimation by the radar-hailpad method was about 50 percent of the average error by other methods. 45 out of 60, or 75 percent, of the hailpads tested by the radar-hailpad method were estimated to within $10 Jm^{-2}$ of their actual energy densities. By comparison, using an arithmetic-mean on the hailpad data gave only 43 percent within $10 Jm^{-2}$. Using distance-weighted means of hailpad data gave only 40 percent within $10 Jm^{-2}$. Similarly, 92 percent of the hailpads

were estimated within $20Jm^{-2}$ by the radar-hailpad method, as compared to 61 and 62 percent by the two hailpads-only methods.

Using the radar-hailpad method, 109 square miles ($282km^2$) were intensively surveyed. Radar estimates of hailfall energy density in this area showed variations having dimensions that are in good agreement with ground observations of small-scale hail patterns. Local estimates of hailfall generally agreed well with the available farmers' reports. Hail energy density was first contoured in the intensive survey region using farmers' reports, and assuming a doubling of energy density with each higher "category" of maximum hail size. When this was done, the energy density at the farmers' report site was within one countour category of the radar estimate at the site or a neighbouring land location in 13 out of 24 cases.

The hailpad energy versus radar estimate relationship was found to be quite different on the two storm days studied here. This implies that radar estimates should be tailored to the date's ground-based measurements.

The method of estimating local hail energy density shows promise in operational applications, but some problems must be overcome. The S-band (10.6cm) radar data collected since 1975 is generally more stable and accurately registered than the C-band data of 1974. The longer wavelength of the S-band will greatly reduce the effect of beam attenuation. Refining the programs used to locate

the hailpads and to select the appropriate radar data will also improve the results. For data from 1975 onward, the output from existing high-precision programs can be used as input for secondary programs which perform these tasks.

7.2 RECOMMENDATIONS FOR FURTHER STUDY

Refined radar-hailpad studies could readily be incorporated into Alberta Hail Project operations and evaluations.

A more sophisticated and accurate method is needed to filter out the contribution of rain to the radar echoes. Information from the circular depolarization ratio (CDR) could, for example, be used, since the CDR is well correlated with the proportion of rain to hail (Barge, 1972). The contribution of the hail signal to the total returned signal increases with the magnitude of the returned signal. The energy estimation formula should therefore be tested at threshold levels greater than 45dBZ.

The radar-hailpad method should be more thoroughly tested. A large amount of high-quality radar data and thousands of hailpad analyses are available from 1975, 1976 and 1977. Use of this data base for testing the radar-hailpad method can more fully establish its reliability and feasibility.

Programs already in use by the Hail Project can extract the estimated rate of rainfall from the radar data for each storm. A similar program, using the energy-

reflectivity relationship appropriate for the characteristics of the radar, could be used to produce maps of raw hail energy density estimates for the entire Hail Project region for a given storm day. This raw estimate pattern could later be adjusted when the hailpads for that date are analysed.

The radar data presented in Chapter 6 raises theoretical questions such as the relationship between reflectivity factor Z and the spectrum of hailstone diameters D. The relationship can be expressed approximately as $Z = \Sigma D^r$, where $4 < r \leq 6$ (Barge, 1977). Examination of more hailpads and the corresponding radar data to determine this relationship more precisely may be of some interest.

Such a procedure can be applied directly to the problem of determining the effect that cloud seeding has on hailfall. Unil now, no fine-scale quantitative data was available to measure this effect. The desired effect of seeding is to shift the entire size spectrum of hail produced by a storm toward smaller sizes. The best single parameter to measure this effect is the energy density of hail at the ground. Calculations can be made of the average energy density of, or total energy yielded by, seeded and unseeded hailswaths, or seeded and unseeded portions of the same hailswath. A comparison, based on many such calculations, could possibly determine the overall effect of seeding. Seeding effects determined by

analyses of hail insurance claims in townships could be verified independently by determining the relationship between the average hailfall energy density and the total hail insurance claims in each township. These methods, which use many energy density estimates over large areas, have the inherent advantage of averaging out the uncertainties in individual energy density estimates.

LIST OF REFERENCES

Barge, B. Radar signal depolarization by hydrometeors in Alberta hailstorms. In: *Proceedings, Fifteenth Radar Meteorology Conference,* American Meteorological Society, Champaign-Urbana, Illinois, 1972, pp. 1-6.

Personal communication. University of Alberta, 1977.

Battan, L. J. *Radar Observation of the Atmosphere,* University of Chicago Press, 1973, p. 44.

Battan, L. J., Brown S. R. and Herman, B. M. *Tables of the radar cross-sections of dry and wet ice spheres.* Institute of Atmospheric Physics, University of Arizona, Tucson, Arizona, 1970.

Beattie, A. G. *A photograhic study of the kinematics of natural hailstones.* M.Sc. thesis, University of Alberta, Edmonton, Alberta, 1975, p. 14.

Brandes, E. A. *Radar rainfall optimizing technique.* NOAA Tech Memo ERL NSSL-67, National Severe Storms Laboratory, Norman, Oklahoma, 1974.

Optimizing rainfall estimates with the aid of radar. *Journal of Applied Meteorology 14* (1975):1339-1345.

Changnon, S. A. Areal-temporal variations of hail intensity in Illinois. *Journal of Applied Meteorology, 6* (1967):536-541.

Hailstreaks. *Journal of the Atmospheric Sciences, 27* (1970):109-125.

Charlton, R. B. Personal communication. Associate professor of meteorology, University of Alberta, 1978.

Decker, F. W. and Calvin, L. D. Hailfall of 20 September 1959 near Medford, Oregon. *Bulletin of the American Meteorological Society, 42* (1961):475-480.

Dimaksian, A. M., Sotimov, N. V. and Zykov, N. A. Results of radar measurements of liquid precipitation. Trans. in: *Soviet hydrology: Selected Papers, 6*(1965):530-537.

Douglas, R. H. Size distributions, ice contents and radar reflectivities of hail in Alberta. *Nubila, III*(1960):5-11.

Size distributions of Alberta hail samples. In: *Sci. Report MW-36*, Stormy Weather Group, McGill University, 1963, pp. 55-70.

The adjustment of radar estimates of storm mean rainfall with raingage data. In: *Proceedings, Twelfth Radar Meteorology Conference*, Norman, Oklahoma, 1966.

Ludlam, F. H. The hail problem. *Nubila, I*(1958):12-95.

Macklin, W. C. Heat transfer from hailstones. *Quarterly Journal of the Royal Meteorological Society, 89*(1963):360-369.

Marshall, J. S., Langille, R. C., and Palmer, W. M. Measurement of rainfall by radar. *Journal of Meteorology, 4*(1947):186-192.

Marshall, J. S. and Palmer, W. M. The distribution of raindrops with size. *Journal of Meteorology, 5*:165-166, 1948.

Mason, B. J. *The Physics of Clouds*. Oxford University: Clarendon Press, 1971, p. 367.

McLeish, D. Personal communication, Assistant professor of mathematics, University of Alberta, 1978.

Rogers, R. R. The effect of variable target reflectivity on weather radar measurements. *Quarterly Journal of the Royal Meteorological Society, 97*(1971):154-168.

Schleusener, R. A. and Jennings, P. C. An energy method for relative estimates of hail intensity. *Bulletin of the American Meteorological Society, 41*(1960):372-376.

Smith, P. L., Myers, C. G. and Orville, H. D. Radar reflectivity factor calculations in numerical cloud models using bulk parameterization of precipitation. *Journal of Applied Meteorology, 14*(1965):1156-1165.

Stout, G. E. and Mueller, E. A. Survey of relationship between rainfall rate and radar reflectivity in the measurement of precipitation. *Journal of Applied Meteorology, 7*(1968):465-473.

Strong, G. *The objective measurement of Alberta hailfall*. M.Sc. thesis, University of Alberta, Edmonton, Alberta, 1974.

Strong, G. and Lozowski, E. P. An Alberta study to objectively measure hailfall intensity. *Atmosphere, 15*:33-53, 1977.

Ulbrich, C. W. Doppler radar relationship for hail at vertical incidence. *Journal of Applied Meteorology, 16:*1349-1359.

Waldvogel, A., Schmid, W. and Federer, B. Z-E relations and kinetic energies of hailfalls. In: *Proceedings of the Eighteenth Radar Meteorology Conference,* Atlanta, Georgia, 1978.

Wilson, J. W. Storm-to-storm variability in the radar reflectivity-rainfall rate relationship. In: *Proceedings of the Twelfth Radar Meteorology Conference,* pp. 229-233.

Integration of radar and raingage data for improved rainfall measurement. *Journal of Applied Meteorology, 9*(1970): 489-497.

Wojtiw, L. Personal communication, University of Alberta, 1975.

Woodley, W. L., Olsen, A., Herndon, A. and Wiggert, V. *Optimizing the measurement of convective rainfall in Florida,* NOAA Tech Memo ERL WMPO-18, Weather Modification Program Office, Boulder, Colorado, 1974.

APPENDIX A

APPENDIX A

SUMMARY OF HAILPAD DATA USED IN THIS STUDY

Date (1974)	Station I.D.	Land Location	Hail Start Time (MDT)	Hailfall Duration (min)	Kinetic Energy (Jm^{-2})	
					Original Analysis	New Calibration[3]
July 30	A18	SW10,48,4,5	1717	13	79.0	23.9
	A19	NE27,48,4,5	1700	30	191.1	76.6
	B21	NE17,47,3,5	1730	15	46.8	14.9
	B33	NW25,47,27,4	1800	5	115.4	43.4
	B36	NW26,47,26,4	1810	4	3.7	0.9
	B39	SE7,47,25,4	1817	2	4.8	1.2
	B46	SE4,47,25,4	1840	5	7.5	1.9
	B51	SE14,47,21,4	1855	10	36.5	9.6
	C27	NW5,46,1,5	1800	3	1.7	0.5
	C36	SE23,46,26,4	1755	10	18.5	10.8
	C39	SE35,46,25,4	1822	2	3.7	1.1
	C48	NW20,46,20,4	1850	<1	8.5	3.1
	D31	SE14,45,28,4	1800	15	4.2	1.2
	D33	SW33,45,27,4	1815	14	76.8	28.6
	D34	SW24,45,27,4	1820	10	17.1	6.0
	D36[1]	SW6,45,26,4	1830	10	17.9	5.1
	D36[1]	SW6,45,26,4			110.6	40.6
	D48	NE25,45,22,4	1906	8	29.8	10.0
	D49	NW12,45,22,4	1700	15	28.0	10.0
	D51	NE3,45,21,4	1920	3	28.0	8.9

[1]Multiple hail bursts: more than one hailpad collected at a site from a single storm.
[2]Total energy density from multiple hail bursts.
[3]See Page 12 of text.

Continued ↓

Appendix A

Summary of Hailpad Data Used in This Study, Continued

July 30	E27	NW22,44,1,5	1815	5	6.4	1.6
	E57	SW6,44,19,4	1935	10	182.4	86.7
	F42	NW16,43,24,4	1901	5	37.1	12.5
	F46	SE4,43,23,4	1915	5	137.1	52.3
	G36	NW30,42,26,4	1830	15	56.6	19.2
	G37	SE24,42,26,4	1845	5	2.8	0.8
	G42	NE34,42,24,4	1907	6	72.7	27.5
	G43	NE12,42,24,4	1900	10	126.4	27.7
	H48	SW1,41,22,4	1934	3	129.6	49.7
	I12	NE7,40,6,5	1740	4	322.7	126.3
	I14	NE13,40,6,5	1750	3	162.2	64.1
August 7	B51	SE14,47,21,4	1630	5	17.9	4.1
	C42	NW5,46,24,4	1445	15	61.0	18.9
	C45	NW11,46,23,4	1555	7		
	C48	NW20,46,20,4	1608	4	66.8	18.2
	D31	SE14,45,28,4	1330	30	92.3	26.5
	D33	SW33,45,27,4			7.6	1.6
	D36	SW6,45,26,4	1430	10	196.6	50.2
	D37	SW13,45,28,4	1447	3	463.1	166.1
	D45	NE17,45,23,4	1305	4	1.6	0.4
	D49	NW12,45,22,4	1615	10	33.7	8.5
	E33	SE28,44,27,4	1500	30	100.2	22.4
	E36	SW22,44,26,4	1446	12	18.8	4.5
	F18	SE24,43,4,5			7.3	1.8
	F30	SE36,43,28,4	1350	10	85.8	19.5
	F33	NW8,43,27,4	1445	1	76.4	17.3
	F34	NE12,43,27,4	1445	10	60.8	15.1
	F36	SW31,43,26,4	1455	6	34.4	8.2
	F39	SE33,43,25,4	1525	5	68.6	21.1
	G27	SW36,42,1,5	1330	1	18.9	4.5

continued ↓

Appendix A

Summary of Hailpad Data Used in This Study, Continued

August 27 (cont'd)	G28	SW24,42,1,5			93.6	23.9
	G39	SW28,42,25,4	1705	8	180.9	59.3
	G43	NE12,41,24,4	1510	15	52.7	16.5
	G45	SW35,42,23,4	1755	6	21.3	4.5
	H37	NE20,41,26,4	1650	5	27.2	8.7
	I54	SE15,40,20,4	1700	5	2.3	0.5
	J6	SW22,39,8,5			17.4	3.5
	J7	SE7,39,8,5			0	0
	M10	SE13,36,8,5			17.6	4.6
	N0	SE12,35,3,5			9.9	2.0
	N6	SW29,35,1,5			4.4	0.9
	N9	SE13,35,1,5			1.3	0.2
	O0	NW18,34,5,5			14.9	3.0
	O35	SW34,34,22,4	2045	10	51.5	17.4
	P12	NE26,33,5,5			0	0
	P17	NW35,33,28,4	2002	3	154.7	58.1
	P21	NW30,33,25,4			76.2	19.1
	P34	NW19,33,17,4	1845	2	1.0	0.2
	Q4	NE13,32,3,5			37.6	8.2
	Q9	NE8,32,1,5			1.4	0.3
	Q11	NW14,32,5,5	2100	5	25.1	7.3
	Q16	NW27,32,28,4			13.0	2.9
	Q18	SW19,32,25,4	1637	3	2.1	0.5
	R4	SE26,31,2,5	2015	3	16.0	5.4
	R20	NE6,31,26,4	1845	5	0.4	0.1
	S9	NW10,30,1,5	1430	1	66.2	23.3
	S11	NW11,30,29,4	1515	20	15.1	4.2
	S12	SW28,30,28,4	1540	20	7.5	1.8
	T4	SE17,29,3,5	1605	15	41.4	10.0
	U36	SE31,28,26,4	1650	1	12.8	4.6

continued ↓

Appendix A

Summary of Hailpad Data Used in This Study, Continued

August 15	J7	SE7,39,8,5			0.1	0.0
	M4	NE32,36,3,5			0	0
	P12	NE26,33,5,5	2020	11	3.1	0.6
	Q80[1]	NE36,32,3,5			0.4	0.4[2]
	Q80[1]	NE36,32,3,5	2045	1	1.5	0.4[2]
	Q82	NE29,32,4,5			14.1	2.9
August 18	J6	SW22,39,8,5			0	0
	K6	SW12,38,4,5			0.5	0.1
	K8	SE9,38,2,5			0	0
	K21	SE12,38,7,5	1755	5	12.9	4.5
	L0	SE24,37,8,5	1815	10	77.5	16.1
	L2	NE19,37,5,5	1815	4	77.7	26.8
	L4	NW15,37,5,5	1817	10	177.1	63.8
	L18	SW15,37,4,5			110.8	33.0
	M0	SW15,36,5,5	1852	3	56.8	14.5
	M1	SE14,36,4,5	1615	10	121.7	39.8
	M4	NE32,36,3,5	1830		260.9	101.9
	M13	SW17,36,2,5	1850	10	310.4	127.7
	N	SE12,35,3,5	1650	5	25.6	7.3
	N2	NE12,35,4,5	1902	13	68.6	17.5
	N9	SE13,35,1,5	1900	2	60.9	18.0
	N22	NE23,35,5,5	1855	10	171.8	56.8
	N80	NE28,35,3,5	1633	18	124.6	41.6
	O4	SE25,34,4,5			73.7	22.4
	O5[1]	SE1,34,4,5			13.2	
	O5[1]	SE1,34,4,5	1920	4	102.8	33.2[2]
	O7	SE32,34,1,5	1905	25	50.3	15.1
	O16	NE29,34,28,4	1730	15	42.7	13.1
	O17	SW12,38,4,5			0.5	3.2
	O18	SE20,34,27,4			10.8	2.3

[1]Multiple hail bursts

[2]Total energy density from multiple hail bursts

continued ↓

Appendix A
Summary of Hailpad Data Used in This Study, Continued

August 18 (Cont'd)	P17	NW35,33,28,4	1730	5	2.2	0.5
	Q1	SE3,32,5,5	1935	-	41.2	13.9
	Q9	NE8,32,1,5	2028	2	37.4	10.5
	Q16	NW27,32,28,4	2001	6	63.9	14.1
	Q18	SW19,32,25,4	2140	2	1.9	0.4
	Q31	NW14,32,22,4	1935	10	2.1	0.6
	R1	NW6,31,3,5	2120	1	116.3	41.9
	R8	SE19,31,2,5	0935	3	40.7	13.7
	R50	NE7,31,19,4	1950	10	9.1	2.0

APPENDIX B

LISTINGS OF MAJOR PROGRAMS

Notes: Page

- PLOT

```
      INTEGER QRT,SEC,TNSHP,RANGE,RRNGE(50),RAZM(50),SPACE(50),IID(4),
     *LTIM,HTIM,ID(4,50),
     *STLTIM,STHTIM,SPLTIM,SPHTIM,BLANK,TIMSTT(3),TIMSTP(3),HR,MIN,SEC,
     *CNTNUM,BIN,HTIM,LTIM
      INTEGER*2 M(3072),LEN,IHTIM,ILTIM
      LOGICAL DOWN,UP
      COMMON ID,INTEN,NUMBER
      COMMON II
      LOGICAL*1 A(6)
      DATA BLANK/' '/
      REAL PAZM(50),INTEN(53),INCEPT
      LTIM(IHTIM,ILTIM)=IHTIM*32768+ILTIM
      BINTIM(HR,MIN,SEC)=HR*216000.+MIN*3600.+SEC*60.
      WRITE(6,300)
300   FORMAT('1 INPUT BEGINNING TIME AND ENDING TIME OF SURVEY',/)
      READ(5,100)TIMSTT,TIMSTP
100   FORMAT(6(I2,1X))
      WRITE(6,305)
305   FORMAT(' ',//,' INPUT SLOPE,INTERCEPT,AND RADAR CONSTANT',/)
C FREAD IS A FORTRAN SPECIAL ROUTINE USED UNDER MTS,U OF A.
      CALL FREAD(5,'3R:',SLOPE,INCEPT,RADAR)
      START=BINTIM(TIMSTT(1),TIMSTT(2),TIMSTT(3))
      TSTOP=BINTIM(TIMSTP(1),TIMSTP(2),TIMSTP(3))
2000  WRITE(6,301)
301   FORMAT(' ',//,' INPUT QUARTER,SECTION,TOWNSHIP,RANGE,'// MERIDIAN,
     * AND IDENTIFICATION FOR EACH LOCATION.')
      NUMBER=50
      DO 1 I=1,50
8     READ(5,101)QRT,SEC,TNSHP,RANGE,MER,(ID(J,I),J=1,4)
      IF(QRT.EQ.BLANK)GO TO 9
101   FORMAT(A2,4I10,4A2)
C CONVERTS SURVEY COORDINATES TO RADAR RANGE (KM) AND AZM
C (631 PER SCAN) WITH ZERO AT 140 DEGREES FROM TRUE NORTH.
5     CALL LAND(QRT,SEC,TNSHP,RANGE,MER,RRNGE(I),RAZM(I),PAZM(I))
C CHECK FOR INVALID LAND LOCATIONS. IF SO,INFORM THE WORLD.
      IF (RRNGE(I).GT.147)GO TO 6
      IF (RRNGE(I).GT.3)GO TO 1
      WRITE(6,302)(ID(J,I),J=1,4)
302   FORMAT(' PAD ',4A2,' IS LESS THAN 3KM.FROM THE RADAR. NO DATA
     *IS AVAILABLE. THE LOCATION IS DELETED')
      GO TO 8
6     WRITE(6,303)(ID(J,I),J=1,4)
303   FORMAT(' PAD ',4A2,' IS MORE THAN 147 KM.FROM THE RADAR.NO DATA
     *IS AVAILABLE.  THE LOCATION IS DELETED.')
      GO TO 8
1     CONTINUE
      GO TO 12
9     NUMBER=I-1
C BUBBLE SORT LOCATIONS TO PREVENT COMMON REFERENCE OF SOURCE.
12    N1=NUMBER-1
      DO 2 I=1,N1
      N2=N1-I+1
      DO 3 J=1,N2
      IF (RAZM(J).LT.RAZM(J+1))GO TO 3
      IF (RAZM(J).EQ.RAZM(J+1).AND.RRNGE(J).LT.RRNGE(J+1))GO TO 3
      DO 15 K=1,4
      IID(K)=ID(K,J)
15    CONTINUE
      IAZM=RAZM(J)
      RPAZM=PAZM(J)
      IR=RRNGE(J)
```

```
      DO 16 K=1,4
      ID(K,J)=ID(K,J+1)
16    CONTINUE
      RAZM(J)=RAZM(J+1)
      PAZM(J)=PAZM(J+1)
      RRNGE(J)=RRNGE(J+1)
      DO 17 K=1,4
      ID(K,J+1)=IID(K)
17    CONTINUE
      RAZM(J+1)=IAZM
      PAZM(J+1)=RPAZM
C CALCULATE NUMBER OF RAYS TO SKIP TO GO FROM ONE LOCATION TO THE NEXT.
      RRNGE(J+1)=IR
3     CONTINUE
2     CONTINUE
      ISUM=0
      WRITE(6,400)NUMBER,((ID(K,I),K=1,4),PAZM(I),RRNGE(I),I=1,NUMBER)
400   FORMAT(' PAD IDENT AZM D RNGE KM',I6/(' ',4A2,2X,F6.0,I6))
      SPACE(1)=RAZM(1)
      DO 4 I=2,NUMBER
      SPACE(I)=RAZM(I)-RAZM(I-1)
4     CONTINUE
C READ ONE RECORD,ALSO INITIALIZE SUM IN SUMARY.
      WRITE(6,402)
402   FORMAT(' ',' ENTER TAPE MOUNT#',/)
222   CALL FREAD(5,'I:',II)
      IF (II.GT.0.AND.II.LE.13)GO TO 224
      WRITE(6,403)
403   FORMAT(' ',' INVALID INPUT..PLS RE-ENTER INPUT'/)
      GO TO 222
224   CALL TPMNT(II)
C CREATE OUTPUT FILE ON WHICH DATA WILL BE WRITTEN.
      CALL CREATF
      WRITE(7)NUMBER,ID,PAZM,RRNGE
C SKIP A NUMBER OF RECORDS (6144 IN LENGTH) DEPENDING ON INPUT TIME.
      CALL SKPREC(II,START,M,CNTNUM)
C GET SOME MORE DATA ON TAPE.
      CALL DATA(M,CNTNUM,&40,&2000)
C INITILAZE SUMARY.
      CALL SUMARY(1)
      DOWN=.TRUE.
      UP=.FALSE.
C SPACE FORWARD TO START TIME.
C GET DOWN PULSE (HEADING MARKER=12).
11    CALL HEDING(M,CNTNUM,DOWN,UP,&11,&40,&2000)
C EVERY BYTE OF DATA HAS TO BE SWITCHED AROUND (PDP11/45,DACZ).
      CALL BYTREV(M,CNTNUM+1)
      CALL BYTREV(M,CNTNUM+2)
C CONVERT FROM SYSTEM TIME TO REAL TIME.
      CLOCK=RTIM(M(CNTNUM+2),M(CNTNUM+1))
      IF(CLOCK.GE.START)GO TO 14
      CNTNUM=CNTNUM+2
      GO TO 11
C SET ELEVATION COUNTER TO ZERO (HEADING MARKER=12 FOLOLOWED BY
C HEADING MARKER=8).
C SKIP TO NEXT HEADING MARKER.IT WILL INDICATE A ZERO DEGREE SCAN.
14    CALL HEDING(M,CNTNUM,.FALSE.,.TRUE.,&14,&40,&2000)
      CALL BYTREV(M,CNTNUM+1)
      CALL BYTREV(M,CNTNUM+2)
      CLOCK=RTIM(M(CNTNUM+2),M(CNTNUM+1))
      HTIM=M(CNTNUM+2)
      LTIM=M(CNTNUM+1)
      CNTNUM=CNTNUM+2
22    ELEV=0.
      CALL TIME(CLOCK,HR,MIN,SEC)
C BTD IS SPECIAL MTS ROUTINE.(CONVERSION OF CHARACTERS)
```

```
      CALL BTD(HR,A(1),2,ND,'0')
      CALL BTD(MIN,A(3),2,ND,'0')
      CALL BTD(SEC,A(5),2,ND,'0')
      WRITE(6,401)A
401   FORMAT(' ',2A1,':',2A1,':',2A1)
      IF (CLOCK.GT.TSTOP)GO TO 40
23    INTEN(NUMBER+1)=HTIM
      INTEN(NUMBER+2)=LTIM
      DO 20 I=1,NUMBER
C SUBTRACT 3 BECAUSE FIRST THREE BINS ARE NOT RECORDED
      BIN=RRNGE(I)-3
      N=SPACE(I)
      IF (N.EQ.0)GO TO 25
      CALL SKPRAY(M,CNTNUM,N,&40,&2000)
      CNTNUM=CNTNUM+2
      IBIN=0
25    CALL DBZRAY(M,CNTNUM,BIN,IBIN,R,SLOPE,INCEPT,RADAR,&40,&2000)
26    INTEN(I)=R
20    CONTINUE
      INTEN(NUMBER+3)=ELEV
      WRITE(7)INTEN
      CALL SUMARY(2)
      CALL HEDING(M,CNTNUM,.FALSE.,.TRUE.,&27,&40,&2000)
      CNTNUM=CNTNUM+2
      IF (ELEV.EQ.22.5)GO TO 115
      ELEV=ELEV+1.5
      GO TO 23
115   CALL HEDING(M,CNTNUM,.FALSE.,.TRUE.,&27,&40,&2000)
      GO TO 115
27    ISUM=ISUM+1
      CALL BYTREV(M,CNTNUM+2)
      CALL BYTREV(M,CNTNUM+1)
      HTIM=M(CNTNUM+2)
      LTIM=M(CNTNUM+1)
      CLOCK=RTIM(M(CNTNUM+2),M(CNTNUM+1))
      IF (ISUM.EQ.17)GO TO 41
      GO TO 22
40    STOP
41    CALL SUMARY(3)
      ISUM=0
      GO TO 22
      END
```

```
C A SUBROUTINE TO BYTE REVERSE INTEGER*2 DATA.

      SUBROUTINE BYTREV(L,I)
      LOGICAL*1 L(6144),LA
      LA=L((I-1)*2+1)
      L((I-1)*2+1)=L(I*2)
      L(I*2)=LA
      RETURN
      END
```

```
C A SUBROUTINE TO DETECT RAYS AND SKIP TO THE BEGINNING
C OF A DESIRED RAY. FORWARD SKIPS ONLY.

      SUBROUTINE SKPRAY(M,CNTNUM,N,*,*)
      INTEGER CNTNUM,N
      INTEGER*2 M(3072)
12    IF (N.LT.0)GO TO 10
3     IF(N.EQ.0)RETURN
1     CNTNUM=CNTNUM+1
      IF(CNTNUM.GT.3072)CALL DATA(M,CNTNUM,&4,&5)
      IF(M(CNTNUM).EQ.144)CALL DATA (M,CNTNUM,&4,&5)
      IF(M(CNTNUM).EQ.0)GO TO 2
      GO TO 1
2     N=N-1
      GO TO 3
4     RETURN1
5     RETURN2
10    CNTNUM=CNTNUM-1
      IF(M(CNTNUM).EQ.0)GO TO 11
      GO TO 10
11    N=N+1
      GO TO 12
      END
```

```
C A SUBROUTINE TO READ DATA FROM TAPE AND
C MODIFY CNTNUM (COUNTER NUMBER) BACK TO 1

      SUBROUTINE DATA (M,CNTNUM,*,*)
      INTEGER CNTNUM,CONTRL(20)
      INTEGER*2 M(3072),LEN
      MOD=0
      LUNIT=0
1     CALL READ(M,LEN,MOD,LNR,LUNIT,&10)
      CNTNUM=1
      RETURN
10    CALL MOUTP(III)
      GO TO (4,3,2),III
2     RETURN1
3     GO TO 1
4     RETURN2
      END
```

```
C A SUBROUTINE TO DETECT HEADING MARKERS AND DOWN PULSES

      SUBROUTINE HEDING (M,CNTNUM,DOWN,UP,*,*,*)
      INTEGER CNTNUM
      INTEGER*2 M(3072)
      LOGICAL DOWN,UP
1     CNTNUM=CNTNUM+1
      IF(CNTNUM.GT.3072)CALL DATA(M,CNTNUM,&2,&4)
      IF(M(CNTNUM).EQ.144)CALL DATA(M,CNTNUM,&2,&4)
      IF(M(CNTNUM).EQ.0)GO TO 3
      IF(M(CNTNUM).EQ.12.AND.DOWN)RETURN
      IF(M(CNTNUM).EQ.8.AND.UP)RETURN
      IF(M(CNTNUM).EQ.12.AND.UP)RETURN1
      GO TO 1
3     CNTNUM=CNTNUM+2
      GO TO 1
2     RETURN2
4     RETURN3
      END
```

```
C SUBROUTINE TO GET A SPECIFIED BIN OF DATA FROM CURRENT RAY
C
C  BIN=RRNGE(I)-3
C
C   -16385=>ERROR FLAG
C   -28672=>END OF RECORD
C    2048=> NEW MARKER
C    3072=> DOWN PULSE


      SUBROUTINE DBZRAY(M,CNTNUM,BIN,IBIN,R,SLOPE,INCEPT,RADAR,*,*)
      REAL INCEPT
      INTEGER CNTNUM,BIN
      INTEGER*2 M(3072)
10    CNTNUM=CNTNUM+1
      IF(CNTNUM.GT.3072)GO TO 15
13    CALL BYTREV(M,CNTNUM)
      IF(M(CNTNUM).GE.0)GO TO 11
      IF(M(CNTNUM).EQ.-16385)GO TO 9
      IF(M(CNTNUM).EQ.-28672)GO TO 15
C SURELY IT IS A POINTER
      IBIN=M(CNTNUM)+145
      IF(IBIN.GT.BIN)GO TO 91
      GO TO 10
C ERROR IN NEXT DATA WORD.SKIP THE WORD.
9     CNTNUM=CNTNUM+2
      GO TO 13
15    CALL DATA(M,CNTNUM,&100,&101)
      GO TO 13
C NUMBER IS POSITIVE SO COULD BE FLAG,TIME OR DATA.
11    IF(M(CNTNUM).EQ.0)GO TO 17
      IF(M(CNTNUM).EQ.2048)GO TO 89
      IF(M(CNTNUM).EQ.3072)GO TO 88
      IF(BIN.EQ.IBIN)GO TO 90
      IBIN=IBIN+1
      GO TO 10
C NEW PULSE.THEREFORE M(BIN) EQUALS ZERO.
17    R=0.
      CNTNUM=CNTNUM-1
      RETURN
C DOWN PULSE: WHAT DO WE DO???
88    CALL BYTREV(M,CNTNUM)
      GO TO 17
C NEW MARKER: WHAT DO WE DO???
89    CALL BYTREV(M,CNTNUM)
      GO TO 17
C CALCULATE RANGE IN KM ALSO DBM AND DBZ.
90    RRANGE=(IBIN*1.048)+2.67
      DBM=SLOPE*M(CNTNUM)+INCEPT
      R=DBM+(20*ALOG10(RRANGE))+RADAR
      RETURN
91    CALL BYTREV(M,CNTNUM)
      GO TO 17
100   RETURN1
101   RETURN2
      END
```

```
C THIS SUBROUTINE CREATES THE HOURLY DATA SUMMARY

      SUBROUTINE SUMARY(II)
      REAL INTEN(53)
      INTEGER SUM(50,10),ID(4,50)
      COMMON ID,INTEN,NUMBER
      GO TO (1000,2000,3000),II
1000  DO 1001 J=1,10
      DO 1002 I=1,50
      SUM(I,J)=0
1002  CONTINUE
1001  CONTINUE
      RETURN
2000  DO 2001 I=1,NUMBER
      IDB=IFIX(INTEN(I)/10.)+1
      IF(IDB.GT.10)IDB=10
      IF(IDB.LT.0)IDB=0
      SUM(I,IDB)=SUM(I,IDB)+1
2001  CONTINUE
      RETURN
3000  WRITE(6,3001)
3001  FORMAT('1SUMARY OF DATA FOR THE LAST PERIOD'/
     *' NUMBER OF TIMES RADAR REFLECTIVITY WAS IN RANGE OF'/
     *' PAD IDENT  0-9 10-19 20-29 30-39 40-49 50-59 60-69'
     *,' 70-79 80-89 90-99 DBZ')
      DO 3002 I=1,NUMBER
      WRITE(6,3003)(ID(J,I),J=1,4),(SUM(I,J),J=1,10)
3003  FORMAT(' ',4A2,10I6)
3002  CONTINUE
      GO TO 1000
      END
```

```
C A SUBROUTINE TO CONVERT REAL TIME INTO HOURS AND MINUTES

      SUBROUTINE TIME(CLOCK,HR,MIN,SEC)
      INTEGER HR,SEC
      HR=INT(CLOCK/216000.)
      MIN=INT(CLOCK/3600.)-HR*60
      SEC=INT(CLOCK/60)-(HR*3600+MIN*60)
      RETURN
      END
```

```
C THE SUBROUTINE TO CREATE THE FILE ON THE OUTPUT TAPE.

      SUBROUTINE CREATF
      LOGICAL*1 FIL(10)
      LOGICAL*1 CHAR(99)/'$','M','O','U','N','T',' ','O','O','3','4','7'
     *,'O',' ','9','T','P',' ','*','T','A','P','E','*',' ','R','I','N','
     *G','=','I','N',' ','P','O','S','N','=','*','E','O','T','*',' ','V'
     *,'O','L','=','O','U','T','P','U','T',' ','F','M','T','=','F','B','
     * ','L','R','E','C','L','=','2','1','2',' ','S','I','Z','E','=','2'
     *,'1','2','0','0',' ','D','S','N','='/
      CALL FTNCMD('ASSIGN 4=NEWDIRECTORY',21)
      CALL FTNCMD('ASSIGN 3=NEWDIRECTORY(*L+1)',27)
      WRITE(6,101)
101   FORMAT(' ',' PLS ENTER NAME OF FILE TO BE CREATED ON TAPE',/)
6     CALL FREAD(5,'STRING:',CHAR(88),11)
4     READ(4,104,END=10)FIL
104   FORMAT(10A1)
      IF(LCOMC(10,FIL,CHAR(88)).EQ.0)GO TO 11
      GO TO 4
10    WRITE(3,103)(CHAR(J),J=88,98)
103   FORMAT(11A1)
      CALL CMD(CHAR,98)
      CALL FTNCMD('ASSIGN 7=*TAPE*',15)
      RETURN
11    WRITE(6,102)
102   FORMAT(' ',' FILE ALREADY EXISTS ON TAPE...PLS RE-ENTER FILE NAME.
     *',/)
      GO TO 6
      END
```

```
C THIS SUBROUTINE SKIPS A NUMBER OF RECORDS DEPENDING
C ON THE POSITION OF MARKER ON TAPE.

      SUBROUTINE SKPREC(II,START,M,CNTNUM)
      INTEGER HR,MIN,SEC,HR1,MIN1
      INTEGER*2 M(3072),IHTIM,ILTIM
      INTEGER CNTNUM
      LOGICAL DOWN,UP
      INTEGER*2 HRS(13)/16,18,13,15,17,19,20,21,14,15,16,17,18/
      INTEGER*2 MINU(13)/05,32,10,55,27,40,18,55,43,35,55,37,36/
      RTIM(IHTIM,ILTIM)=IHTIM*32768+ILTIM
      CLOCK=START
      CALL TIME(CLOCK,HR,MIN,SEC)
      TOTAL=(HR*60+MIN)-(HRS(II)*60+MINU(II))
9     IF (TOTAL.LE.12.AND.TOTAL.GE.0)RETURN
      CALL SKIP(0,INT((TOTAL/6)*75),0,&4)
      CALL DATA(M,CNTNUM)
10    CALL HEDING(M,CNTNUM,.TRUE.,.FALSE.,&10)
      CALL BYTREV(M,CNTNUM+1)
      CALL BYTREV(M,CNTNUM+2)
      CLOCK=RTIM(M(CNTNUM+2),M(CNTNUM+1))
      CALL TIME(CLOCK,HR1,MIN1,SEC)
      TOTAL=(HR*60+MIN)-(HR1*60+MIN1)
      GO TO 9
4     RETURN
      END
```

```
C THIS SUBROUTINE CHOOSES A RADAR DATA TAPE FROM A NUMBERED SERIES
C AND MOUNTS IT.

      SUBROUTINE TPMNT(II)
      INTEGER*2 LEN/24/,LEN1/80/
      INTEGER CONTR(20)
      GO TO (1,2,3,24,25,26,27,8,9,10,11,12,13),II
      WRITE(6,101)
101   FORMAT(' PLS ENTER TAPE MOUNT',/)
      READ(5,102)CONTR
102   FORMAT(80A1)
C MOUNT IS ANOTHER SPECIAL MTS FORTRAN ROUTINE.
      CALL MOUNT(CONTR,LEN1)
      GO TO 6
1     CALL MOUNT('003271 9TP *T* SIZE=6144',LEN)
      GO TO 6
2     CALL MOUNT('003272 9TP *T* SIZE=6144',LEN)
      GO TO 6
3     CALL MOUNT('003260 9TP *T* SIZE=6144',LEN)
      GO TO 6
24    CALL MOUNT('003261 9TP *T* SIZE=6144',LEN)
      GO TO 6
25    CALL MOUNT('003262 9TP *T* SIZE=6144',LEN)
      GO TO 6
26    CALL MOUNT('003263 9TP *T* SIZE=6144',LEN)
      GO TO 6
27    CALL MOUNT('003264 9TP *T* SIZE=6144',LEN)
      GO TO 6
8     CALL MOUNT('003265 9TP *T* SIZE=6144',LEN)
      GO TO 6
9     CALL MOUNT('003266 9TP *T* SIZE=6144',LEN)
      GO TO 6
10    CALL MOUNT('003267 9TP *T* SIZE=6144',LEN)
      GO TO 6
11    CALL MOUNT('003268 9TP *T* SIZE=6144',LEN)
      GO TO 6
12    CALL MOUNT('003269 9TP *T* SIZE=6144',LEN)
      GO TO 6
13    CALL MOUNT('003270 9TP *T* SIZE=6144',LEN)
6     CALL FTNCMD('ASSIGN 0=*T*',12)
      RETURN
      END
```

```
C THIS SUBROUTINE CHANGES THE DATA TAPE DURING PRINT-OUT OF THE DATA
C SUMMARY.

      SUBROUTINE MOUTP(III)
      REAL INTEN(50)
      INTEGER ID(4,50)
      COMMON ID,INTEN,NUMBER
      INTEGER*2 LEN
      COMMON II
      CALL SUMARY(3)
      WRITE(6,100)
100   FORMAT(' ',' END-OF-FILE ON TAPE#',//,' WHAT DO YOU WANT TO DO
     1WITH TAPE?',//,' ENTER NUMBER CORRESPONDING TO THE FOLLOWING:',//,
     *' 1=>REWIND AND RE-USE.',/,' 2=>UNLOAD AND MOUNT NEW TAPE.',
     */,' 3=>UNLOAD AND STOP.',/)
4     CALL FREAD(5,'I:',III)
      GO TO (5,6,7),III
      WRITE(6,102)
102   FORMAT(' ',' INVALID INPUT...PLS RE-ENTER INPUT',/)
      GO TO 4
5     CALL REWIND(0)
      RETURN
6     WRITE(6,103)
103   FORMAT(' PLS ENTER NEW TAPE#')
19    CALL FREAD(5,'I:',II)
      IF(II.GT.0.AND.II.LE.13)GO TO 600
      WRITE(6,102)
      GO TO 19
600   CALL TPMNT(II)
      RETURN
7     RETURN
      END
```

PLOTPAD

```
      REAL PAZM(50),INTEN(53),ELEV(15),A(2),HEIGHT(15)
      REAL IHTIM,ILTIM,TIM1,TIM2,CLOCK
      INTEGER RRNGE(50),HIST(15,20),A1(20),ID(4,50),WRONG(2)
     *,PAD(4),HR
      DATA WRONG/'ST','OP'/
      LOGICAL EQUC
      LOGICAL*1 FIL(10)
      LOGICAL*1 A2(6)
      RTIM(IHTIM,ILTIM)=IHTIM*32768+ILTIM
      LOGICAL*1 CHAR(28)/'$','C','O','N',' ','*','T','A','P','E','*',' '
     *,'P','O','S','N','='/
      WRITE(6,700)
700   FORMAT(' ',' PLS INPUT NAME OF OUTPUT FILE',/)
      CALL FTNCMD('ASSIGN 4=NEWDIRECTORY',26)
1112  CALL FREAD(5,'STRING:',CHAR(18),11)
      REWIND 4
1109  READ(4,407,END=1111)FIL
407   FORMAT(10A1)
      IF(LCOMC(10,FIL,CHAR(18)).EQ.0)GO TO 1110
      GO TO 1109
1111  WRITE(6,401)(CHAR(I),I=18,28)
401   FORMAT(' ','FILE ',11A1,'DOES NOT EXIST..PLS RE-ENTER FILENAME',/)
      GO TO 1112
1110  CALL FTNCMD(CHAR,28)
      CALL FTNCMD('$COPY *TAPE* -Y',15)
      CALL FTNCMD('ASSIGN 7=-Y',11)
      CALL FTNCMD('$RELEASE *TAPE*',15)
605   READ(7,END=600)NUMBER,ID,PAZM,RRNGE
C READ ID OF DESIRED PAD.
      WRITE(6,200)
200   FORMAT('  INPUT DESIRED PAD IDENTIFICATION OR "STOP"'/)
3     READ(6,100)PAD
100   FORMAT(4A2)
      IF(PAD(1).EQ.WRONG(1).AND.PAD(2).EQ.WRONG(2))STOP
604   DO 1 IP=1,NUMBER
      DO 80 K=1,4
      IF(PAD(K).NE.ID(K,IP))GO TO 1
80    CONTINUE
      GO TO 2
1     CONTINUE
      WRITE(6,201)PAD
201   FORMAT('  PAD ',4A2,' CANNOT BE FOUND. PLS RE-ENTER IDENT'/)
      GO TO 3
2     N1=NUMBER+1
      N2=NUMBER+2
      N3=NUMBER+3
      DO 10 I=1,15
      HEIGHT(16-I)=(RRNGE(IP))*1.5*(I-1)*3.1415927/180.
10    CONTINUE
      DO 11 J=1,20
      DO 12 K=1,15
      HIST(K,J)=0
12    CONTINUE
11    CONTINUE
      DO 13 J=1,20
      A1(J)=0
13    CONTINUE
6     READ(7,END=601)INTEN
14    TIM2=INTEN(N1)
      TIM1=INTEN(N2)
      MIH=0
      II=0
```

```
      A1(1)=0
7     CALL EXTRAC(HIST,1,ELEV,INTEN,N3,IP,LIH,II)
      IF(LIH.GT.MIH)MIH=LIH
      IF(II.EQ.-1)GO TO 601
      IF(II.EQ.1.AND.LIH.EQ.0)GO TO 14
      IF(LIH.EQ.0)GO TO 6
      CLOCK=RTIM(TIM2,TIM1)
      CALL TIME(CLOCK,HR,MIN,SEC)
      HIST(1,1)=0
      DO 4 I=2,20
      IF(II.EQ.0)READ(7,END=601)INTEN
      II=0
      A1(I)=IFIX(((INTEN(N1)-TIM2)*32768.+(INTEN(N2)-TIM1))/3600.)
      CALL EXTRAC(HIST,I,ELEV,INTEN,N3,IP,LIH,II)
      IF(LIH.GT.MIH)MIH=LIH
      IF(II.EQ.-1)GO TO 500
4     CONTINUE
500   IF(MIH.EQ.0)GO TO 601
      CALL BTD(HR,A2(1),2,ND,'0')
      CALL BTD(MIN,A2(3),2,ND,'0')
      CALL BTD(SEC,A2(5),2,ND,'0')
      WRITE(6,202)PAD,A2,RRNGE(IP),PAZM(IP)
202   FORMAT('1',6X,' TIME-HEIGHT-REFLECTIVITY FOR PAD ',4A2,/6X,
     *' START TIME=',2A1,':',2A1,':',2A1,'  DISTANCE=',I3,' KM.  AZIMUTH
     *=',F4.0,' DEG',/,'DEG',63X,'KM.')
      DO 5 J=1,15
      WRITE(6,203)ELEV(J),(HIST(J,K),K=1,20),HEIGHT(J)
203   FORMAT(' ',F4.1,'?',20I3,'?',F4.1)
5     CONTINUE
      WRITE(6,204)(A1(J),J=1,20)
204   FORMAT(' ',4X,'.....',/,
     *'.....',/,'  TIME',20I3,' MIN'////)
      MIH=0
      DO 8 J=1,20
      DO 9 K=1,15
      HIST(K,J)=0
9     CONTINUE
8     CONTINUE
      DO 15 J=1,20
      A1(J)=0
15    CONTINUE
      IF(II.EQ.-1)GO TO 601
      IF(LIH.EQ.0)GO TO 6
      IF(II.EQ.0)READ(7,END=601)INTEN
      II=0
      A1(1)=IFIX(((INTEN(N1)-TIM2)*32768+(INTEN(N2)-TIM1))/3600.)
      GO TO 7
600   WRITE(6,602)
602   FORMAT(' END-OF-FILE READ WHILE READING PREAMBLE???')
      REWIND 7
      GO TO 605
601   CONTINUE
      REWIND 7
      GO TO 605
      END
```

```
C THIS SUBROUTINE EXTRACTS DBZ'S FROM THE OUTPUT TAPE

      SUBROUTINE EXTRAC(HIST,I,ELEV,INTEN,N3,IP,LIH,II)
      REAL ELEV(15),INTEN(53)
      INTEGER HIST(15,20)
      ELEV(15)=INTEN(N3)
      IH=IFIX(INTEN(IP))
      HIST(15,I)=IH
      LIH=IH
      DO 5 J=2,15
      READ(7,END=1)INTEN
      IF(INTEN(N3).EQ.0.0)GO TO 11
      ELEV(16-J)=INTEN(N3)
      IH=IFIX(INTEN(IP))
      HIST((16-J),I)=IH
      IF(IH.GT.LIH)LIH=IH
5     CONTINUE
      READ(7,END=1)INTEN
      IF(INTEN(N3).EQ.22.5)RETURN
      HIST(1,I)=0
11    II=1
13    IF(INTEN(N3).EQ.0.0)RETURN
      READ(7,END=1)INTEN
      GO TO 13
1     CONTINUE
      II=-1
      RETURN
      END
```

```
C A SUBROUTINE TO CONVERT REAL TIME INTO HOURS AND MINUTES

      SUBROUTINE TIME(CLOCK,HR,MIN,SEC)
      INTEGER HR,SEC
      HR=INT(CLOCK/216000.)
      MIN=INT(CLOCK/3600.)-HR*60
      SEC=INT(CLOCK/60)-(HR*3600+MIN*60)
      RETURN
      END
```

```
PADEN

      REAL PAZM(50),INTEN(53),ELEV(15),A(2),HEIGHT(15),ENSUM(4)
      REAL IHTIM,ILTIM,TIM1,TIM2,CLOCK
      INTEGER RRNGE(50),HIST(15,20),ID(4,50),WRONG(2),A1(20)
     *,PAD(4),HR
      DATA WRONG/'ST','OP'/
      LOGICAL EQUC
      LOGICAL*1 FIL(10)
      LOGICAL*1 A2(6)
      RTIM(IHTIM,ILTIM)=IHTIM*32768+ILTIM
      LOGICAL*1 CHAR(28)/'$','C','O','N',' ','*','T','A','P','E','*',' '
     *,'P','O','S','N','='/
      WRITE(6,199)
199   FORMAT(' ENERGY INTEGRALS LISTED IN DECREASING ORDER OF THRESHOLD
     *DBZ:45,40,35,30'///' PLS INPUT NAME OF OUTPUT FILE',/)
      CALL FTNCMD('ASSIGN 4=NEWDIRECTORY',26)
1112  CALL FREAD(5,'STRING:',CHAR(18),11)
      REWIND 4
1109  READ(4,407,END=1111)FIL
407   FORMAT(10A1)
      IF(LCOMC(10,FIL,CHAR(18)).EQ.0)GO TO 1110
      GO TO 1109
1111  WRITE(6,401)(CHAR(I),I=18,28)
401   FORMAT(' ','FILE ',11A1,'DOES NOT EXIST..PLS RE-ENTER FILENAME',/)
      GO TO 1112
1110  CALL FTNCMD(CHAR,28)
      CALL FTNCMD('$COPY *TAPE* -Y',15)
      CALL FTNCMD('ASSIGN 7=-Y',11)
      CALL FTNCMD('$RELEASE *TAPE*',15)
605   READ(7,END=600)NUMBER,ID,PAZM,RRNGE
C READ ID OF DESIRED PAD.
      WRITE(6,200)
200   FORMAT('  INPUT DESIRED PAD IDENTIFICATION OR "STOP"'/)
3     READ(6,100)PAD
100   FORMAT(4A2)
      IF(PAD(1).EQ.WRONG(1).AND.PAD(2).EQ.WRONG(2))STOP
604   DO 1 IP=1,NUMBER
      DO 80 K=1,4
      IF(PAD(K).NE.ID(K,IP))GO TO 1
80    CONTINUE
      GO TO 2
1     CONTINUE
      WRITE(6,201)PAD
201   FORMAT('  PAD ',4A2,' CANNOT BE FOUND. PLS RE-ENTER IDENT'/)
      GO TO 3
2     N1=NUMBER+1
      N2=NUMBER+2
      N3=NUMBER+3
      DO 10 I=1,15
      HEIGHT(16-I)=(RRNGE(IP))*1.5*(I-1)*3.1415927/180.
10    CONTINUE
C SET UPPER AND LOWER ELEVATION BOUNDS FOR DBZ CALCULATION.
      MAX=0
      DO 20 I=1,15
      IF(HEIGHT(I).GE.4.0)GO TO 20
      MAX=I
      GO TO 21
20    CONTINUE
21    MINI=0
      DO 22 I=MAX,15
      IF(HEIGHT(I).GE.1.5)GO TO 22
      MINI=I-1
      GO TO 23
```

```
22    CONTINUE
23    INT=MINI-MAX+1
      DO 11 J=1,20
      DO 12 K=MAX,MINI
      HIST(K,J)=0
12    CONTINUE
11    CONTINUE
6     READ(7,END=601)INTEN
14    TIM2=INTEN(N1)
      TIM1=INTEN(N2)
      MIH=0
      II=0
7     CALL EXTRAC(HIST,1,ELEV,INTEN,N3,IF,LIH,II)
      IF(LIH.GT.MIH)MIH=LIH
      IF(II.EQ.-1)GO TO 601
      IF(II.EQ.1.AND.LIH.E Q.0)GO TO 14
      IF(LIH.EQ.0)GO TO 6
      CLOCK=RTIM(TIM2,TIM1)
      CALL TIME(CLOCK,HR,MIN,SEC)
      HIST(1,1)=0
      DO 4 I=2,20
      IF(II.EQ.0)READ(7,END=601)INTEN
      II=0
      CALL EXTRAC(HIST,I,ELEV,INTEN,N3,IF,LIH,II)
      IF(LIH.GT.MIH)MIH=LIH
      IF(II.EQ.-1)GO TO 500
4     CONTINUE
500   IF(MIH.EQ.0)GO TO 601
      CALL BTD(HR,A2(1),2,ND,'0')
      CALL BTD(MIN,A2(3),2,ND,'0')
      CALL BTD(SEC,A2(5),2,ND,'0')
      WRITE(6,202)PAD,A2
202   FORMAT('1','HOURLY RADAR-ENERGY INTEGRALS FOR PAD ',4A2,/' START T
     *IME=',2A1,':',2A1,':',2A1/)
      THRESH=45.0
      DO 1000 I=1,4
      ENSUM(I)=0.
      DO 1001 J=MAX,MINI
      DO 1001 K=1,20
      FIST=FLOAT(HIST(J,K))
      IF(FIST.GE.THRESH)ENSUM(I)=ENSUM(I)+4.76*10**(FIST/12.-7.)*(2
     *11./FLOAT(INT))
1001  CONTINUE
      WRITE(6,203)ENSUM(I)
203   FORMAT(' ',F10.3)
1000  THRESH=THRESH-5.0
      MIH=0
      DO 8 J=1,20
      DO 9 K=MAX,MINI
      HIST(K,J)=0
9     CONTINUE
8     CONTINUE
      IF(II.EQ.-1)GO TO 601
      IF(LIH.EQ.0)GO TO 6
      IF(II.EQ.0)READ(7,END=601)INTEN
      II=0
      GO TO 7
600   WRITE(6,602)
602   FORMAT(' END-OF-FILE READ WHILE READING PREAMBLE???')
      REWIND 7
      GO TO 605
601   CONTINUE
      REWIND 7
      GO TO 605
      END
```

PPI

```
C PROGRAM TO GET DATA ON TAPE AND CONVERT IT TO DBZ'S.

      INTEGER*2 IHTIM,ILTIM,M(3072),RBINS(130,20)
      REAL INCEPT
      REAL RAZM(100),MILES(100)
      LOGICAL*1 A(6)
      LOGICAL UP,DOWN,SKIP/.FALSE./
      INTEGER MIN,SEC,HR,CNTNUM
      INTEGER TIMSTT(3)
      RTIM(IHTIM,ILTIM)=IHTIM*32768+ILTIM
      BINTIM(HR,MIN,SEC)=HR*216000.+MIN*3600.+SEC*60.
      COMMON RAZM,MILES
      COMMON SLOPE,INCEPT,RADAR,IPTR
      WRITE(6,300)
300   FORMAT('1INPUT BEGINNING TIME.')
      READ(5,101)TIMSTT
101   FORMAT(3(I2,1X))
      WRITE(6,301)
301   FORMAT(//,' INPUT SLOPE,INTERCEPT,RADAR,AND AZIMUTH(DEGREES).')
      CALL FREAD(5,'3R,I:',SLOPE,INCEPT,RADAR,N)
      N1=N
      N=((N*1.0)-140.0)*631./360.
      IF(N.LT.0)N=N+631.
      IAZ=N
      START=BINTIM(TIMSTT(1),TIMSTT(2),TIMSTT(3))
      WRITE(6,304)
304   FORMAT(' ',//' INPUT BEGINNING ELEVATION AND ENDING ELEVATION.',/)
      CALL FREAD(5,'2R:',ELEV1,ELEV2)
      TELEV=ELEV1
      WRITE(6,305)
305   FORMAT(' ',//' INPUT STARTING RANGE AND ENDING RANGE.',/)
      CALL FREAD(5,'2I:',IR1,IR2)
      WRITE(6,306)
306   FORMAT(' ',//,' START OF DATA?"Y(0) OR N(1)"',/)
      CALL FREAD(6,'I:',III)
      IF(III.EQ.1)SKIP=.TRUE.
      IRANGE=IR2-IR1
C CALCULATE RAZM FOR PRINT-OUT PURPOSES.
      DO 1 I=1,100
1     RAZM(I)=((N+(I-1))*(360./631.))+140
C CALCULATE MILES FROM KILOMETERS.
      DO 2 I=1,IRANGE
2     MILES(I)=(IR1+(I-1))/1.609
      N=IAZ
C BY NOW WE HAVE READ EVERYTHING IN. LET'S MOUNT THE TAPE AND USE THE
C WONDERFUL SUBROUTINE SKPREC.
      WRITE(6,100)
100   FORMAT(' ','PLS ENTER MOUNT#',/)
222   CALL FREAD(5,'I:',II)
C DO A BIT OF CHECKING.
      IF(II.GT.0.AND.II.LE.13)GO TO 224
      WRITE(6,403)
403   FORMAT(' ',' INVALID INPUT...PLS RE-ENTER MOUNT#'/)
      GO TO 222
224   CALL TPMNT(II)
C TAPE MOUNTED...READY FOR THE HARD PART.
      CALL SKPREC(II,START,M,CNTNUM)
      CALL DATA(M,CNTNUM,&40,&27)
      DOWN=.TRUE.
      UP=.FALSE.
C SPACE FORWARD TO START TIME AND GET DOWN PULSE.
11    CALL HEDING(M,CNTNUM,DOWN,UP,&11,&27,&27)
```

```
      CALL BYTREV(M,CNTNUM+1)
      CALL BYTREV(M,CNTNUM+2)
      CLOCK=RTIM(M(CNTNUM+2),M(CNTNUM+1))
      IF(CLOCK.GE.START)GO TO 14
      CNTNUM=CNTNUM+2
      GO TO 11
14    IF(SKIP)GO TO 15
      CALL SKPRAY(M,CNTNUM,200,&27,&27)
C SET ELEVATION COUNTER TO ZERO AND SKIP TO NEXT HEADING MARKER.
16    CALL HEDING(M,CNTNUM,.FALSE.,.TRUE.,&16,&27,&27)
      CNTNUM=CNTNUM+2
15    IF(ELEV1.EQ.0.0)GO TO 30
      DOWN=.FALSE.
      UP=.TRUE.
C GET PROPER ELEVATION.
      ELEV=0.0
26    CALL SKPRAY(M,CNTNUM,200,&27,&27)
      CALL HEDING(M,CNTNUM,DOWN,UP,&27)
      ELEV=ELEV+1.5
      IF(ELEV.LT.ELEV1)GO TO 26
30    CALL SKPRAY(M,CNTNUM,N,&27,&27)
      N=IAZ
      CALL BYTREV(M,CNTNUM+1)
      CALL BYTREV(M,CNTNUM+2)
      CLOCK=RTIM(M(CNTNUM+2),M(CNTNUM+1))
      CALL TIME(CLOCK,HR,MIN,SEC)
      CALL BTD(HR,A(1),2,ND,'0')
      CALL BTD(MIN,A(3),2,ND,'0')
      CALL BTD(SEC,A(5),2,ND,'0')
      CNTNUM=CNTNUM+2
C TAPE IS NOW POSITIONED AT PROPER TIME,ELEVATION,AND AZIMUTH.
C LET'S PRINT SOME STATISTICS.
      WRITE(6,401)A,N1,IRANGE,ELEV1
401   FORMAT(//,4X,'STARTING TIME=>',2A1,':',2A1,':',2A1,
     */,4X,'STARTING AZIMUTH=>',I4,'DEGREES',
     */,4X,'AZIMUTH COVERED=>60 DEGREES(100RAYS)',
     */,4X,'RANGE COVERED=>',I3,'KM'
     */,4X,'STARTING ELEVATION=>',F5.2,'DEGREES',//)
23    WRITE(6,400)(RAZM(IPTR),IPTR=1,20)
400   FORMAT(/,1X,'AZIMUTH ',20(F5.1,1X))
      WRITE(6,404)(I,I=1,20)
404   FORMAT(3X,'RAY#',3X,(20(I3,3X)))
C LET'S DO SOME WORK WITH THOSE BINS.
      CALL DBZRAY(M,CNTNUM,RBINS,IRANGE,IR1,IR2,&27,&27,&40)
      IF(ELEV1.EQ.ELEV2)GO TO 40
      CALL HEDING(M,CNTNUM,.FALSE.,.TRUE.,&27)
      ELEV1=ELEV1+1.5
C SINCE WE ARE DEALING WITH A NP.,SKIP TO PROPER AZIMUTH.
      IF(ELEV1.GT.ELEV2)GO TO 40
      CALL SKPRAY(M,CNTNUM,N,&27,&27)
      N=IAZ
      CALL BYTREV(M,CNTNUM+1)
      CALL BYTREV(M,CNTNUM+2)
      CLOCK=RTIM(M(CNTNUM+2),M(CNTNUM+1))
      CNTNUM=CNTNUM+2
      CALL TIME(CLOCK,HR,MIN,SEC)
      CALL BTD(HR,A(1),2,ND,'0')
      CALL BTD(MIN,A(3),2,ND,'0')
      CALL BTD(SEC,A(5),2,ND,'0')
      WRITE(6,407)A,ELEV1
407   FORMAT(/,'TIME=>',2A1,':',2A1,':',2A1,
     */'ELEVATION=>',F5.2,/)
      GO TO 23
27    WRITE(6,408)
408   FORMAT(' TROUBLES...TROUBLES..')
      STOP
```

```
40    CALL HEDING(M,CNTNUM,.TRUE.,.FALSE.,&40,&27)
      CNTNUM=CNTNUM+2
      ELEV1=TELEV
      GO TO 15
    END
```

PERMS

```
      DIMENSION ERR(3),KOUNT(3),RER(3),SIGN(3),OBS(60),OBSR(60),EST(3,60
     *),PER(3)
      COMMON /RN/IPERM(60)
      READ(3,1)((EST(I,J),I=1,3),J=1,60)
1     FORMAT(3F8.3)
      READ(4,2)(OBS(I),I=1,60)
2     FORMAT(10F6.1)
      CALL TIME(0,0)
      DO 3 K=1,3
       PER(K)=0.
       ERR(K)=0.
       RER(K)=0.
3      KOUNT(K)=0
C CALCULATION OF ACTUAL MEAN ERRORS OF ESTIMATION METHODS
      DO 4 J=1,60
       DO 4 I=1,3
4       ERR(I)=ERR(I)+ABS(EST(I,J)-OBS(J))/60.
      ISEED=16807
C CALCULATION OF MEAN RANDOMIZED ERRORS (REPEATED NUMEROUS TIMES)
      DO 5 I=1,10000
       CALL PERM(ISEED)
       DO 6 J=1,60
       JJ=IPERM(J)
6       OBSR(J)=OBS(JJ)
       DO 7 J=1,60
        DO 7 K=1,3
7         RER(K)=RER(K)+ABS(OBSR(J)-EST(K,J))/60.
C COMPARISON OF MEAN ACTUAL ERROR WITH MEAN RANDOMIZED ERROR.THIS IS
C TALLIED IF THE MEAN RANDOMIZED ERROR IS LESS THAN THE MEAN ACTUAL
C ERROR.
       DO 8 L=1,3
        PER(L)=PER(L)+RER(L)/10000
        IF(RER(L).LT.ERR(L))KOUNT(L)=KOUNT(L)+1
8       RER(L)=0.
5     CONTINUE
      DO 9 I=1,3
9      SIGN(I)=KOUNT(I)/100.
      CALL TIME(15,1)
      WRITE(6,10)(SIGN(I),I=1,3)
10    FORMAT('1PERCENTAGE OF CASES IN WHICH MEAN ERROR OF ESTIMATE BY VA
     *RIOUS METHODS WAS LESS THAN MEAN ERROR OF RANDOMLY PERMUTED OBSERV
     *ATIONS'//' METHOD 1   METHOD 2.  METHOD 3'//3(F5.2,6X))
C LIST POPULATION MEAN RANDOMIZED ERRORS FOR THE RESPECTIVE METHODS
      WRITE(6,11)(PER(L),L=1,3)
11    FORMAT('0',3F10.3)
      STOP
      END
```

```
      SUBROUTINE PERM(ISEED)
      COMMON /RN/IV(60)
      DO 20 I=1,60
20     IV(I)=I
      CALL RNDP(ISEED)
      RETURN
      END
```

```
      SUBROUTINE RNDP(ISEED)
      DIMENSION D(60)
      COMMON /RN/IV(60)
      N=60
C GGU3 IS A *IMSL ROUTINE THAT GENERATES RANDOM NUMBERS.
      CALL GGU3(ISEED,N,D)
      DO 20 I=2,60
       J=N-I+1
       K=J*D(I)+1
       W=IV(K)
       IV(K)=IV(J)
20.    IV(J)=W
      RETURN
      END
```

APPENDIX C

Hailpad triplets are described on p. of the text. In the following listing, "hailpad I.D.'s" designated by W,X,Y or Z refer to locations known to have received no hail, but are not official hailpad locations. These are:

W3: SW6,43,1,5
W4: NE32,45,27,4
W5: SW3,45,2,5
W6: SW2,46,26,4
W7: SE17,46,27,4
W8: SW21,40,5,5

X1: SW30,30,27,4
X2: NE12,30,28,4
X3: NE29,31,28,4
SE6,31,1,5
X6: SE16,41,25,4
Y4: SE3,33,2,5

Z3: SW33,32,2,5
Z4: SW10,33,3,5
Z6: NW27,34,27,4
Z7: SW30,35,28,4
NE21,34,5,5
NW7,37,1,5

Kinetic energy densities are calculated from Equations 2.2 and 2.3.

Date (1974)	Triplet I.D.	Hailpad I.D.'s			Kinetic Energy Densities (Jm^{-2})			Distances (miles)	
		H_1	H_C	H_2	E_1	E_C	E_2	d_1	d_2
July 30	3001	A18	B21	C27	23.9	14.9	0.5	7.0	14.0
	3002	B21	C27	D31	14.9	0.5	1.2	14.0	8.5
	3003	C27	D31	D36	0.5	1.2	45.7	8.5	8.0
	3004	E27	D31	D33	1.6	1.2	28.6	6.5	5.5
	3005	W4	D33	D34	0	28.6	6.0	1.0	3.5
	3006	B33	W7	D33	43.4	0	28.6	9.0	2.0
	3007	B21	B33	B36	14.9	43.4	0.9	24.0	5.0
	3008	B36	B39	C39	0.9	1.2	1.1	4.5	5.5
	3009	B39	C36	W6	1.2	10.8	0	4.0	3.0
	3010	B39	C36	D34	1.2	10.8	6.0	4.0	8.0
	3011	D33	D34	D36	28.6	6.0	45.7	3.5	3.0
	3012	W5	C27	B33	0	0.5	43.4	7.5	16.0
	3013	C27	W7	C36	0.5	0	10.8	10.0	9.0
	3014	W7	C36	C39	0	10.8	1.1	9.0	6.5
	3015	B39	C39	B46	1.2	1.1	1.9	5.5	9.0
	3016	C36	C39	B46	10.8	1.1	1.9	6.5	9.0
	3017	D34	W6	C39	6.0	0	1.1	6.0	8.0
	3018	D34	C36	C39	6.0	10.8	1.1	8.5	6.5
	3019	C39	B46	B51	1.1	1.9	9.6	9.0	14.5
	3020	W2	E27	D36	0	1.6	45.7	3.5	13.0

continued ↓

July 30 (Cont'd)	3021	G37	G36	F42	0.8	19.2	12.5	1.5	8.C
	3022	F42	F46	G42	12.5	52.3	27.5	7.0	8.0
	3023	G42	G43	H48	27.5	27.7	48.7	4.5	7.5
	3024	D48	D49	G42	10.0	10.0	27.5	3.0	14.5
	3025	D49	D48	B51	10.0	10.0	9.6	3.0	10.5
	3026	D49	D51	E57	10.0	8.9	86.7	4.0	11.0
	3027	D48	D51	E57	10.0	8.9	86.7	5.5	11.0
	3028	B51	C48	E57	9.6	3.1	86.7	6.0	16.5
	3029	B46	D48	D51	1.9	10.0	8.9	14.5	4.0
	3030	B46	D48	E57	1.9	10.0	86.7	14.5	15.0
	3031	A18	C27	D31	23.9	0.5	1.2	21.0	8.5
	3032	A19	B21	C27	76.6	14.9	0.5	10.0	14.0
	3033	E27	D31	W4	1.6	1.2	0	6.5	5.5
	3034	B36	C36	W6	0.9	10.8	0	7.5	3.0
	3035	I12	I14	W8	126.3	64.1	0	6.0	2.5
	3036	D33	C36	C39	28.6	10.8	1.1	9.5	6.5
	3037	W4	C36	C39	0	10.8	1.1	10.0	6.5
	3038	W3	E27	D31	0	1.6	1.2	10.0	6.5
August 7	701	S9	S11	X2	23.3	4.2	0	3.5	7.5
	702	S12	X1	R20	1.8	0	0.1	6.0	5.5
	703	R4	X4	S11	5.4	0	4.2	5.5	6.5
	704	S12	X3	Q16	1.8	0	2.9	6.5	6.5
	705	X3	Q16	P17	0	2.9	58.1	6.5	7.0
	706	R20	Q18	P21	0.1	0.5	19.1	10.0	7.5
	707	Q4	R4	X4	8.2	5.4	0	7.0	4.5
	708	R4	Q9	A16	5.4	0.3	2.9	4.5	9.5
	709	O0	P12	Q16	3.0	0	2.9	6.0	13,5
	710	O0	P12	Q4	3.0	0	8.2	6.0	15,5
	711	N0	Q16	R20	2.0	2.9	0.1	22.5	14.0
	712	N0	P17	Q18	2.0	58.1	0.5	19.5	16.5
	714	F18	G28	H37	1.8	23.9	8.7	19.0	14.5
	715	F18	G27	H37	1.8	4.5	8.7	18.0	15.5
	716	H37	X6	G43	8.7	0	16.5	7.5	9.0
	717	G27	F30	E33	4.5	19.5	22.4	7.0	6.0
	718	G28	F30	E33	23.9	19.5	22.4	9.0	6.0
	719	F30	F33	F36	19.5	17.3	8.2	3.5	3.0
	720	F34	F36	D36	15.1	8.2	50.2	3.5	7.0
	721	F33	E33	D33	17.3	22.4	1.6	5.5	6.0
	722	D37	E33	F36	166.1	22.4	8.2	5.5	6.0
	723	D31	E33	F36	25.6	22.4	8.2	5.5	6.0
	724	D33	D36	E36	1.6	50.2	4.5	5.0	4.5
	725	F33	F36	F39	17.3	8.2	21.1	3.0	8.5
	726	D36	E36	F39	50.2	4.5	21.1	4.5	7.0
	727	E33	D36	C42	22.4	50.2	18.9	4.0	14.5

continued ↓

August 7 (Cont'd)	728	F34	E36	C42	15.1	4.5	18.9	8.5	14.0
	729	F39	G39	X6	21.1	59.3	0	7.0	8.0
	730	E36	G39	G43	4.5	59.3	16.5	13.0	12.5
	731	C42	D45	D49	18.9	0.4	8.5	7.5	9.5
	733	F30	E33	D36	19.5	22.4	50.2	6.0	4.0
	734	D37	E33	E36	166.1	22.4	4.5	5.5	6.5
	735	D31	E33	E36	25.6	22.4	4.5	5.5	6.5
	736	D37	D36	E36	166.1	50.2	4.5	7.5	4.5
	737	D31	D36	E36	25.6	50.2	4.5	8.0	4.5
	738	F30	E36	D45	19.5	4.5	0.4	10.5	17.5
	739	F33	E36	D45	17.3	4.5	0.4	7.5	17.5
	740	F30	D36	C42	19.5	50.2	18.9	9.5	14.5
	741	F33	E36	C42	17.3	4.5	18.9	7.5	14.0
	742	D37	D33	C42	166.1	1.6	18.9	4.5	16.5
	743	D31	D33	C42	25.6	1.6	18.9	5.0	16.5
	744	D31	D37	D36	25.6	166.1	50.2	0.5	7.5
	745	F36	E36	C42	8.2	4.5	18.9	5.0	14.0
August 15	153	Q82	Q80	Y4	2.9	0.4	0	10.0	4.0
August 18	1801	K21	L2	L4	4.5	26.8	63.8	8.0	2.5
	1802	J6	K21	L2	0.0	4.5	26.8	12.5	8.0
	1803	L2	L4	L18	26.8	63.8	33.0	2.5	6.0
	1804	L0	L2	L4	16.1	26.8	63.8	13.0	2.5
	1805	M0	L18	K6	14.5	33.0	0.1	8.5	5.5
	1806	K21	K6	K8	4.5	0.1	0	17.5	2.5
	1807	L4	L18	M4	63.8	33.0	101.9	6.0	5.0
	1808	K6	M4	N80	0.1	101.9	41.6	8.0	7.0
	1809	L18	M1	N2	33.0	39.8	17.5	6.0	7.0
	1810	M1	N2	O4	39.8	17.5	22.4	7.0	3.5
	1811	N2	O4	O5	17.5	22.4	33.3	3.5	4.0
	1812	O4	O5	R1	22.4	33.3	41.9	4.0	12.5
	1813	Q1	R1	R8	13.9	41.9	13.7	8.5	7.0
	1814	R8	Q9	Q16	13.7	10.5	14.1	8.5	9.5
	1815	Q16	Q18	Q31	14.1	0.4	0.6	15.5	23.0
	1816	P17	O17	O18	0.5	3.2	2.3	2.0	3.0
	1817	N9	O16	O18	18.0	13.1	2.3	5.0	6.5
	1818	N9	O16	O17	18.0	13.1	3.2	5.0	5.0
	1819	N9	O16	P17	18.0	13.1	0.5	5.0	5.5
	1820	K8	M13	O7	0	127.7	15.1	11.0	11.5
	1822	K8	M13	N	0	127.7	7.3	11.0	7.0
	1823	L18	M4	M13	33.0	101.9	127.7	5.5	6.5
	1824	M4	M7	N9	101.9	127.7	18.0	6.5	12.5
	1825	M4	M1	O7	101.9	127.7	15.1	6.5	11.5
	1826	M1	N80	N	39.8	41.6	7.3	5.5	4.5
	1827	N2	N80	M13	17.5	41.6	127.7	4.0	6.0

continued ↓

August 18 (Cont'd)	1828	L4	M1	N80	63.8	39.8	41.6	10.0	5.5
	1829	N2	N	O7	17.5	7.3	15.1	6.0	8.5
	1831	M0	N22	O4	14.5	56.8	22.4	5.0	9.0
	1832	N22	M1	M4	56.8	39.8	101.9	7.5	5.0
	1833	M1	M4	K8	39.8	101.9	0	4.5	10.5
	1834	L4	M1	N	63.8	39.8	7.3	10.0	5.5
	1835	M0	N22	O5	14.5	56.8	33.3	5.0	12.0
	1837	O5	Z3	Q9	33.3	0	10.5	11.0	6.5
	1838	Z4	N	M13	0	7.3	127.7	12.5	7.5
	1839	O7	O16	Z6	15.1	13.1	0	7.5	6.5
	1840	O7	N9	Z7	15.1	18.0	0	5.0	2.0
	1841	Z8	N22	L18	0	56.8	33.0	6.5	11.5
	1842	M4	M13	Z7	101.9	127.7	0	6.5	12.0
	1843	N80	M13	Z9	41.6	127.7	0	6.0	7.5

Appendix D

CENTER-PAD ESTIMATES AND ERRORS OF TRIPLETS (IN Jm^{-2})

The following is a list of the center-pad estimates and the errors of these estimates described on pp. 72 and 74 of the text.

Triplet I.D.	Method 1 Estimate	$\|E_c'-E_c\|$	Method 2 Estimate	$\|E_c'-E_c\|$	Method 3 Estimate	$\|E_c'-E_c\|$
701	11.7	7.5	15.9	11.7	5.7	1.5
702	1.0	1.0	0.9	0.9	5.0	5.0
703	4.8	4.8	4.8	4.8	5.0	5.0
704	2.4	2.4	2.4	2.4	5.0	5.0
705	29.1	26.2	28.0	25.1	5.0	2.1
706	9.6	9.1	11.0	10.5	6.7	6.2
707	4.1	1.3	3.2	2.2	5.0	0.4
708	4.2	3.9	4.6	4.3	5.0	4.7
709	3.0	3.0	3.0	3.0	5.8	5.8
710	5.6	5.6	4.6	4.6	5.8	5.8
711	1.1	1.9	0.8	2.1	5.0	2.1
712	1.3	56.9	1.2	56.9	6.4	51.7
714	5.3	18.7	5.7	18.2	21.3	2.6
715	5.3	0.8	5.5	1.0	65.3	60.8
716	12.6	12.6	12.2	12.3	5.0	5.0
717	13.5	6.1	14.1	5.4	12.5	7.0
718	23.2	3.7	23.1	3.6	12.5	7.0
719	13.8	3.5	13.4	3.9	19.9	2.6
720	32.7	24.5	26.8	18.6	13.8	5.6
721	9.5	13.0	9.8	12.6	24.4	2.0
722	87.2	64.8	90.6	68.2	24.4	2.0
723	16.9	5.5	17.3	5.1	24.4	2.0
724	3.1	47.2	3.1	47.1	36.3	14.1
725	19.2	11.0	18.3	10.1	13.8	5.6
726	35.7	27.5	38.8	30.6	7.8	5.6
727	20.7	29.6	21.6	28.6	5.0	14.1
728	17.0	12.5	16.5	12.0	5.0	3.3
729	10.6	48.8	11.8	48.0	6.2	54.3
730	10.5	48.8	10.6	48.7	24.4	54.3
731	13.7	13.3	14.3	13.9	24.4	5.7
733	34.9	12.5	37.9	15.5	24.4	2.0

continued ↓

734	85.3	62.9	92.0	69.6	24.0	2.0
735	15.1	7.4	15.9	6.5	24.4	2.0
736	85.3	35.1	65.1	14.9	36.3	14.1
737	15.1	35.2	12.1	38.1	36.3	14.1
738	10.0	5.5	12.3	7.8	7.8	3.3
739	8.9	4.4	12.2	7.7	7.8	3.3
740	19.2	31.0	19.3	30.9	36.3	14.1
741	18.1	13.6	17.9	13.4	7.8	3.3
742	92.5	90.9	134.6	133.0	10.0	8.4
743	22.3	20.7	24.0	22.4	10.0	8.4
744	108.2	82.6	158.9	133.3	166.1	155.0
745	13.6	9.1	11.0	6.5	7.8	3.3
153	1.5	1.1	0.8	0.4		
1801	34.2	7.4	49.7	22.9	28.7	1.9
1802	13.4	8.9	16.3	11.8	0.8	3.7
1803	29.9	33.9	28.6	35.2	44.9	18.9
1804	40.0	13.2	56.1	29.3	28.7	1.9
1805	7.3	25.7	5.8	27.2	24.5	8.5
1806	2.3	2.2	1.6	1.5	5.5	5.4
1807	82.9	49.9	84.6	51.6	24.5	8.5
1808	20.9	81.1	22.2	79.7		
1809	25.3	14.6	25.8	14.0		
1810	31.1	13.6	28.2	10.7		
1811	25.4	3.0	24.9	2.5		
1812	32.2	1.2	27.1	6.2		
1813	13.8	28.1	13.8	28.1		
1814	13.9	3.4	13.9	3.4		
1815	7.4	7.0	2.5	2.1	0.0	0.4
1816	1.4	1.8	1.2	2.0	1.7	1.5
1817	10.2	3.0	11.2	1.9	0.0	13.1
1818	10.6	2.5	10.6	2.5	0.0	13.1
1819	9.3	3.9	9.7	3.4	0.0	13.1
1820	7.6	120.2	7.4	120.3		
1822	3.7	124.1	4.5	123.2		
1823	80.4	21.6	76.4	25.5		
1824	60.0	67.8	73.2	54.5		
1825	58.5	69.2	70.6	57.1		
1826	23.6	18.1	21.9	19.7	47.5	5.9
1827	72.6	31.0	61.6	20.0	47.5	5.9
1828	52.7	12.9	49.5	9.7		
1829	16.3	9.0	16.5	9.2		
1831	18.5	38.4	17.3	39.5		
1832	79.4	39.6	83.9	44.1		
1833	19.9	82.0	27.9	74.0		
1834	35.6	4.3	27.3	12.5		

continued↓

1835	23.9	32.9	20.0	36.8		
1837	21.9	21.9	19.0	19.0	0.0	0.0
1838	63.9	56.6	79.8	72.5	10.3	3.0
1839	7.6	5.6	7.0	6.1	0.0	13.1
1840	7.6	10.5	4.3	13.7		
1841	16.5	40.3	11.9	44.9		
1842	51.0	76.8	66.1	61.6		
1843	20.8	106.9	23.1	104.6		
3001	12.2	2.7	16.1	1.2		
3002	8.1	7.6	6.4	5.9		
3003	23.1	21.9	23.8	22.6		
3004	15.1	13.9	16.2	15.0		
3005	3.0	25.6	1.3	27.3		
3006	36.1	36.1	31.4	31.4		
3007	7.9	35.5	3.3	40.1		
3008	1.1	0.2	1.0	0.2		
3009	0.6	10.2	0.5	10.3		
3010	3.6	7.2	2.8	8.0		
3011	37.2	31.2	37.8	31.8		
3012	21.7	21.2	13.9	13.4		
3013	5.7	5.7	5.9	5.9		
3014	0.6	10.2	0.7	10.1		
3015	1.6	0.5	1.5	0.4		
3016	6.4	5.3	7.1	6.0		
3017	3.6	3.6	3.9	3.9		
3018	3.6	7.3	3.2	7.6		
3019	5.4	3.5	4.4	2.5		
3020	22.9	21.3	9.7	8.1		
3021	6.7	12.6	2.6	16.6		
3022	20.0	32.3	19.5	32.8		
3023	38.6	10.9	35.8	8.1		
3024	18.8	8.8	13.0	3.0		
3025	9.8	0.2	9.9	0.1		
3026	48.4	39.5	30.5	21.6		
3027	48.4	39.5	35.6	26.7		
3028	48.2	45.1	30.2	27.1		
3029	5.4	4.6	7.4	2.6		
3030	44.3	34.3	43.6	33.6		
3031	12.6	12.1	7.7	7.2		
3032	38.6	23.7	44.9	30.0		
3033	0.8	0.4	0.7	0.5		
3034	0.5	10.4	0.3	10.5		
3035	63.2	1.0	37.1	27.0		
3036	14.9	4.1	12.3	1.5		
3037	0.6	10.3	0.7	10.1		
3038	0.6	1.0	0.7	0.9		

Appendix E

The table on the following pages lists all the analyses used in determining the accuracy of registration of the C-band radar output. The results of these analyses are summarized in Secion 6.3 of the text. The radar data from the hail-free locations Z1 to Z5 and Z7 to Z9 were studied, and used for registration analyses. The land locations Z3, Z4, Z5, Z7, Z8 and Z9 have already been noted in Appendix C. The two remaining locations are:

Z1: SW26,33,1,5 Z2: NW36,33,1,5

INDEX TO TABLE HEADINGS

r_m	map range in kilometers
a_m	map azimuth in degrees
r_{PLOT}	range given by program PLOT kilometers)
a_{PLOT}	azimuth given by PLOT (degrees)
r_{PPI}	range given by PPI
a_{PPI}	azimuth given by PPI
X_R^{PLOT}	range error in kilometers (PLOT relative to map)
X_T^{PLOT}	tangential error in kilometers (PLOT relative to map)
X_R^{PPI}	range error (PPI relative to map)
X_T^{PPI}	tangential error (PPI relative to map)
X_{TOTAL}^{PLOT}	total error, in kilometers (PLOT relative to map)
X_{TOTAL}^{PPI}	total error (PPI relative to map)

AUGUST 7, 1974 "PLOT" vs. MAP ANALYSES

PAD I.D.	MAP		PLOT		PLOT ERROR		
	r_m	a_m	r_{PLOT}	a_{PLOT}	X_R^{PLOT}	X_T^{PLOT}	X_{TOTAL}^{PLOT}
B51	115.5	32.5	115	33	0.5	1.0	1.1
C42	89.6	18.2	89	18	0.6	0.3	0.7
C48	112.8	36.6	111	360	1.8	1.2	2.2
D33	82.5	0.5	82	360	0.5	0.7	0.9
D45	88.0	32.5	87	33	0.5	1.0	1.1
D49	94.6	35.4	93	35	1.6	0.6	1.7
F18	70.6	327.5	70	328	0.6	0.6	0.8
F39	66.5	18.8	66	19	0.5	0.2	0.8
G27	53.9	350.3	53	350	0.9	0.3	0.9
G39	56.3	24.3	56	23	0.3	1.3	1.3
G43	52.3	45.2	52	44	0.3	1.1	1.1
G45	68.4	40.5	69	39	1.0	1.8	2.1
H37	42.5	16.4	42	14	0.5	1.8	1.9
I54	80.0	68.6	79	68	1.0	0.8	1.3
J6	83.7	284.7	83	285	0.7	0.4	0.8
M10	78.3	262.9	77	263	1.3	0.1	1.3
N0	35.4	232.9	35	232	0.4	0.5	0.6
N6	22.8	223.5	22	223	0.8	0.2	0.8
N9	21.6	202.9	21	203	0.6	0.0	0.6
P17	33.6	178.5	33	181	0.6	0.8	1.0
P21	42.3	146.2	41	148	1.3	1.3	1.8
Q4	55.7	210.0	55	210	0.7	0.0	0.7
Q11	69.3	226.1	69	226	0.3	0.1	0.3
Q16	44.7	181.0	44	180	0.7	0.8	1.1
Q18	52.8	153.6	53	153	0.2	0.6	0.6
R20	62.8	166.5	62	166	0.8	0.5	0.9
S9	70.0	190.0	70	190	0.0	0.0	0.0
S11	69.5	185.9	69	187	0.5	1.3	1.4
S12	65.2	182.9	65	182	0.2	1.0	1.0
T4	85.3	203.6	85	204	0.3	0.6	0.7

AUGUST 7, 1974: DETAILED ANALYSES ("PLOT", "PPI" AND MAP)

PAD I.D.	MAP		PLOT		PPI		PLOT ERROR			PPI ERROR		
	r_m	a_m	r_{PLOT}	a_{PLOT}	r_{PPI}	a_{PPI}	X_R^{PLOT}	X_T^{PLOT}	X_{TOTAL}^{PLOT}	X_R^{PPI}	X_T^{PPI}	X_{TOTAL}^{PPI}
D31	77.4	346.4	77	355	77	355	0.4	1.9	1.9	1.3	1.7	2.1
D36	74.7	5.9	74	5	74	4.8	0.7	1.2	1.4	0.7	1.4	1.6
D37	77.4	357.4	77	356	77	355.7	0.4	1.9	1.9	0.4	2.3	2.3
E33	71.1	1.6	71	2	71	1.9	0.1	0.5	0.5	0.1	0.4	0.4
E36	70.5	10.1	70	11	70	11.1	0.5	1.1	1.2	0.5	1.2	1.3
F30	62.9	357.4	62	358	62	357.4	0.9	0.6	1.1	0.9	0.0	0.9
F33	57.1	359.5	57	360	57	359.7	0.1	0.5	0.5	0.1	0.3	0.3
F34	57.6	6.7	57	7	57	7.6	0.6	0.3	0.7	0.6	0.9	1.1
F36	63.4	6.7	63	7	63	7.6	0.4	0.3	.5	0.9	0.4	1.0
G28	50.7	349.4	50	350	50	349.4	0.7	0.5	0.9	0.7	0.0	0.7
O0	63.2	243.0	63	243	63	242.7	0.2	0.0	0.2	0.2	0.3	0.4
P12	60.2	234.5	60	235	60	234.1	0.2	0.5	0.5	0.2	0.4	0.5
Q9	52.0	196.8	51	197	51	196.5	1.0	0.2	1.0	1.0	0.3	1.0
R4	58.9	199.8	58	200	58	199.3	0.9	0.2	0.9	0.9	0.5	1.0

AUGUST 18, 1974: "PLOT" vs. MAP ANALYSES

PAD I.D.	MAP		PLOT		PLOT ERROR			
	r_m	a_m	r_{PLOT}	a_{PLOT}	X_R^{PLOT}	X_T^{PLOT}	PLOT TOTAL	
K6	39.1	281.4	39	282	0.1	0.4	0.4	
K8	24.3	288.9	24	290	0.3	0.0	0.3	
M1	40.7	256.0	40	255	0.7	0.7	1.0	
M4	34.8	263.0	39	270	0.8	4.3	4.4	REJECTED
N2	43.0	241.5	42	241	1.0	0.4	1.1	
N9	21.6	203.3	21	203	0.6	0.1	0.6	
O4	45.9	235.5	45	235	0.9	0.4	1.0	
O5	49.9	229.0	45	229	0.9	0.0	0.9	
O7	29.0	211.0	28	211	1.0	0.0	1.0	
O16	25.7	187.4	25	191	0.7	1.6	1.7	
Q1	72.4	224.6	72	224	0.4	0.8	0.9	
Q16	44.7	180.9	44	180	0.7	0.7	1.0	
Q18	52.9	153.5	53	153	0.1	0.5	0.5	
Q31	77.2	128.4	76	129	1.2	0.8	1.5	
R1	71.3	211.1	71	211	0.3	0.1	0.3	
R8	62.9	204.9	63	205	0.1	0.1	0.1	
R50	95.9	129.0	102	125	6.1	7.1	9.4	REJECTED
Z1	37.7	195.8	37	194	0.7	1.2	1.4	
Z2	34.9	195.2	34	195	0.9	0.1	0.9	
Z3	50.0	208.5	50	208	0.0	0.4	0.4	
Z4	52.0	218.2	51	218	1.0	0.2	1.0	
Z5	55.0	227.0	54	227	1.0	0.0	1.0	
Z7	18.3	204.9	18	204	0.3	0.3	0.4	
Z8	56.5	243.5	56	244	0.5	0.5	0.7	
Z9	17.5	266.8	17	270	0.5	1.0	1.1	

AUGUST 18, 1974: DETAILED ANALYSES ("PLOT", "PPI" AND MAP)

PAD I.D.	MAP		PLOT		PPI		PLOT ERROR			PPI ERROR		
	r_m	a_m	r_{PLOT}	a_{PLOT}	r_{PPI}	a_{PPI}	X_R^{PLOT}	X_T^{PLOT}	X_{TOTAL}^{PLOT}	X_R^{PPI}	X_T^{PPI}	X_{TOTAL}^{PPI}
J6	84.0	285.0	83	285	83	284.9	1.0	0.0	1.0	1.0	0.1	1.0
K21	67.4	277.9	67	278	67	277.5	0.4	0.4	0.6	0.4	0.4	0.6
L0	76.6	271.0	76	270	76	269.5	0.6	1.3	1.4	0.6	2.0	2.0
L2	55.5	271.5	55	270	56	269.5	0.5	1.5	1.6	0.5	1.9	2.0
L4	51.5	271.0	51	270	51	269.5	0.5	0.9	1.0	0.5	1.3	1.4
L18	41.7	269.5	41	270	41	269.5	0.7	0.4	0.8	0.7	0.0	0.7
M0	52.7	259.4	52	259	52	258.7	0.7	0.4	0.8	0.7	0.6	0.9
M13	27.4	248.7	27	248	27	247.8	0.4	0.4	0.6	0.4	0.4	0.6
N	35.2	232.7	35	232	35	231.9	0.2	0.5	0.5	0.2	0.5	0.5
N22	52.0	251.0	51	251	51	250.1	1.0	0.0	1.0	1.0	0.8	1.3
N80	36.4	244.8	36	244	36	243.8	0.4	0.6	0.8	0.4	0.6	0.8
O17	31.1	175.5	31	178	31	178.2	0.1	1.4	1.4	0.1	1.5	1.5
O18	29.0	167.1	28	170	29	169.7	1.0	1.4	1.7	0.0	1.3	1.3
P17	33.6	178.6	33	181	33	180.5	0.6	1.4	1.5	0.6	1.1	1.3

Appendix F

LAND LOCATION NOTATION

Most inhabited areas of Alberta are parcelled out according to the Dominion of Canada Survey. The United States border marks the southern limit of the survey. The largest divisions in the Survey are delineated by meridians, which are longitude lines spaced at four-degree intervals. The eastern border of Alberta coincides with the fourth meridian, while the fifth meridian lies about 13 kilometers west of Red Deer, Alberta. The Survey divides the land further into townships, sections and quarter-sections. Smaller divisions exist, but they are not important here. The location of a township, which normally covers 36 square miles, is identified by the township number, which increases northward from 1 at the U.S. border, and the range number, which increases westward from the meridian, beginning with Range 1. Because of the geometry of the survey system, some townships immediately to the east of the meridian line will not cover a full 36 square miles. With these exceptions, each township contains 36 sections, each covering 1 square mile, while each section is divided into 4 quarter-sections. The following diagram shows the labelling. Referring to the diagram, a typical land location might be NW15,39,2,5 or NW15,T39,R2,W5. This is read as "Northwest quarter, section 15, township 39, range 2, west of the Fifth Meridian." Sections or quarter-sections are sometimes referred to explicitly in the text.

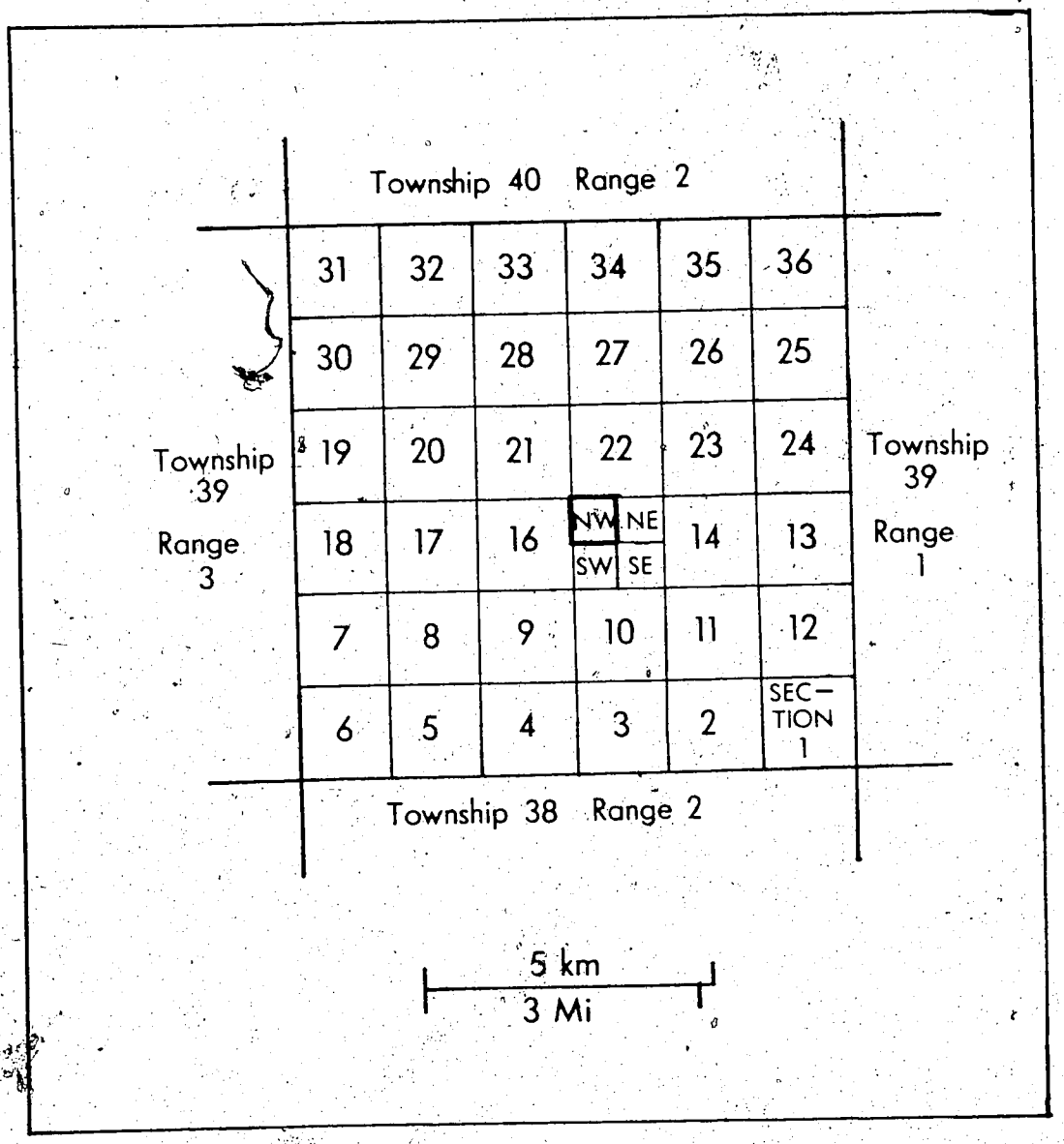

Figure A-1. Land locations. The township shown in detail is Township 39, Range 2. The Fifth Meridian is at the eastern border of Township 39, Range 1. The heavily outlined quarter-section is described as "Northwest Quarter, Section 15, Township 39, Range 2, west of the Fifth Meridian." In the text, this would be written as "NW15,39,2,5".